

DISSOLVED ORGANIC CARBON AND DISSOLVED INORGANIC CARBON ALONG
AN URBANIZATION GRADIENT IN CHARLOTTE, NORTH CAROLINA

by

Taylor Wilson Kiker

A thesis submitted to the faculty of
The University of North Carolina at Charlotte
in partial fulfillment of the requirements
for the degree of Master of Science in
Earth Sciences

Charlotte

2018

Approved by:

Dr. David Vinson

Dr. Sandra Clinton

Dr. Craig Allan

©2018
Taylor Wilson Kiker
ALL RIGHTS RESERVED

ABSTRACT

TAYLOR WILSON KIKER. Dissolved Organic Carbon and Dissolved Inorganic Carbon Along an Urbanization Gradient in Charlotte, North Carolina. (Under the direction of DR. DAVID VINSON)

Streams and rivers are an integral component of the freshwater carbon cycle as they provide the lateral transport of carbon from terrestrial environments to the ocean. Urbanization is one of the fastest growing land uses and it has major impacts on streams and rivers. This study examined twenty-eight watersheds varying in land uses from pre-restoration forested to urban in Charlotte, North Carolina. Their impervious cover ranged from 0.5-55%. The objective of this study was to examine alterations to freshwater carbon processes among watersheds of various land uses in multiple streams in Mecklenburg County, Charlotte, NC.

Surface water was collected at each site in addition to discharge measurements. Water quality parameters were analyzed including: DOC concentration, Specific UV Absorbance of DOC, DIC concentration, alkalinity concentration, $\delta^{13}\text{C-DIC}$, major cations (Na^+ , K^+ , Mg^{2+} , and Ca^{2+}), and anions (F^- , Cl^- , PO_4^{3-} , NO_3^- and SO_4^{2-}). DOC concentration ranged from 1.1-18 mg/L and SUVA values ranged from 0.2-18 L/mg*m. Alkalinity concentrations ranged from 0.1-3.8 meq/L and DIC concentrations ranged from 0.2-3.8 mM. $\delta^{13}\text{C-DIC}$ values ranged from -18.0‰ to -7.4‰. Overall, DOC concentrations and SUVA values had weak negative relationships with percent impervious cover. DIC concentrations, alkalinity concentrations, $\delta^{13}\text{C-DIC}$ values, all cations, and F^- , Cl^- , and SO_4^{2-} had strong positive relationships with percent impervious cover. PO_4^{3-} and NO_3^- had weak correlations with percent impervious cover. The increase in DIC, alkalinity, $\delta^{13}\text{C-DIC}$, and cations with high impervious cover was largely due to the increased chemical weathering of concrete materials in urban areas.

ACKNOWLEDGEMENTS

Thank you to my advisor Dr. Vinson and my committee Dr. Clinton and Dr. Allan. Thank you to Dr. Clinton's laboratory from May 2016 to May 2018 for all of their help in gathering samples and analyzes. Thank you to Jon Watkins in the Earth Sciences department for the endless help with laboratory machines and analyzes. Thank you to the City of Charlotte Storm Water for funding the research on the Reedy Creek Restoration project.

TABLE OF CONTENTS

LIST OF TABLES	vii
LIST OF FIGURES	viii
1. Introduction.....	1
1.1 The Freshwater Carbon Cycle.....	1
1.2 The Urban Carbon Cycle	2
1.3 Dissolved Organic Carbon.....	3
1.3.1 Specific UV Absorbance.....	3
1.4 Dissolved Inorganic Carbon and Alkalinity.....	5
1.4.1 Terrestrial sourced DIC.....	5
1.4.2 Instream sourced DIC	6
1.4.3 Alkalinity	6
1.4.4 Urban effects on DIC and alkalinity	6
1.4.5 $\delta^{13}\text{C}$ - DIC	8
1.5 Study Locations and Sample Groups	9
1.5.1 Reedy Creek Watershed (RC group).....	11
1.5.2 Toby Creek (TC group).....	14
1.5.3 Additional urban watersheds in Mecklenburg County, NC (MC group).....	16
1.6 Objectives.....	21
2. Hypotheses.....	21
3. Methods	22
3.1 Field methods.....	22
3.2 Laboratory methods	23
4. Results	25
4.1 Stream discharge.....	25
4.2 Dissolved organic carbon and SUVA	26
4.2.1 Inter-site variation.....	26
4.2.2 Temporal variation.....	35
4.3 Dissolved inorganic carbon, alkalinity, and pH.....	42
4.3.1 Inter-site variation.....	42
4.3.2 Temporal variation.....	52
4.4 $\delta^{13}\text{C}$ -DIC	59
4.4.1 Inter-site variation.....	59
4.4.2 Temporal variation.....	63
4.5 Cation and anion concentrations	68
4.5.1 Cations	68

4.5.2	Anions.....	73
4.6	Correlation coefficients.....	82
4.7	Percent forest cover.....	83
5.	Discussion.....	89
5.1	Watershed-scale discharge.....	89
5.2	Watershed-scale fluxes of DOC and DIC	91
5.3	DOC concentrations, DOC fluxes, and SUVA values: Response to urbanization and comparison to other studies.....	96
5.3.1	Comparison of DOC concentrations and SUVA values to other urban stream systems in the Piedmont region.....	96
5.3.2	Urbanization as a controlling variable on DOC fluxes and reactivity in streams of the study	97
5.4	DIC, alkalinity, and $\delta^{13}\text{C}$ -DIC.....	99
5.4.1	Comparison of DIC, alkalinity, and $\delta^{13}\text{C}$ -DIC to other urban stream studies.....	99
5.4.2	Role of urban land cover controlling, DIC, alkalinity, and $\delta^{13}\text{C}$ -DIC fluxes.....	101
5.5	Cations and anions	103
5.5.1	Comparison of cations and anions to other urban stream studies	103
5.6	Percent forest cover.....	105
5.7	Hypotheses testing.....	105
6.	Conclusions	108
	References.....	109
	APPENDIX A: Data table of all parameters for the MC and TC groups	114
	APPENDIX B: Data table of all parameters for RC group.....	116

LIST OF TABLES

Table 1: Subwatershed land uses of Toby Creek (TC group).....	14
Table 2: USGS ID and drainage area (km ²) of MC group (USGS data)	16
Table 3: Watershed area (km ²), percent forest, crop land, urban development, impervious area, and canopy-free impervious area of each watershed.	20
Table 4: StreamStats datasets and associated land use description.....	24
Table 5: Area and discharge of each watershed. Green highlight indicates forest/undeveloped land use, orange indicates agriculture land use, purple indicates urban/developed land use, unshaded indicates watershed outlet or mixed uses, blank spaces mean discharge was not measured that day.....	25
Table 6: Means and standard deviations of DOC and DIC concentrations, alkalinity, SUVA, and $\delta^{13}\text{C}$ -DIC for all 28 sampling sites (green highlight= undeveloped/forest, orange highlight=agriculture, purple highlight= urban/developed, unshaded=watershed outlet or mixed uses)	67
Table 7: Means and standard deviations of cation concentrations (Na, K ⁺ , Mg ²⁺ , and Ca ²⁺) for the 28 sampling sites (green highlight= undeveloped/forest, orange highlight=agriculture, purple highlight= urban/developed, unshaded=watershed outlet or mixed uses)	80
Table 8: Means and standard deviations of anion concentrations (F ⁻ , Cl ⁻ , NO ₃ ⁻ , PO ₄ ³⁻ , SO ₄ ²⁻) for the 28 sampling sites. Where a peak was not detected, a concentration of 0 was used to calculate means. (green highlight= undeveloped/forest, orange highlight=agriculture, purple highlight= urban/developed, unshaded=watershed outlet or mixed uses)	81
Table 9: Correlation coefficient of multiple parameters versus percent impervious cover. Green shading indicates there is an association between the two parameters and red shading indicates there is no association.	82
Table 10: Mean DOC and DIC baseflow fluxes (kg C/hectare/year) for all 28 watersheds	92

LIST OF FIGURES

Figure 1: Global carbon cycle. Pools are expressed in 10^{15} grams of C and fluxes are expressed in 10^{15} grams C/ year (Schlesinger and Bernhardt 2013).....	2
Figure 2: DIC species change with pH. Note that DIC and alkalinity are dominated by the bicarbonate ion at the pH range of this study (Clark & Fritz, 1997).....	5
Figure 3: DIC yield ($\text{mol/m}^2\cdot\text{yr}$) for watersheds with different land uses (Barnes and Raymond, 2009)	7
Figure 4: ArcGIS map of the six study watersheds in Mecklenburg County, NC.....	10
Figure 5: ArcGIS map of Reedy Creek (RC group) Watersheds and the study watersheds (11 total). Yellow outlines the watershed boundary and green dots represent the subwatershed outlet.....	13
Figure 6: ArcGIS map of Toby Creek (TC group), Mecklenburg County, NC. 11 total subwatersheds	15
Figure 7a-f: Aerial imagery of the MC group watersheds (ArcGIS World Imagery basemap) Green dots indicate represent watershed outlet and sampling point.	17
Figure 8: Hypothesized trends between SUVA, DIC concentration, and alkalinity with increasing impervious cover.....	21
Figure 9: Box plot of DOC concentration vs. increasing percent impervious cover	29
Figure 10: Box plot of SUVA values vs. increasing percent impervious cover	30
Figure 11: Scatter plot of DOC concentration vs. percent impervious cover (May 2016- October 2017)	31
Figure 12: Scatter plot of DOC concentration vs. percent impervious cover (June 2017- October 2017)	32
Figure 13: Scatter plot of SUVA vs. percent impervious cover (May 2016- October 2017)	33
Figure 14: Scatter plot of SUVA values vs. percent impervious cover (June 2017- October 2017)	34
Figure 15: Time series of DOC concentration for the RC group, showing the occurrence of scattered higher DOC concentrations during late summer-early fall (May 2016- October 2017)	36
Figure 16: Time series of SUVA values for the RC group (May 2016- October 2017).....	37
Figure 17: Time series of DOC concentration for the MC group (June 2017- September 2017). Dotted lines represent RC concentrations	38
Figure 18: Time series of SUVA values for the MC group (June 2017- September 2017). Dotted lines represent RC values.....	39
Figure 19: Time series of DOC concentration for the TC group (June 2017- October 2017). Dotted lines represent RC concentrations.	40
Figure 20: Time series of SUVA values for the TC group (June 2017- October 2017). Dotted lines represent RC values	41
Figure 21: pH vs. percent impervious cover (June 2017- October 2017).....	45
Figure 22: Box plots of alkalinity concentration vs. percent impervious cover	46
Figure 23: Box plot of DIC concentration vs. increasing percent impervious cover.....	47
Figure 24: Alkalinity concentration vs. percent impervious cover (May 2016- October 2017)....	48
Figure 25: Alkalinity concentration vs. percent impervious cover (June 2017- October 2017)....	49
Figure 26: DIC concentration vs. percent impervious cover (May 2016- October 2017)	50
Figure 27: DIC concentration vs. percent impervious cover (June 2017- October 2017)	51
Figure 28: Time series of alkalinity concentration for the RC group (May 2016- September 2017)	53
Figure 29: Time series of DIC concentration for the RC group (May 2016- October 2017)	54

Figure 30: Time series of alkalinity concentration for the MC group (June 2017- September 2017). Dotted lines represent RC concentrations.....	55
Figure 31: Time series of DIC concentration for the MC group (June 2017- September 2017). Dotted lines represent RC concentrations	56
Figure 32: Time series of alkalinity concentration for the TC group (June 2017- October 2017). Dotted lines represent RC concentrations	57
Figure 33: Time series of DIC concentration for the TC group (June 2017- October 2017). Dotted lines represent RC concentrations	58
Figure 34: Box plot of $\delta^{13}\text{C}$ -DIC vs. increasing percent impervious cover	60
Figure 35: $\delta^{13}\text{C}$ -DIC vs. percent impervious cover (May 2016- October 2017).....	61
Figure 36: $\delta^{13}\text{C}$ -DIC vs. percent impervious cover (June 2017-October 2017).....	62
Figure 37: Time series of $\delta^{13}\text{C}$ -DIC for the RC group (May 2016- October 2017).....	64
Figure 38: Time series of $\delta^{13}\text{C}$ -DIC for the MC group (June 2017- September 2017). Dotted lines represent RC values.....	65
Figure 39: Time series of $\delta^{13}\text{C}$ -DIC for the TC group (June 2017- October 2017). Dotted lines represent RC values	66
Figure 40: Sodium (Na^+) concentration vs. percent impervious cover (May 2016- October 2017)	69
Figure 41: Potassium (K^+) concentration vs. percent impervious cover (May 2016- October 2017)	70
Figure 42: Magnesium (Mg^{2+}) concentration vs. percent impervious cover (May 2016- October 2017).....	71
Figure 43: Calcium (Ca^{2+}) concentration vs. percent impervious cover (May 2016- October 2017)	72
Figure 44: Fluoride (F^-) concentration vs. percent impervious cover (May 2016- October 2017) 74	
Figure 45: Chloride (Cl^-) concentration vs. percent impervious cover (May 2016- October 2017)	75
Figure 46: Nitrate concentration (NO_3^-) vs. percent impervious cover (May 2016- October 2017). Nondetectable concentrations are plotted as zero.	76
Figure 47: Phosphate (PO_4^{3-}) concentration (in ppm) vs. percent impervious cover (May 2016- October 2017). Nondetectable concentrations are plotted as zero values.....	77
Figure 48: Sulfate (SO_4^{2-}) concentration (in ppm) vs. percent impervious cover (May 2016- October 2017)	78
Figure 49: Fluoride/Chloride ratio vs. percent impervious cover (May 2016- October 2017).....	79
Figure 50: Percent forest cover vs. DOC concentration (June 2017- October 2017)	84
Figure 51: Percent forest cover vs. SUVA (June 2017- October 2017).....	85
Figure 52: Percent forest cover vs. DIC concentration (June 2017- October 2017).....	86
Figure 53: Percent forest cover vs. alkalinity concentration (June 2017- October 2017).....	87
Figure 54: Percent forest cover vs. $\delta^{13}\text{C}$ -DIC (June 2017- October 2017)	88
Figure 55: Watershed area vs. estimated yearly baseflow in a log scale. Blue dots represent field measurements of discharge and green triangles represent discharge measured by USGS gauges. Note: discharge measurements were during baseflow.	90
Figure 56: Percent impervious cover vs. baseflow per unit watershed area. Blue dots represent field measurements of discharge and green triangles represent discharge measured by USGS gauges. Note: discharge measurements were during baseflow.....	91
Figure 57: Mean DOC baseflow flux vs. Mean DIC baseflow flux	93
Figure 58: DOC flux vs. SUVA.....	94
Figure 59: DIC flux vs. SUVA	95
Figure 60: Percent impervious cover vs. mean baseflow DOC flux for all 28 watersheds.....	99
Figure 61: Percent impervious cover vs. Mean DIC baseflow flux (kg C/ha/year) for all 28 watersheds	102

Figure 62: DIC concentration (mM) vs. SUVA (L/mg*m) for all sites June 2017-October 2017.
 Correlation coefficient -0.19. Green represent low percent impervious cover (0.49-5.33%).
 Blue represent intermediate percent impervious cover (13.7-23.0%). Orange represent high
 percent impervious cover (25.5-55.8%)..... 106

Figure 63: Alkalinity (meq/L) vs. SUVA (L/mg*m) for all sites June 2017-October 2017.
 Correlation coefficient -0.15. Green represent low percent impervious cover (0.49-5.33%).
 Blue represent intermediate percent impervious cover (13.7-23.0%). Orange represent high
 percent impervious cover (25.5-55.8%)..... 107

1. Introduction

1.1 The Freshwater Carbon Cycle

Carbon is exchanged among reservoirs within the biosphere, hydrosphere, atmosphere, geosphere and the pedosphere. Freshwater systems, including lakes, soil waters, shallow groundwater, and streams are important components to the global carbon cycle. Streams and rivers provide the lateral transport of carbon from the terrestrial environment to the oceans. Miller et al. (2016) estimated that 1.4 to 2.9 petagrams (10^{15} grams) of carbon per year derived from land enters freshwaters and is processed and released back to the atmosphere, deposited into terrestrial deposits (e.g. lake sediments) or is delivered to the ocean. Most channel miles of large river systems are in small/headwater streams and their structure and function are directly linked to watershed inputs (Parr et al. 2015). These headwater streams are primary sources of particulate organic matter (Kaushal & Bent 2012) and they store and transform more carbon per unit area than larger streams (Hotchkiss et al. 2015). Additionally, headwater streams degas more carbon dioxide to the atmosphere than larger streams (Marx et al. 2017). Globally, it is estimated that streams and rivers export up to 0.5 petagrams per year of organic carbon (Cole et al. 2007). Additionally, inorganic carbon is transported from freshwaters to oceans at a rate of 0.3 petagrams per year (Cole et al. 2007; Kaushal et al. 2013). In freshwaters, inorganic carbon can occur as bicarbonate alkalinity, among other forms. Weathering of silicates and carbonates and consumption of acidity by biogeochemical processes such as iron reduction are natural sources of bicarbonate alkalinity (Kaushal et al. 2013). Figure 1 illustrates the global carbon cycle and that rivers export 0.4 petagrams of DOC and DIC to the ocean per year (Schlesinger and Bernhardt 2013).

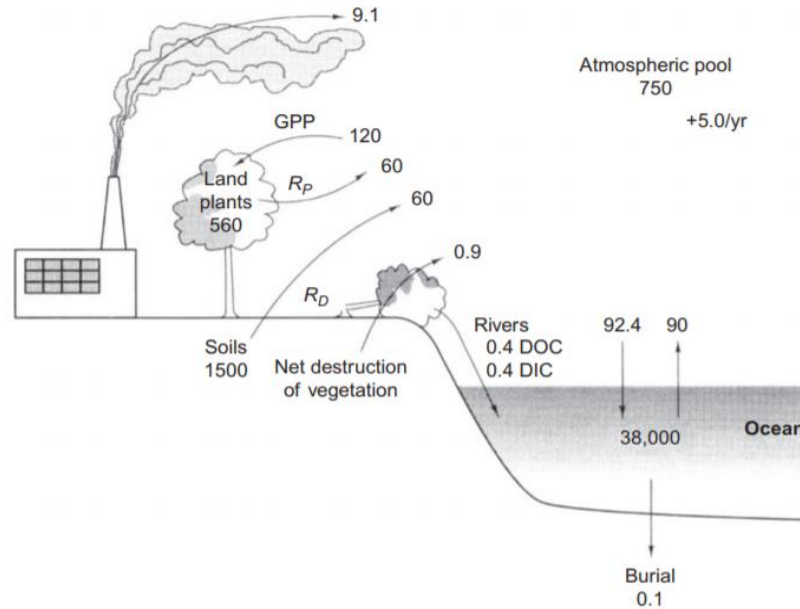


Figure 1: Global carbon cycle. Pools are expressed in 10^{15} grams of C and fluxes are expressed in 10^{15} grams C/ year (Schlesinger and Bernhardt 2013)

1.2 The Urban Carbon Cycle

Urban areas are one of the fastest growing land uses worldwide (Moore et al. 2017). Anthropogenic land uses have major consequences on surrounding streams and rivers. The term “urban stream syndrome” (Meyer et al. 2005) is used to describe how urbanization and increased impervious areas impacts streams. Effects include: increased surface runoff, increased flood discharge, increased sediment loads, increased temperatures, increased nutrient concentrations, decreased channel density, and increased bank incision (Paul & Meyer, 2001). The increase of sediments from urbanization leads to bank erosion which diminishes the interaction between floodplains, groundwater, and surface water. Limited interaction between groundwater and surface water can affect streams’ ability to rebound from disturbances and its overall health (O’Driscoll et al., 2010). Urbanization impacts physical hydrology of freshwaters; it also impacts carbon cycling. Increased temperatures due to climate change can increase the rates at which organic carbon breaks down in river sediments (Smith and Kaushal, 2015). Urbanization increases organic carbon loading due to increased storm runoff (Kaushal et al., 2014). Inorganic carbon, specifically bicarbonate

alkalinity, is increasing in urban watersheds due to liming and weathering of building materials (Smith and Kaushal, 2015). Since pre-industrial times, humans have increased the flux of carbon via rivers by 1 petagram. This increase of carbon in rivers also increases atmospheric CO₂ as some carbon during transport via rivers is exported to the atmosphere (Regnier et al. 2013). Human activities change the physical hydrologic connection between soil water to the ocean via freshwater bodies, which further impacts the global carbon cycle (Regnier et al. 2013).

1.3 Dissolved Organic Carbon

Headwater and low-order streams influence the global carbon cycle, specifically by their transport of organic carbon from continents to ocean. Dissolved organic carbon (DOC) and particulate organic carbon (POC) comprise total organic carbon. POC falls into streams as leaves, twigs, branches, trunks of vegetation and it is decomposed and dissolved downstream (DOC) (Schlesinger & Bernhardt, 2013). Headwater streams are tightly linked to their terrestrial environment, and their organic carbon is mostly dissolved organic carbon (Singh et al., 2016). Dissolved organic carbon supplies energy and food resources to aquatic microorganisms. Organic carbon “influences light and temperature regimes. [It] affects [the] transport and bioavailability of heavy metals and controls pH in low-alkalinity water (Stanley et al. 2011).” Concentrations of dissolved organic carbon are useful when determining the levels of DOC between watersheds, but it does not fully describe the routing of DOC through aquatic systems due to the many sources and consumption pathways of DOC. Dissolved organic carbon concentrations can often overlap between land uses, which further makes it difficult to use alone when assessing land use effects.

1.3.1 Specific UV Absorbance

An adjustment to DOC concentration, which does address the reactive attributes of carbon, is specific ultraviolet absorbance (SUVA). SUVA is equal to the UV absorbance at 254 nanometers divided by the DOC concentration (Weishaar et al., 2003). Therefore, SUVA is the UV absorbance per unit of DOC.

$$\text{SUVA (L/ mg*m)} = \text{UV DOC at 254 nanometers (m}^{-1}\text{)} \div \text{DOC concentration (mg/L)} \quad (1)$$

SUVA estimates the relative prevalence of the humic fraction of dissolved organic carbon and therefore approximates the reactivity of the humic substances. Weishaar et al. (2003) stated that SUVA and aromatic carbon content are strongly correlated “because it provides an integrated estimate of aromatic content across functional classes.” High SUVA values indicate that the carbon in the freshwater is more aromatic and that the dissolved organic carbon is sourced from terrestrial inputs. Aromatic carbon is more stable because the hexagonal bonding is harder to degrade than a single bond. Allochthonous inputs, i.e. terrestrial, from plants and soil dominate the organic matter in most forested and/or first or second order streams which are characterized by high SUVA values (Aitkenhead- Peterson et al., 2009). Lower SUVA values indicate that the carbon is less aromatic and the dissolved organic carbon is sourced from within the stream (autochthonous). Autochthonous inputs are derived from *in situ* primary production of aquatic organisms, i.e. algae. *In situ* primary production often occurs in streams without links to their terrestrial environment. Urban streams are frequently disconnected to vegetation/soil and thus have larger DOC contributions from autochthonous inputs (i.e. algae). Algae produce more labile organic inputs, and urban streams are expected to have an autochthonous source of DOC represented by low SUVA values (Imberger et al., 2014). Smith and Kaushal (2015) stated that nutrient loading and tree canopy removal in urban landscapes can increase autochthonous DOC sources due to algal growth. In agricultural land uses, organic carbon can shift from allochthonous inputs to autochthonous inputs due to the removal of tree canopy and high nutrients (Hagen et al. 2010). However, high SUVA values (allochthonous) can be found in agricultural streams due to high sediment loads which decreases light availability and thus limits algal growth (Hagen et al. 2010).

1.4 Dissolved Inorganic Carbon and Alkalinity

1.4.1 Terrestrial sourced DIC

Dissolved inorganic carbon (DIC) is the sum of inorganic carbon species including carbonic acid, bicarbonate ion, and carbonate.

$$\text{DIC (mmol/L)} = [\text{H}_2\text{CO}_3] + [\text{HCO}_3^-] + [\text{CO}_3^{2-}] \quad (2)$$

DIC is produced via rock weathering and soil microbial respiration (CO_2) (Finlay, 2003). Terrestrial inputs of carbon (DIC) are important for freshwaters because those waters rely on terrestrial carbon to sustain its ecosystem. Globally, DIC provides a carbon flux of 0.3 petagrams from rivers to the ocean (Helie, et al., 2002). At acidic pH, H_2CO_3 is the major component of DIC. Therefore, DIC concentration (mmol/L) often exceeds alkalinity (meq/L) in slightly acidic to neutral pH. The dominant DIC species depends on pH. Figure 2 illustrates that DIC is dominated by bicarbonate ions at near-neutral pH with minor contributions from H_2CO_3 .

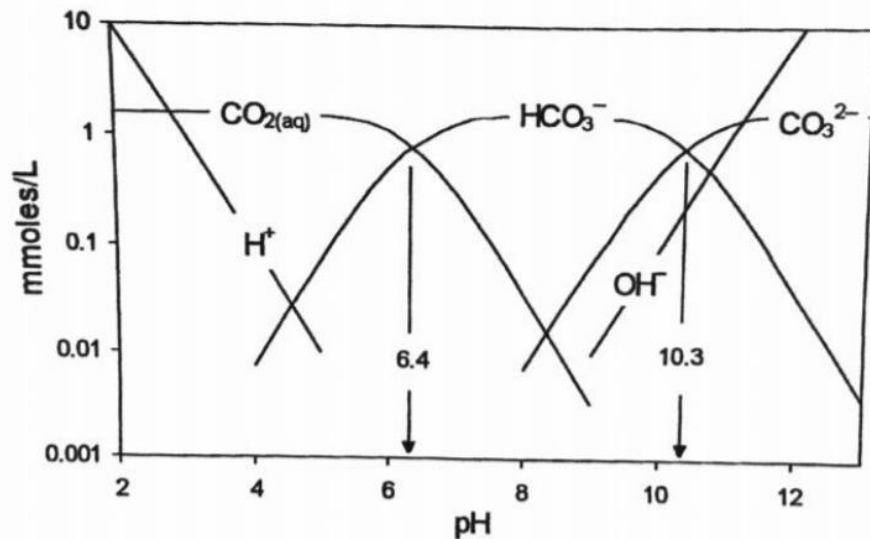


Figure 2: DIC species change with pH. Note that DIC and alkalinity are dominated by the bicarbonate ion at the pH range of this study (Clark & Fritz, 1997).

Stream waters represent a mixture of DIC sources from precipitation, water-rock interaction, and biological processes. Terrestrial sourced DIC can form in an open system or a closed system. In an open system, water is exposed to soil gas (CO_2) at a constant partial pressure

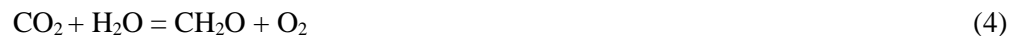
($p\text{CO}_2$). This constant exposure to CO_2 occurs in rainwater, surface water, shallow groundwater, and soil water. In rainwater, $p\text{CO}_2$ is $10^{-3.5}$ atm but in soil water, $p\text{CO}_2$ is one to two orders of magnitude greater than $10^{-3.5}$ atm due to microbial respiration. Therefore, shallow groundwater near the water table is expected to have higher $p\text{CO}_2$ than rain. Higher $p\text{CO}_2$ leads to higher dissolved carbonic acid and thus a slightly acidic pH. In a closed system the water is no longer in contact with the unsaturated zone, this occurs below the water table and in deeper groundwater. In a closed system, water can come in contact with carbonate minerals and calcite dissolution can occur, which releases additional DIC, alkalinity, consumes protons, increasing pH. Thus, open system pH is generally lower than closed system pH.

1.4.2 Instream sourced DIC

In addition to terrestrial inputs of DIC, instream processes produce DIC. Atmospheric exchange of CO_2 with freshwaters' surfaces produces a portion of DIC (carbonic acid). Dissolved inorganic carbon can also be formed from dissolved organic carbon through instream respiration. Algae and microorganisms undergo cellular respiration, which oxidizes DOC to DIC:



Additionally, DIC can be converted into DOC through photosynthesis.



1.4.3 Alkalinity

A major component of dissolved inorganic carbon is alkalinity. Alkalinity is defined as water's ability to neutralize acid. In most freshwaters, total alkalinity is carbonate alkalinity (Clark and Fritz, 1997):

$$\text{Carbonate Alkalinity (meq/L)} = [\text{HCO}_3^-] + 2[\text{CO}_3^{2-}] \quad (5)$$

1.4.4 Urban effects on DIC and alkalinity

Human land uses can influence the source of DIC and alkalinity and their concentrations in streams. Kaushal et al. (2017) found that DIC concentrations increased with increasing percent impervious cover. Moore et al. (2017) found that DIC concentrations increased ten times from

forested to urban watersheds. Compared to forest watersheds, agricultural and urban watersheds export significantly more DIC (Barnes and Raymond, 2009). Increased DIC concentrations in urban areas can be sourced from chemical weathering of carbonate structures, road salts, sewage, and decreased vegetation (Kaushal et al., 2017). Figure 3, from Barnes and Raymond (2009), shows how DIC yields differed between forested, agricultural, and urban watersheds.

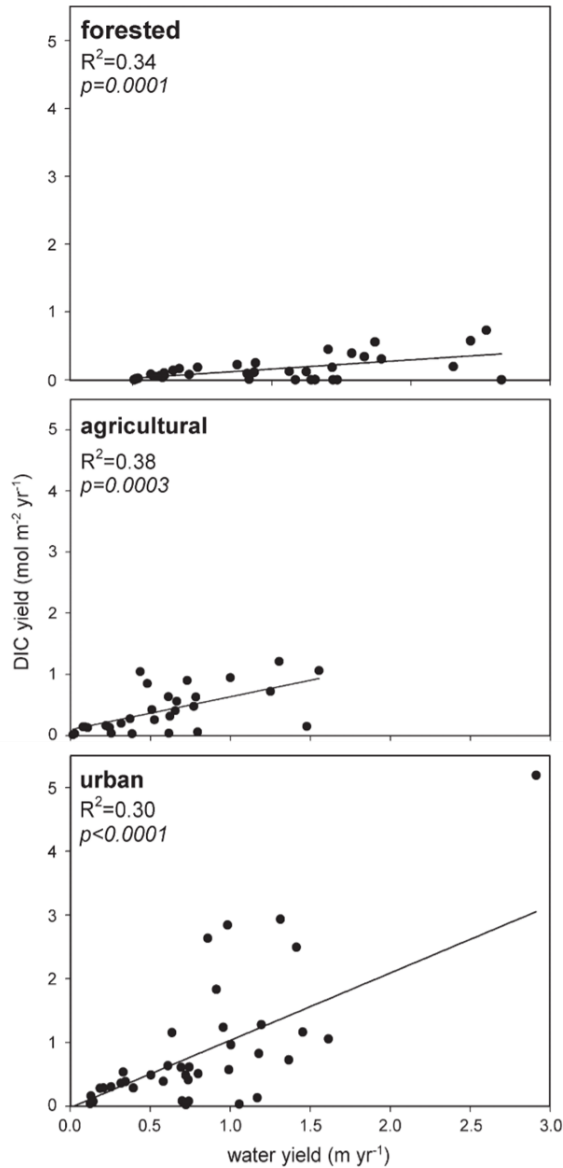
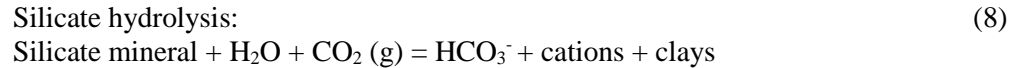


Figure 3: DIC yield (mol/m²*yr) for watersheds with different land uses (Barnes and Raymond, 2009)

Naturally, alkalinity occurs as bicarbonate from carbonate weathering, calcite dissolution, silicate hydrolysis, and soil respiration (Clark and Fritz, 1997; Kaushal et al., 2017).



Urban land use increases weathering rates which increases alkalinity in streams and rivers (concrete weathering). Additionally, liming of soils and crops in agriculture can alter alkalinity in freshwaters. Barnes and Raymond (2009) reported that agriculture watersheds exported four times more DIC (specifically bicarbonate/ HCO_3^-) than undeveloped watersheds. Raymond and Cole (2003) found that the increase of alkalinity in the Mississippi River over the last few decades was mainly due to increased chemical weathering rates from increased rainfall and temperature. Tippler et al. (2014), found that bicarbonate was 18 times greater in urban streams due to the presence of concrete.

1.4.5 $\delta^{13}\text{C}$ - DIC

Beyond DIC concentration, $\delta^{13}\text{C}$ of DIC is widely used to fingerprint the evolution of natural waters buffered by the carbonate system. $\delta^{13}\text{C}$ is a way of expressing the carbon-13 to carbon-12 ratio relative to internationally-accepted reference material. $\delta^{13}\text{C}$ can be used as a tracer because there are expected differences between the $\delta^{13}\text{C}$ values of soil waters and the $\delta^{13}\text{C}$ values of groundwaters. Soil waters obtain their DIC from soil CO_2 and this shifts the $\delta^{13}\text{C}$ to be more negative. Due to their lower pH and alkalinity, soil water and shallow groundwaters have more negative $\delta^{13}\text{C}$ -DIC values because $\delta^{13}\text{C}$ -DIC is dominated by CO_2 from microbial respiration. $\delta^{13}\text{C}$ -DIC evolves to more moderate values as waters reach neutral pH with higher alkalinity due to mineral sources and exchange with the atmosphere. If carbonate minerals are present, groundwaters evolve towards more positive $\delta^{13}\text{C}$ values along flowpaths due to carbonate

dissolution (Doctor et al., 2008). $\delta^{13}\text{C}$ values are reported relative to the Vienna Pee Dee Belemite (VPDB), which is a marine carbonate whose $\delta^{13}\text{C}$ is defined to be 0 ‰. Measured $\delta^{13}\text{C}$ values of freshwaters are expected to be negative (Clark and Fritz, 1997). $\delta^{13}\text{C}$ -DIC is used as a marker of where the water lies along a geochemical evolution path.

$\delta^{13}\text{C}$ -DIC values are an informative measure of what processes drive DIC yields to further demonstrate differences in land use types. Barnes and Raymond (2009) found that urban watersheds produced 7.8 times more DIC per unit water yield compared to forest watersheds. Additionally, the average $\delta^{13}\text{C}$ -DIC of forested watersheds was more enriched (less negative) than the average $\delta^{13}\text{C}$ -DIC of urban watersheds. This enrichment in $\delta^{13}\text{C}$ -DIC in forested watersheds is likely due to CO_2 loss to the atmosphere during transport from soil to streams and photosynthesis (Barnes & Raymond, 2009, Campeau et al., 2018). Urban streams tend to have more negative $\delta^{13}\text{C}$ -DIC than forested streams due to disturbances to the land, such as construction, and increased carbonate weathering rates. Urban land uses, lawns and green spaces, typically produce more CO_2 and thus a more negative $\delta^{13}\text{C}$ -DIC signature. Lastly, septic and sewer systems increase the amount of carbon transport into streams which increases CO_2 and bicarbonate export (Barnes & Raymond, 2009).

1.5 Study Locations and Sample Groups

Mecklenburg County, North Carolina, has an extensive headwater and low-order urban stream network. Charlotte, Mecklenburg County, was developed on a network of headwaters and this study provides an interesting look on urban headwater streams. In this study, six watersheds were selected based on their land use characteristics, ranging from forested to urban: Reedy Creek, Toby Creek, Little Sugar Creek, Little Hope Creek, Briar Creek, Briar Creek Tributary, Edward's Branch, and Beaverdam Creek (Figure 4). Reedy Creek and Toby Creek watersheds were divided into subwatersheds since there were different land uses dominating throughout their larger watershed.

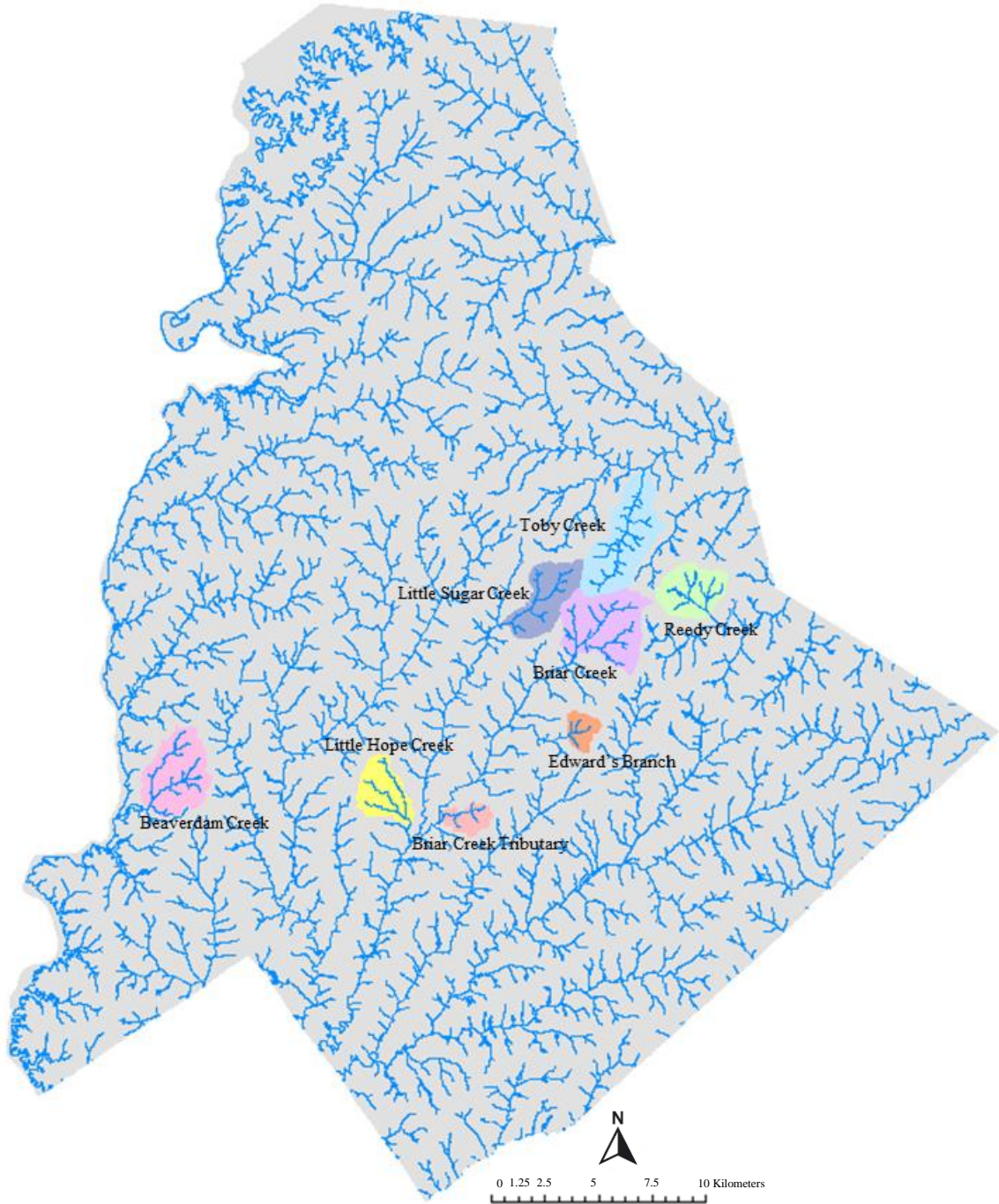


Figure 4: ArcGIS map of the six study watersheds in Mecklenburg County, NC

1.5.1 Reedy Creek Watershed (RC group)

The headwaters of Reedy Creek watershed have an area of 6.5 square kilometers upstream of the Plaza Road Extension bridge (USGS gauging station 212427947). Reedy Creek is a second-order stream that flows into Rocky River, which flows into the Pee Dee River. The creek flows across a flat, floodplain-like surface that overlies crystalline bedrock and saprolite. Saprolite is chemically weathered residual in-place bedrock that maintains the fabric of the original bedrock while significant silicate hydrolysis reactions have taken place, replacing rock-forming silicates with clays. In many places, these outcrops of bedrock and saprolite constrain the channel. Elsewhere, especially on lower Reedy Creek, a meandering to braided sand and gravel bed is present.

Historically, the Reedy Creek watershed was dominated by agriculture as was the case through much of the North Carolina and South Carolina Piedmont region. Over time, the dredging and straightening of the stream caused its degradation. The creek has been severely incised and eroded, and it has flashy discharge with an overload of sediment. Due to its degraded nature, the City of Charlotte is in the process of a major stream restoration project. The goal of the stream restoration is to improve the creek's hydrology, water quality, macroinvertebrate communities, ecological functions, organic matter supply, and sediment load.

In this study, the watershed is divided into five subwatersheds (Figure 5). Subwatersheds were determined based on land use: R is the main stem of the creek (Reedy), A is dominated by agriculture, D represents residential development, P represents the presence of a pond and low-density development, and C is the control or undeveloped subwatershed (McMillan and Clinton, 2013). The agriculture, developed, and control land uses have subwatersheds and sampling points nested within the larger watershed (Figure 5). Additionally, each watershed land use has two shallow monitoring wells. The agriculture watershed has four surface water sampling points: A1, A2, A3, and A4 along with two wells: A1 Riparian and A1 Upland. The main stem has two surface water sampling points: R1 and R2 and two wells: R2 Riparian and R2 Upland. The developed

watershed has surface water sampling points at D1 and D2 and two groundwater wells: D1 Riparian and D1 Upland. The pond influence watershed has one surface water sampling point at P1 and two wells: P1 Riparian and P1 Upland. The control watershed has two surface water sampling points at C1 and C2 and two wells: C1 Riparian and C1 Upland. Each of the surface water sampling points are located upstream of a confluence (Figure 5).

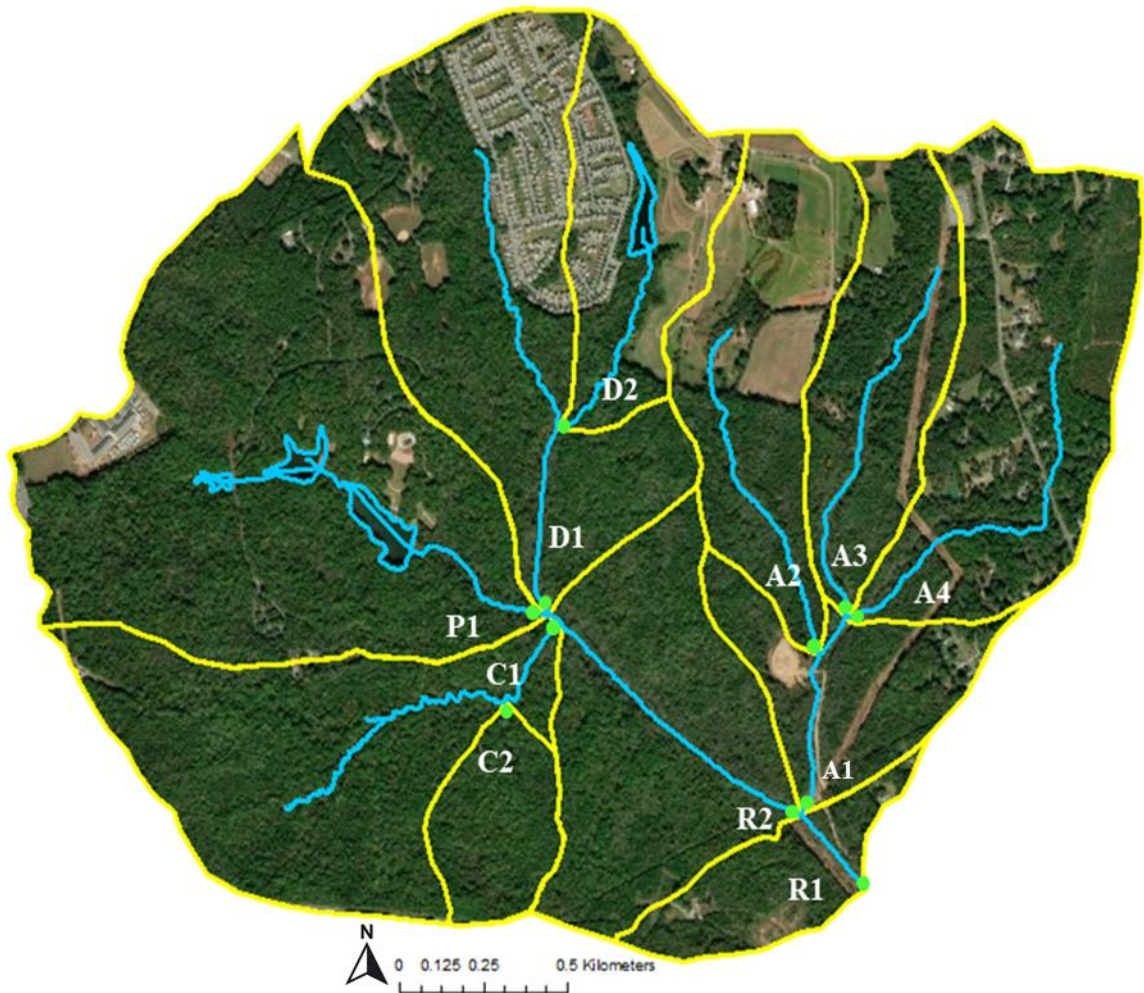


Figure 5: ArcGIS map of Reedy Creek (RC group) Watersheds and the study watersheds (11 total). Yellow outlines the watershed boundary and green dots represent the subwatershed outlet.

1.5.2 Toby Creek (TC group)

Toby Creek is a multiple land use urban watershed in Charlotte, North Carolina with an area of 11.9 square kilometers. The lower reach of Toby Creek flows through the University of North Carolina at Charlotte campus. Eleven subwatersheds were selected based on inferred land uses (Table 1 and Figure 6).

Table 1: Subwatershed land uses of Toby Creek (TC group)

Subwatershed	Land use
T1	Entire Toby Creek watershed
T2	Watershed above UNCC campus
T3	Upper watershed at Rocky River Road
TD 1	Watershed at Town Center Plaza (commercial and residential)
TD 2	Watershed at Newell Community Park
UD 1	Development on UNCC campus
UD 2	Development on UNCC campus
UD 3	Development on UNCC campus
UP 1	Pond influence on UNCC campus
UU 1	Semi-undeveloped on UNCC campus
UU 2	Semi-undeveloped on UNCC campus

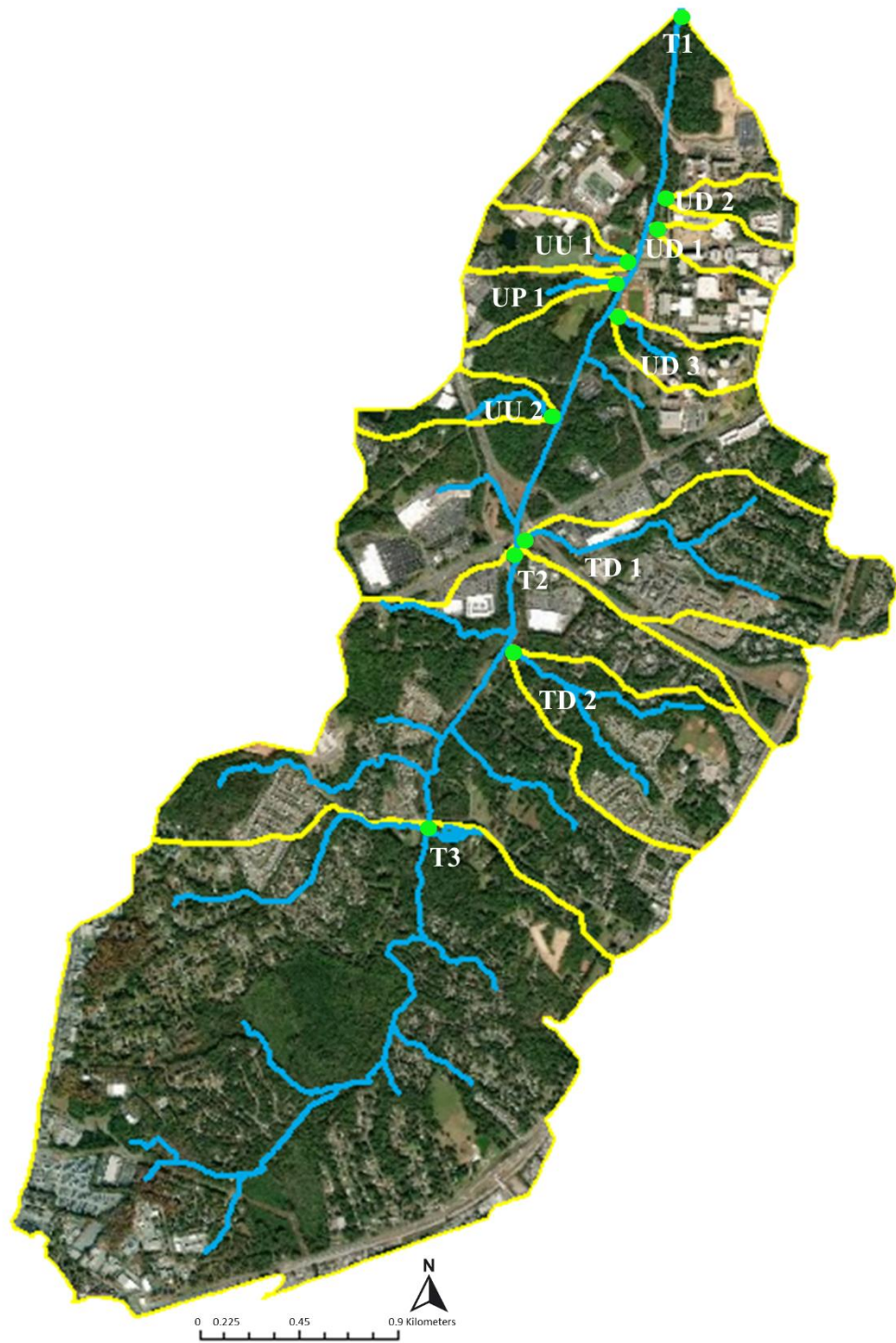


Figure 6: ArcGIS map of Toby Creek (TC group), Mecklenburg County, NC. 11 total subwatersheds

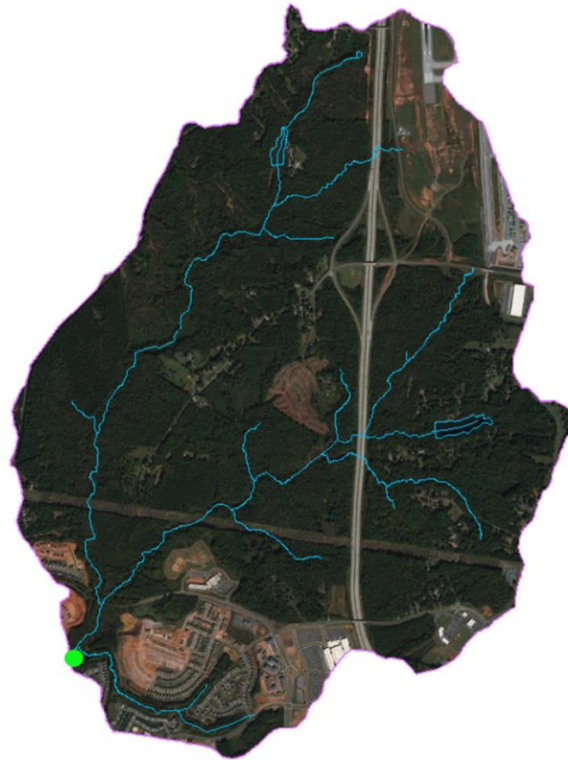
1.5.3 Additional urban watersheds in Mecklenburg County, NC (MC group)

In addition to Reedy Creek and Toby Creek, this study incorporates six urban streams in the Charlotte metropolitan area: Beaverdam Creek, Little Sugar Creek, Little Hope Creek, Edwards Branch, Briar Creek, and Briar Creek tributary (Figure 7a-f). These six streams were included in this study because of their urban attributes and their USGS gauging stations. It is noted that the sampling point of Little Sugar Creek is located upstream of a wastewater treatment plant. Table 2 lists the watershed with its corresponding USGS ID and drainage area.

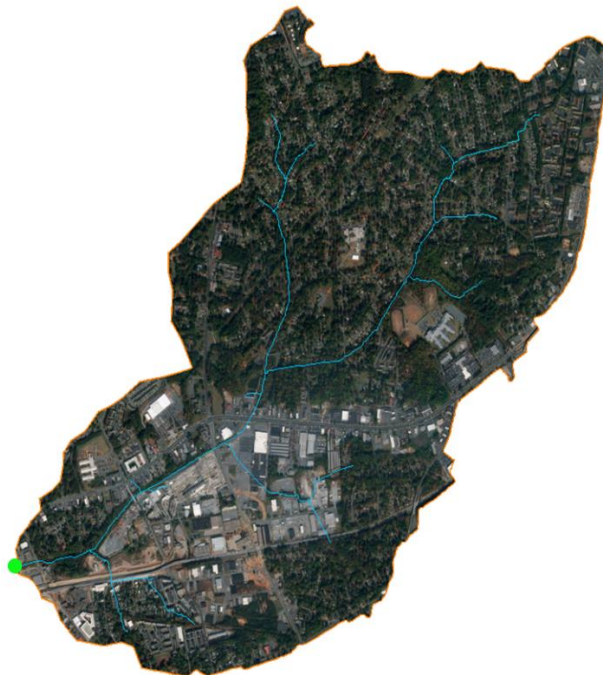
Table 2: USGS ID and drainage area (km²) of MC group (USGS data)

Site	USGS ID	Drainage area (km ²)
Beaverdam Creek (Bvr)	214297160	9.62
Little Sugar Creek (LSC)	214640410	8.86
Little Hope Creek (LHC)	2146470	6.81
Edward's Branch (EB)	214643820	2.51
Briar Creek (BC)	214642825	13.4
Briar Creek tributary (BCT)	21464080	3.08

Figure 7a-f: Aerial imagery of the MC group watersheds (ArcGIS World Imagery basemap)
Green dots indicate represent watershed outlet and sampling point.



a. Beaverdam Creek



b. Little Sugar Creek



c. Little Hope Creek



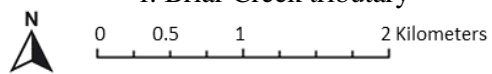
d. Edward's



e. Briar Creek



f. Briar Creek tributary



Percent forest, cropland, urban development, and impervious were calculated using StreamStats. Percent canopy-free impervious area was calculated by Minrui Zheng from the Center for Applied GIS at UNC Charlotte (CAGIS) (Table 3).

Table 3: Watershed area (km²), percent forest, crop land, urban development, impervious area, and canopy-free impervious area of each watershed.

Group	Watershed	Watershed area (km ²)	% forest	% crop land	% urban development	% impervious area	% canopy-free impervious area
RC	C1	0.9	94	0.6	3.7	0.5	1.6
RC	C2	0.3	90.9	0	8.9	1.1	
RC	A1	2	60.3	14.1	22.9	2.1	1.1
RC	A2	0.5	55.2	40.3	2.8	0.6	0.5
RC	A3	0.6	46.5	13.5	33.5	3.4	1.4
RC	A4	0.7	63	1.1	35.2	2.7	1.3
RC	D1	1.5	40	14.3	42.8	14.1	5
RC	D2	0.5	16	32.6	49.7	13.7	2.3
RC	P1	1.3	83.4	3.9	3.2	1.5	1.2
RC	R2	4.3	73.4	6.2	16.3	5.3	0.2
RC	Reedy Creek (R1)	6.2	68.7	8.9	18.8	4.2	1.7
MC	Beaverdam Creek	9.6	60.1	3.6	26.5	4.6	2.3
MC	Briar Creek	11.3	3.6	0	95.7	25.5	8.4
MC	Briar Tributary	2.4	2	0	98	14.6	6.3
MC	Edward's Branch	1.9	7.3	0.7	92	31.8	10.1
MC	Little Hope Creek	5.5	0	0	100	33.3	9.8
MC	Little Sugar	7.2	1.6	0	98.4	37.5	11
TC	T1	11.9	13.9	0.9	82.4	23	7.9
TC	T2	7.4	15.4	0.6	81.9	18.3	7.2
TC	T3	4.7	12.7	0.7	86	17.9	6.2
TC	TD 1	0.8	0.5	0	99.1	32.1	9.5
TC	TD 2	0.6	8.5	0	90.4	21.8	7.4
TC	UD 1	0.1	7.7	0	92.3	55.8	19.8
TC	UD 2	0.1	6.1	0	93.3	51.3	17.2
TC	UD 3	0.2	4.2	0	95.7	37.7	11
TC	UP 1	0.2	16	0.2	83.8	35.8	11
TC	UU 1	0.2	14.3	4.7	78.5	22.7	13.5
TC	UU 2	0.2	17.6	0.6	81.5	34.8	11.5

1.6 Objectives

The main objective of this study is to examine alterations to freshwater carbon processes among watersheds of various land uses in multiple streams in Mecklenburg County, Charlotte, North Carolina using a baseflow stream sampling approach.

2. Hypotheses

It is hypothesized that watersheds in Charlotte with anthropogenic land uses will have lower SUVA values and undeveloped forested watersheds will have higher SUVA values. The urban component of this effect can be represented by percent impervious cover (Figure 8). No specific hypothesis is made about DOC concentrations or fluxes across land uses as these have been shown to overlap in the literature.

It is hypothesized that watersheds with anthropogenic land uses will have higher DIC and alkalinity concentrations and fluxes than undeveloped forested watersheds (Figure 8).

It is hypothesized that undeveloped forested watersheds will have different $\delta^{13}\text{C}$ -DIC values than anthropogenic watersheds. However, the direction of any possible trend is not predicted because $\delta^{13}\text{C}$ -DIC can respond to multiple factors including groundwater inputs and instream processing of DOC and the lack of prior data in the literature.

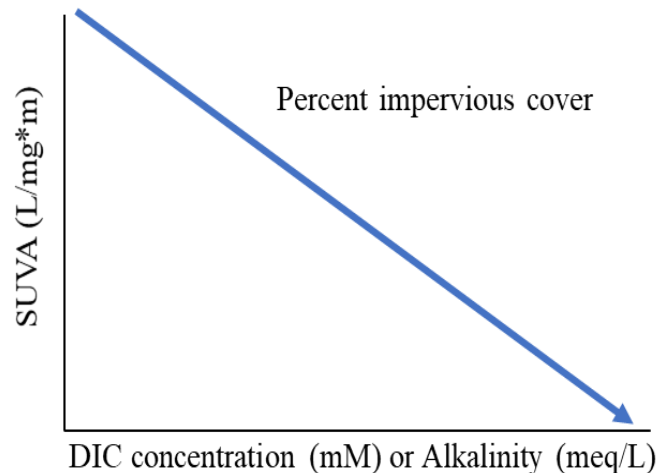


Figure 8: Hypothesized trends between SUVA, DIC concentration, and alkalinity with increasing impervious cover

3. Methods

3.1 Field methods

Surface water samples were collected at the Reedy Creek watershed (sites A1, R2, C1, C2, and D1) weekly from June 2016-October 2017 during baseflow conditions. All eleven surface water sites at the Reedy Creek watershed were sampled monthly. Beaverdam Creek, Briar Creek, Briar Tributary, Edwards Branch, Little Hope Creek, and Little Sugar Creek were sampled four times from June 2017 to September 2017 (6/29/2017, 8/04/2017, 8/30/2017, 9/26/2017). Each surface water point at Toby Creek was sampled four times from June 2017 to October 2017 (6/28/2017/6/30/2017, 7/27/2017, 9/05/2017-9/06/2017, 9/27/2017-10/02/2017). UD2 and UU 2 (TC group) only have a total of three surface water sampling dates because they were not flowing on 10/02/2017.

Surface water samples were collected by filling acid washed- 1 liter polyethylene bottles while facing upstream, shaking and emptying downstream, then filling completely and capping tightly to minimize head space. These bottles were transported to the laboratory for analysis. In addition to water sample collection, pH, temperature, dissolved oxygen, and specific conductivity were measured at each sampling location using a YSI multiparameter probe.

Additionally, discharge measurements were taken at the Reedy Creek and Toby Creek subwatersheds at select sampling events between August and October 2017. All stream discharge measurements were taken during baseflow. Discharge was measured manually at RC group and TC group. MC group and the Reedy outlet have USGS gauging sites, which automatically measures stream stage which is converted to discharge. At each sampling site, a location was chosen where the creek was flowing and not stagnant. The wetted width was measured in addition to the bank width (in centimeters). Based on the wetted width, the cross section was divided into 5 to 10 subsections, of approximately 10 centimeters. At each subsection, depth of the water was measured (in centimeters). At forty percent of each depth, flow was measured using a Swiffer 2100 Current Velocity Meter. Flow was measured in m/s. The measurements taken in the field

were recorded and brought back to the lab. The following equations were used to calculate discharge in liters/second:

$$\text{Flow cross sectional area (cm}^2\text{)} = \text{width (cm)} \times \text{flow depth (cm)} \quad (9)$$

$$\text{Area (m}^2\text{)} \times \text{flow rate (m/s)} = \text{Discharge (m}^3\text{/s)}$$

3.2 Laboratory methods

Water samples were analyzed for DOC and DIC concentrations, $\delta^{13}\text{C}$ -DIC values, SUVA, major anion concentrations (fluoride, chloride, nitrate, and sulfate), major cation concentrations (sodium, potassium, magnesium, and calcium), and alkalinity. Samples were brought back to the UNC Charlotte hydrology and biogeochemistry laboratory and were vacuum filtered immediately upon return. DOC and SUVA samples were filtered using 0.45 μm glass fiber (GFF) filters. DIC, $\delta^{13}\text{C}$ -DIC, alkalinity, anions, and cation samples were filtered using 0.2-micron polyethersulfone filters. Anion and cation samples were filtered into 50 mL polypropylene centrifuge tubes and were refrigerated until analysis. Additionally, high-purity nitric acid at a final concentration of 0.5% was added to the cation samples to preserve the samples. DIC/ $\delta^{13}\text{C}$ -DIC and alkalinity samples were filtered into 20 mL crimp top vials and were stored in the refrigerator.

To measure DOC concentration, a Shimadzu TOC carbon analyzer was used. The standard TOC-TN Analyzer Operational Procedure was followed. Two known standards, 10 mg/L and 20 mg/L of DOC were used throughout the analyses to calibrate. A UV Spectrophotometer was used to analyze SUVA. UV absorbance was obtained using the spectrophotometer at 254 nanometers and recording the value (Weisher et al., 2003). DOC concentration (mg/L) was divided by UV absorbance and multiplied by 100 to obtain SUVA (L/mg*m). DIC concentrations and $\delta^{13}\text{C}$ -DIC values were measured using a Picarro cavity ring-down spectrometer. Cations and anions were measured by ion chromatography using a Dionex DX-500 IC system with AS14A and AG14 analytical columns. Alkalinity titrations followed the Gran titration method.

Impervious cover was calculated through ArcGIS and USGS StreamStats. Watersheds were delineated on ArcMap using 2012 Mecklenburg County LiDAR data (provided from maps.co.mecklenburg.nc.us). Once delineated, watershed areas were calculated using ArcMap. Percent forest, crop land, and urban development were provided from USGS StreamStats 4. USGS StreamStats used area-weighted mean (ArcGIS) to calculate percent forest, crop land, and urban development. Table 4 describes which datasets were used in StreamStats:

Table 4: StreamStats datasets and associated land use description

StreamStats datasets	Description
LC11DEV	Percentage of developed (urban land) from NLCD 2011 classes 21-24
LC11FOREST	Percentage of forest from NLCD 2011 classes 41-43
LC11IMP	Average percentage of impervious area determined from NLCD 2011 impervious dataset
LC11CRPHAY	Percentage of cultivated crops and hay, classes 81 and 82 from NLCD 2011

(streamstats.usgs.gov/ss/ and mrlc.gov.nlcd11_leg.php)

Minrui Zheng (Center for Applied Geographic Information Science at UNCC) used the Mecklenburg County 2012 Tree Canopy/ Landcover dataset and classified seven land covers: 1) tree cover, 2) grass/shrub, 3) bare earth, 4) water, 5) buildings, 6) roads, 7) other paved surfaces. Buildings, roads, and other paved surfaces were used in the percent impervious cover estimation. Impervious cover was an underestimate because tree-covered impervious was counted as tree cover. The calculated impervious cover is canopy-free impervious cover. In this study, impervious area calculated from StreamStats was used in the results.

Additionally, dissolved organic carbon and dissolved inorganic carbon fluxes were calculated. Watershed area was converted from square kilometers to hectares. Discharge was converted to from cubic meters per second to cubic meters per year. DOC and DIC concentrations were converted to kilograms/cubic meter. DOC and DIC in kg/m³ was multiplied by m³/year giving the final number of DOC or DIC in kg/hectare/year.

4. Results

4.1 Stream discharge

Discharge measurements were taken at each site on different dates from August 2017 to October 2017 and yearly baseflow was estimated by converting cubic meters per second to cubic meters per year (Table 5).

Table 5: Area and discharge of each watershed. Green highlight indicates forest/undeveloped land use, orange indicates agriculture land use, purple indicates urban/developed land use, unshaded indicates watershed outlet or mixed uses, blank spaces mean discharge was not measured that day.

Group	Watershed	Watershed area (km ²)	Discharge (m ³ /s) 8/2/17	Discharge (m ³ /s) 8/28/17	Discharge (m ³ /s) 9/20/17	Discharge (m ³ /s) 10/18/17	Estimated yearly baseflow (m ³ /year)
RC	C1	0.88			0.001	0.003	6.2×10 ⁴
RC	C2	0.34	0.001	0.002	0.001	0.001	4.1×10 ⁴
RC	A1	2.02	0.004	0.003	0.003	0.001	7.6×10 ⁴
RC	A2	0.49			0.002	0.002	6.5×10 ⁴
RC	A3	0.60			0.001	0.000	1.2×10 ⁴
RC	A4	0.70			0.000	0.000	4.7×10 ³
RC	D1	1.45	0.017	0.002	0.003	0.001	1.8×10 ⁵
RC	D2	0.47			0.000	0.000	2.0×10 ³
RC	P1	1.27	0.002	0.001	0.001	0.000	3.0×10 ⁴
RC	R1	6.23			0.015	0.002	4.5×10 ⁵
RC	R2	4.30	0.015	0.007	0.014	0.005	3.2×10 ⁵
RC	RC USGS	6.23	0.015	0.016	0.018	0.007	4.5×10 ⁵
Group	Watershed	Watershed area (km ²)	Discharge (m ³ /s) 8/2/2017	Discharge (m ³ /s) 8/28/2017	Discharge (m ³ /s) 9/20/2017	Discharge (m ³ /s) 10/18/2017	Estimated yearly baseflow (m ³ /year)
MC	Bvr	9.60	0.015	0.016	0.018	0.007	4.5×10 ⁵
MC	BC	11.3	0.024	0.017	0.030	0.010	6.3×10 ⁵
MC	BCT	2.35	0.001	0.003	0.003	0.003	7.8×10 ⁴
MC	EB	1.99	0.001	0.001	0.003	0.001	4.0×10 ⁴
MC	LHC	5.46	0.013	0.009	0.010	0.009	3.2×10 ⁵
MC	LSC	7.19	0.096	0.108	0.069	0.071	3.2×10 ⁵
Group	Watershed	Watershed area (km ²)	Discharge (m ³ /s) 9/27/2017				Estimated yearly baseflow (m ³ /year)
TC	T1	11.9	0.127				4.0×10 ⁶

Group	Watershed	Watershed area (km ²)	Discharge (m ³ /s) 9/27/2017	Estimated yearly baseflow (m ³ /year)
TC	T2	7.39	0.080	2.5×10 ⁶
TC	T3	4.74	0.025	7.9×10 ⁵
TC	TD 1	0.84	0.008	2.4×10 ⁵
TC	TD 2	0.63	0.002	6.0×10 ⁴
TC	UD 1	0.11	0.001	3.8×10 ⁴
TC	UD 2	0.12	0.001	4.7×10 ⁴
TC	UD 3	0.15	0.002	5.1×10 ⁴
TC	UP 1	0.14	0.003	6.6×10 ⁴
TC	UU 1	0.17	0.002	5.7×10 ⁴
TC	UU 2	0.15	0.001	1.9×10 ⁴

T1 (TC group) had the largest estimated yearly baseflow of 4.0×10^6 m³/year. D2 (RC group) had the smallest estimated yearly baseflow of 2.0×10^3 m³/year.

4.2 Dissolved organic carbon and SUVA

4.2.1 Inter-site variation

In the RC group, control site (C2) had a mean DOC concentration of 2.83 mg/L. C1 and C2 had DOC concentrations ranging from 1.43 mg/L to 8.33 mg/L. The agriculture sites (A1, A2, A3, A4) had mean DOC concentrations ranging from 2.48 to 4.70 mg/L. Within the agricultural sites, A4 had the lowest DOC concentration of 1.60 mg/L and A3 had the highest DOC concentration of 15.9 mg/L. D1 and D2 had DOC concentrations ranging from 1.07 mg/L to 5.68 mg/L. P1 DOC concentrations ranged from 1.10 mg/L to 17.8 mg/L. The main stem of Reedy (R1 and R2) had DOC concentrations ranging from 1.69 mg/L to 8.56 mg/L (Figure 9, Figure 11).

MC group had mean DOC concentrations ranging from 1.74 mg/L at Edward's to 4.99 mg/L at Beaverdam Creek. DOC concentrations at Beaverdam Creek ranged from 3.73 to 7.30 mg/L. Briar Creek and Briar Creek Tributary DOC concentrations ranged from 2.12 to 4.91 mg/L. Edward's DOC concentrations were 1.19 mg/L to 2.55 mg/L. Little Hope Creek had DOC

concentrations ranging from 1.89 mg/L to 3.07 mg/L. Little Sugar Creek DOC concentrations were 1.81 to 6.60 mg/L (Figure 9, Figure 11).

TC group (Toby Creek) had mean DOC concentrations ranging from 2.43 mg/L at TD 1 to 4.02 mg/L at T3. T1 DOC concentrations ranged from 2.74 mg/L to 3.75 mg/L. T2 DOC concentrations were 2.10 mg/L to 4.34 mg/L. T3 DOC concentrations ranged from 1.57 mg/L to 10.05 mg/L. TD 1 and TD 2 had DOC concentrations ranging from 2.00 to 5.24 mg/L. UD 1, UD 2, and UD 3 had DOC concentrations ranging from 2.42 mg/L at UD 1 to 4.65 mg/L at UD 3. UP 1 DOC concentrations ranged from 3.23 mg/L to 4.43 mg/L. UU 1 had DOC concentrations of 2.32 mg/L to 6.21 mg/L. UU 2 DOC concentrations ranged from 2.00 mg/L to 3.31 mg/L (Figure 9, Figure 11). Overall, there was no systematic trend observed in DOC concentration among sites.

Control sites C1 and C2 (RC group) had SUVA values ranging from 0.29 L/mg*m to 4.92 L/mg*m. Agricultural sites SUVA values ranged from 0.28 L/mg*m at A3 to 18.7 L/mg*m at A2. The developed sites had SUVA values ranging from 2.20 L/mg*m to 11.3 L/mg*m. P1 had SUVA values of 0.25 L/mg*m to 9.59 L/mg*m. The main stem of Reedy had SUVA values of 0.55 L/mg*m to 4.57 L/mg*m (Figure 10, Figure 13).

Beaverdam Creek (MC group) had SUVA values ranging from 2.14 L/mg*m to 4.39 L/mg*m. Briar Creek and Briar Creek Tributary had SUVA values of 2.46 L/mg*m to 4.32 L/mg*m. Edward's had SUVA values ranging from 2.83 L/mg*m to 5.70 L/mg*m. Little Hope Creek had SUVA values of 2.91 L/mg*m to 3.77 L/mg*m. Little Sugar Creek SUVA values ranged from 2.93 L/mg*m to 3.42 L/mg*m (Figure 10, Figure 13).

T1 (TC group) had SUVA values ranging from 2.72 L/mg*m to 3.07 L/mg*m. T2 had SUVA values of 1.50 L/mg*m to 4.44 L/mg*m. T3 SUVA values ranged from 1.31 L/mg*m to 3.65 L/mg*m. TD 1 and TD 2 had SUVA values ranging from 2.16 L/mg*m to 5.34 L/mg*m. UD 1 and UD 2 had SUVA values of 1.35 L/mg*m to 3.08 L/mg*m. UD 3 had SUVA values ranging from 3.68 L/mg*m to 7.40 L/mg*m. UP 1 had SUVA values of 2.16 L/mg*m to 3.35

L/mg*m. UU 1 and UU 2 had SUVA values ranging from 2.29 L/mg*m to 3.93 L/mg*m (Figure 10, Figure 13).

From the results above, it may seem that there are no discernable differences between sites for SUVA, but Figure 14 suggests inter-site differences occur. As percent impervious cover increases, SUVA values generally decrease.

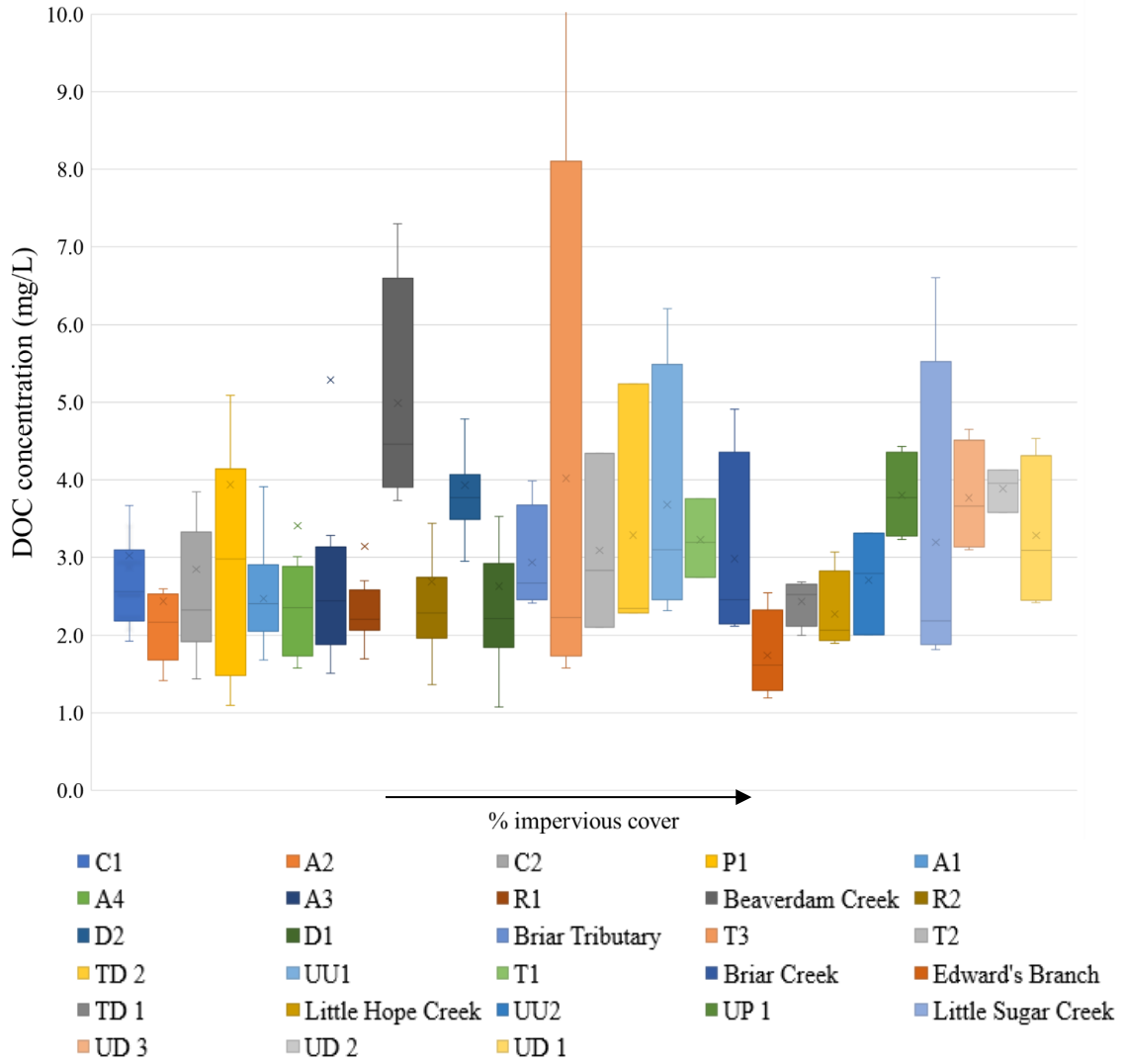


Figure 9: Box plot of DOC concentration vs. increasing percent impervious cover

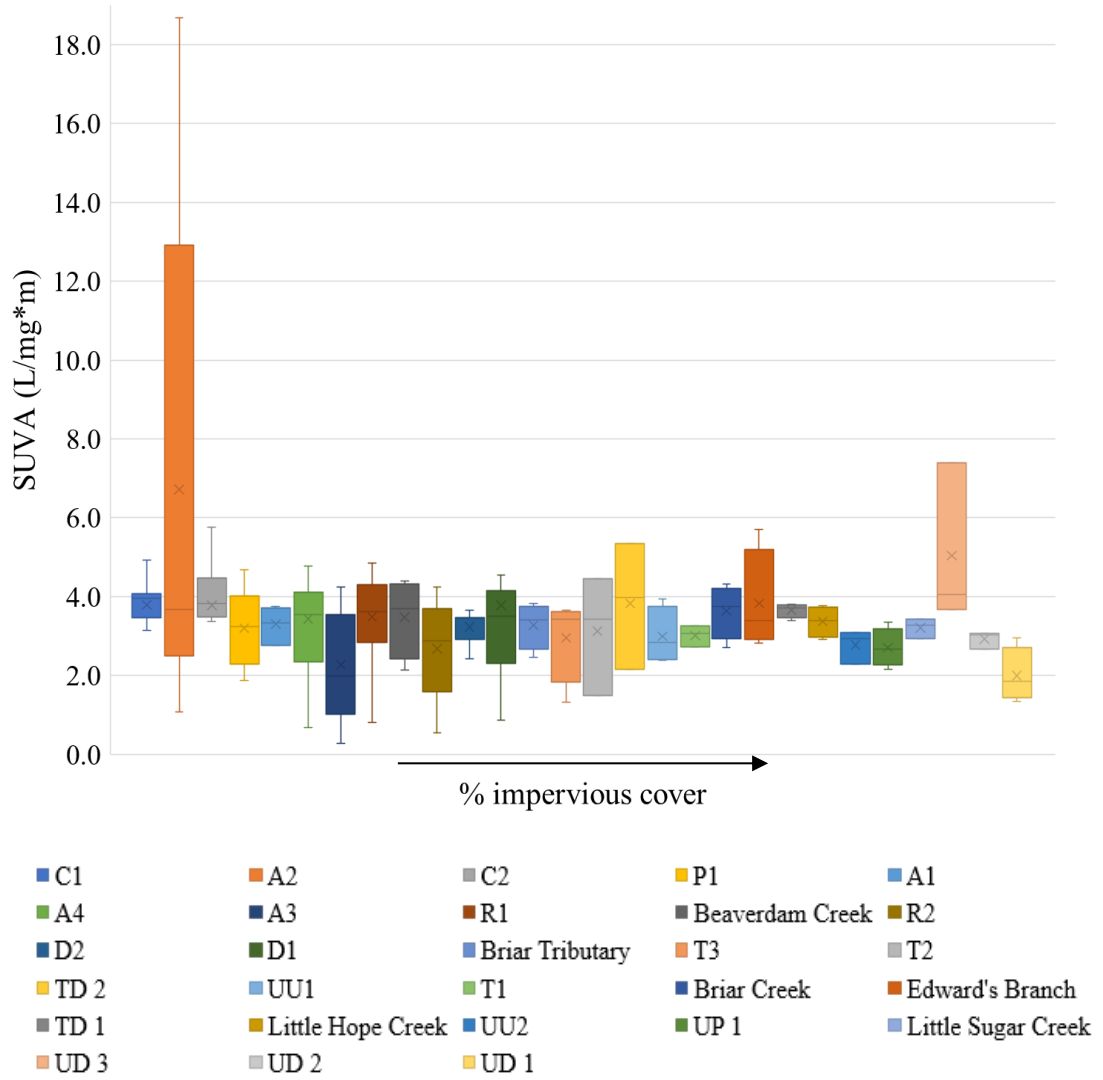


Figure 10: Box plot of SUVA values vs. increasing percent impervious cover

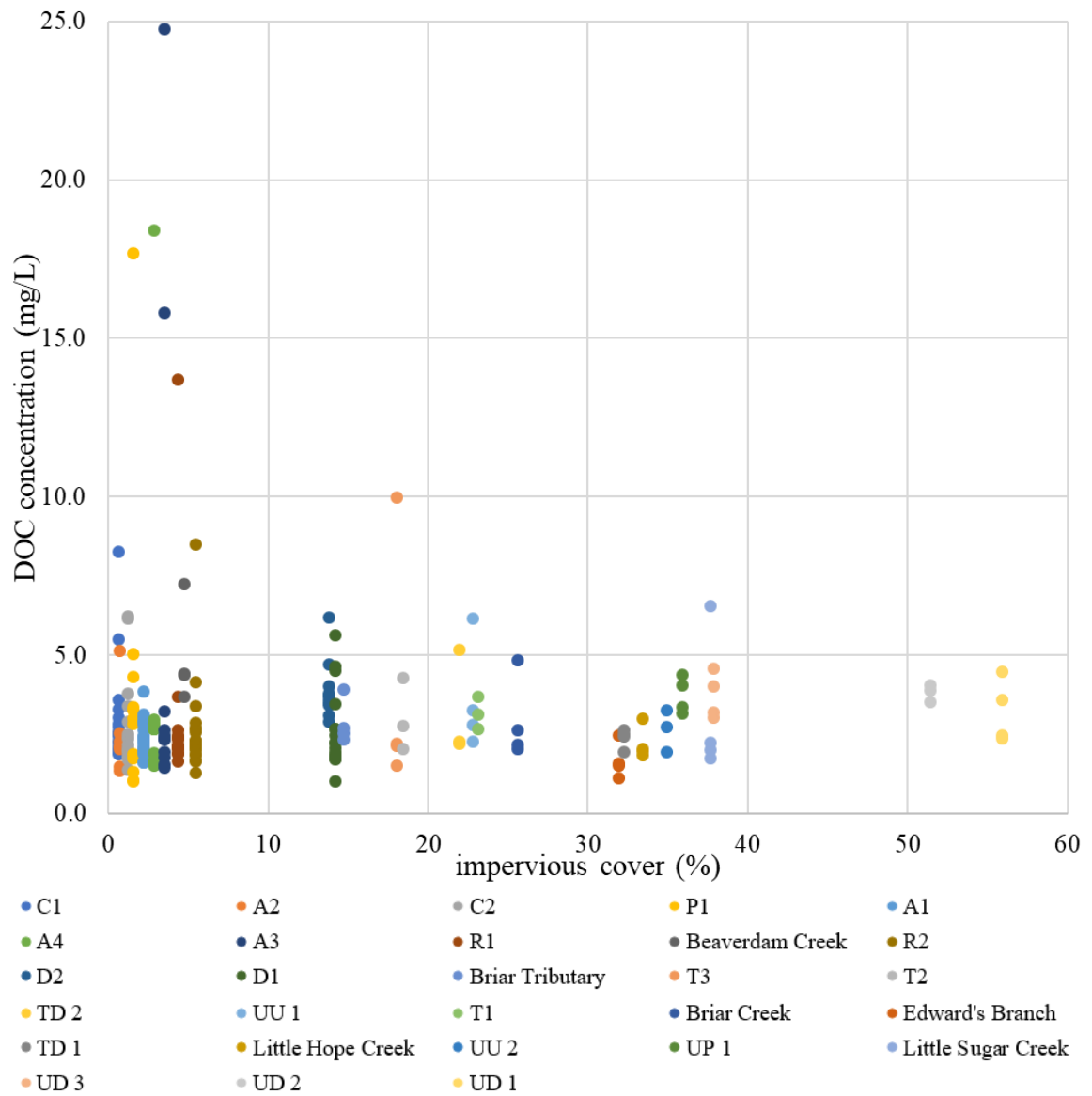


Figure 11: Scatter plot of DOC concentration vs. percent impervious cover (May 2016- October 2017)

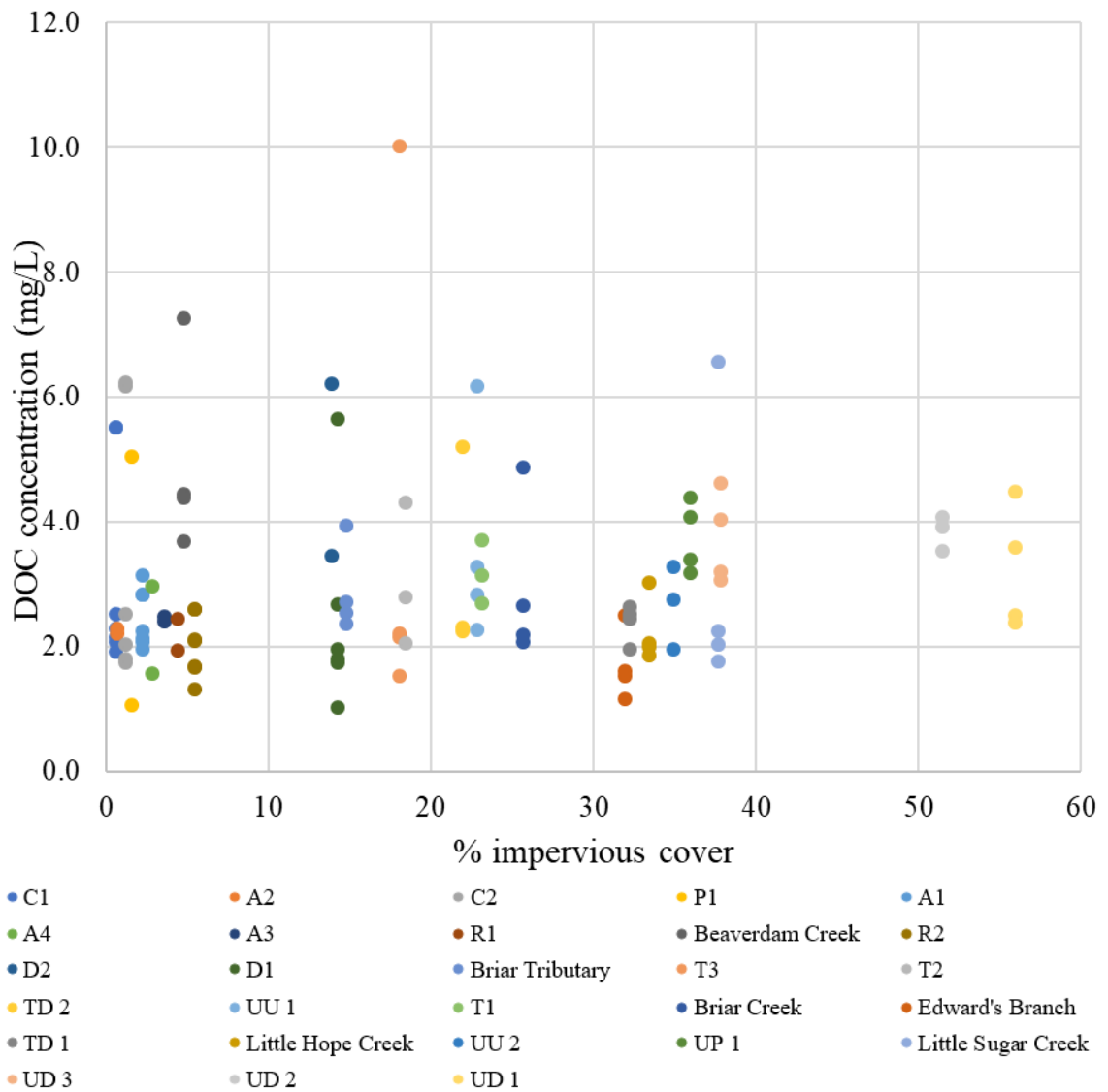


Figure 12: Scatter plot of DOC concentration vs. percent impervious cover (June 2017- October 2017)

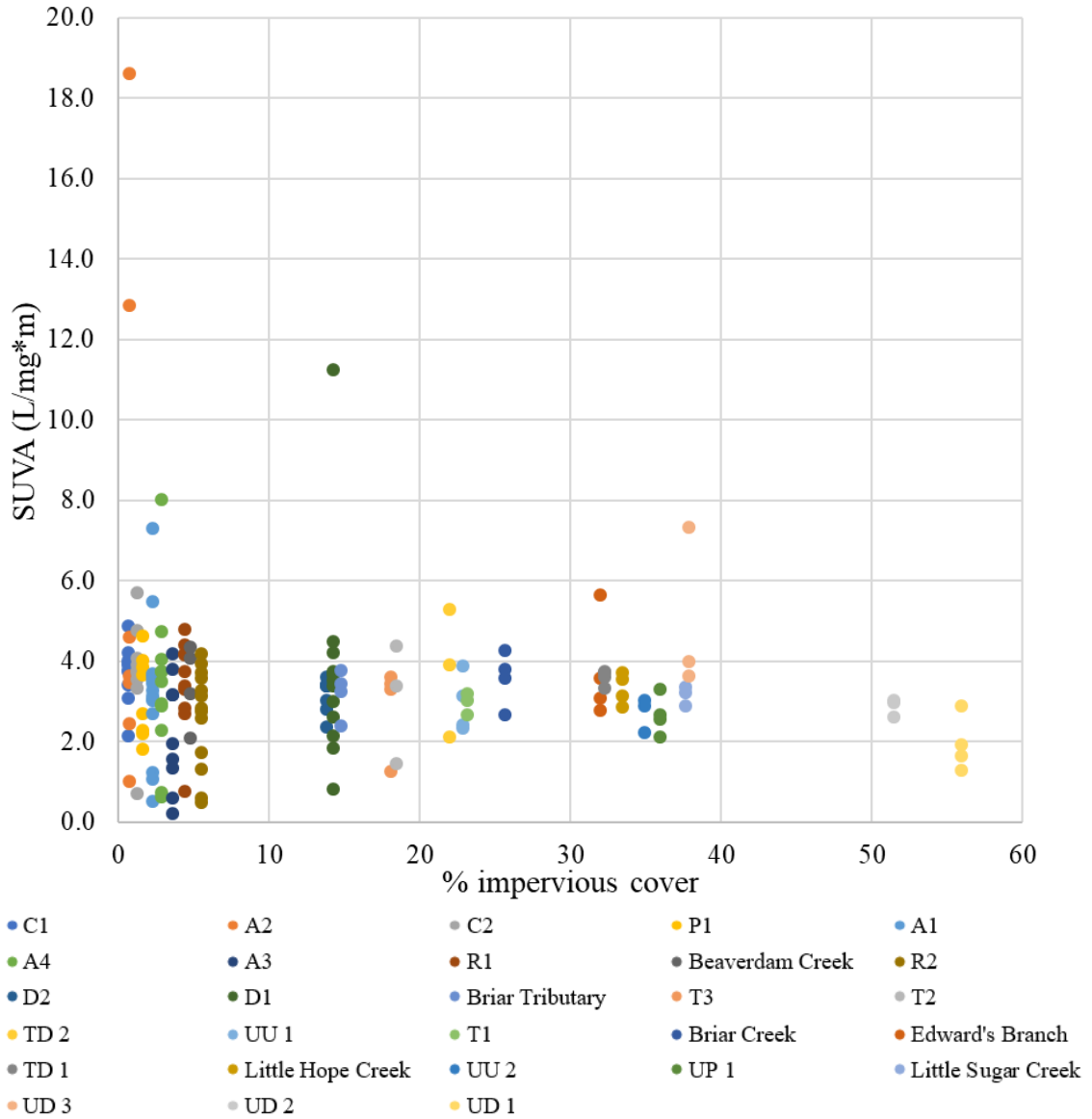


Figure 13: Scatter plot of SUVA vs. percent impervious cover (May 2016- October 2017)

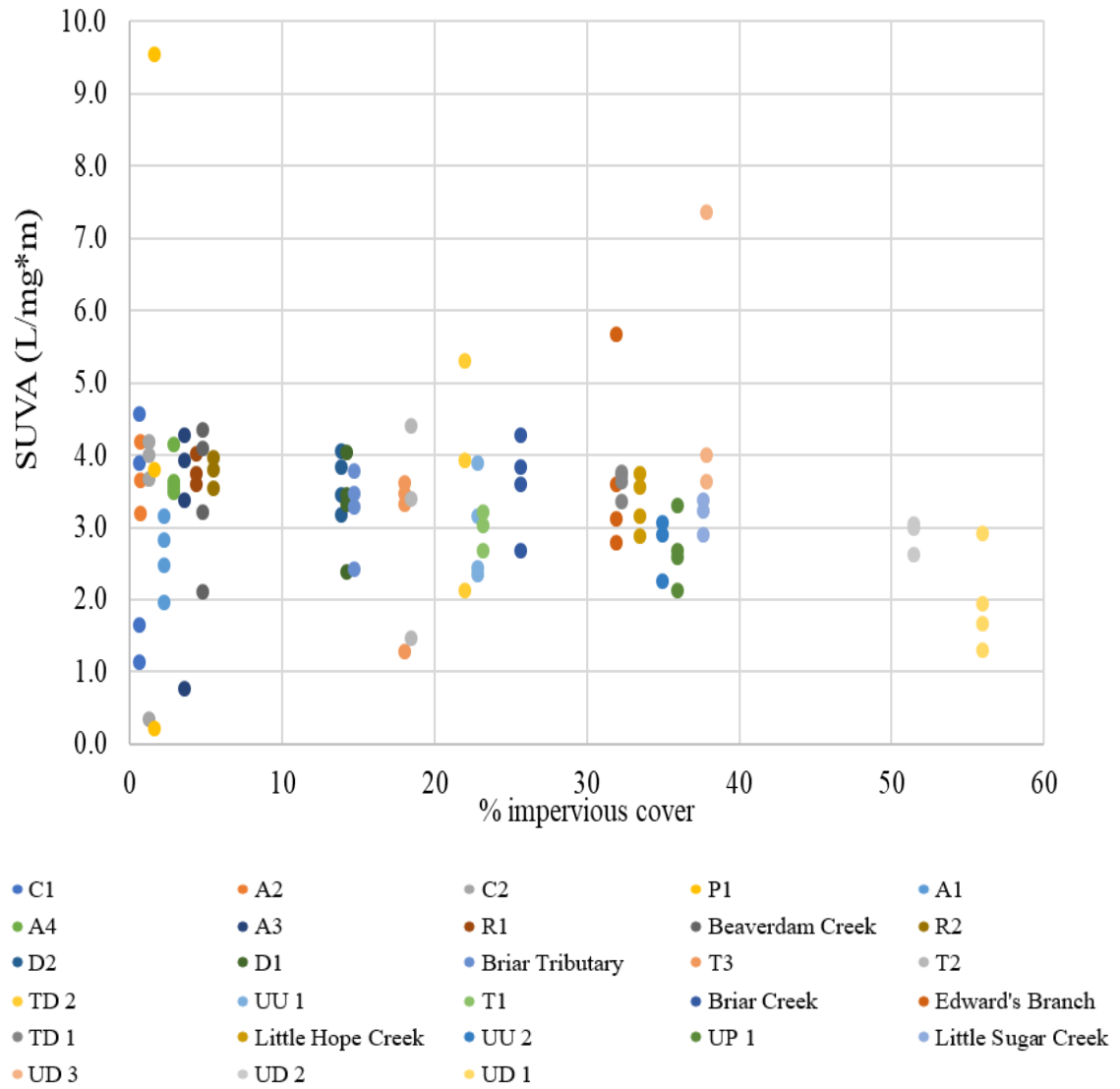


Figure 14: Scatter plot of SUVA values vs. percent impervious cover (June 2017- October 2017)

4.2.2 Temporal variation

A3 (RC group) had the highest DOC concentration of 24.8 mg/L on 8/4/2016. Additionally, A4 DOC concentration reached 18.5 mg/L on 9/20/2016. Spikes of DOC occurred in August-September 2016 and October 2017. DOC concentrations remained fairly consistent through late October 2016 to October 2017 (Figure 15). However, DOC concentrations reached a maximum of 17.8 mg/L at P1 and 15.9 mg/L at A3 on 10/20/2017. SUVA values were highest at A2 on 5/31/2016 and 8/4/2016 with values of 18.7 L/mg*m and 12.9 L/mg*m respectively. D1 peaked to 11.3 L/mg*m on 10/12/2016. SUVA values were mostly consistent from November 2016 to May 2017 (Figure 16). DOC concentrations (mg/L) of the MC group were fairly stable for 6/29/2017, 8/4/2017, and 8/30/2017. On 9/26/2017, DOC concentrations increased for all MC sites (Figure 17). SUVA values were also fairly stable on all sampling dates (Figure 18). Little Sugar Creek did not have a sample on 9/26/2017 due to sample vials breaking. TD 1 had the highest DOC concentration of 10.1 mg/L on 6/28/2017 of the TC group. T1 was highest on 7/27/2017 at 6.6 mg/L. UU 1 DOC concentration was highest on 9/5/2017 at 6.2 mg/L (Figure 19). SUVA values were fairly level for the four sampling dates. However, there was an increase on 7/27/2017 (Figure 20).

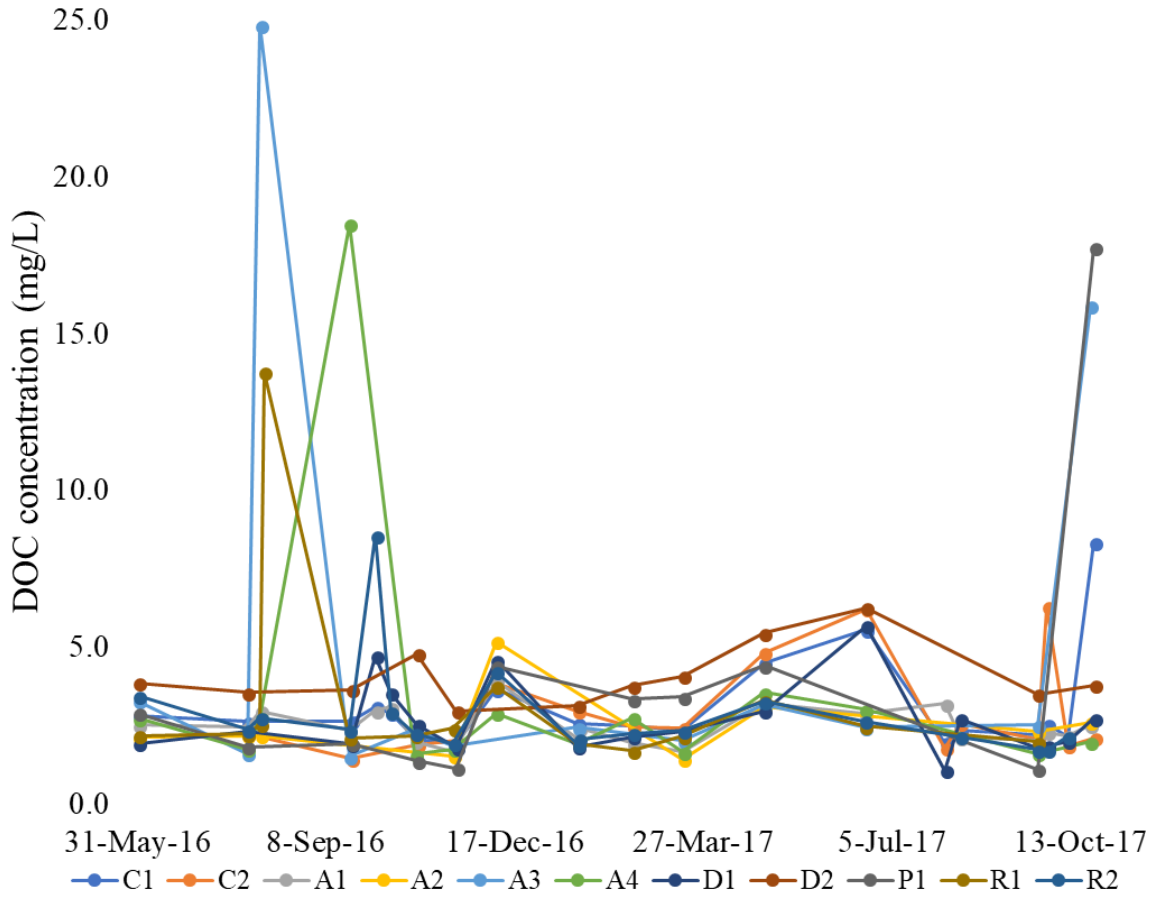


Figure 15: Time series of DOC concentration for the RC group, showing the occurrence of scattered higher DOC concentrations during late summer-early fall (May 2016- October 2017)

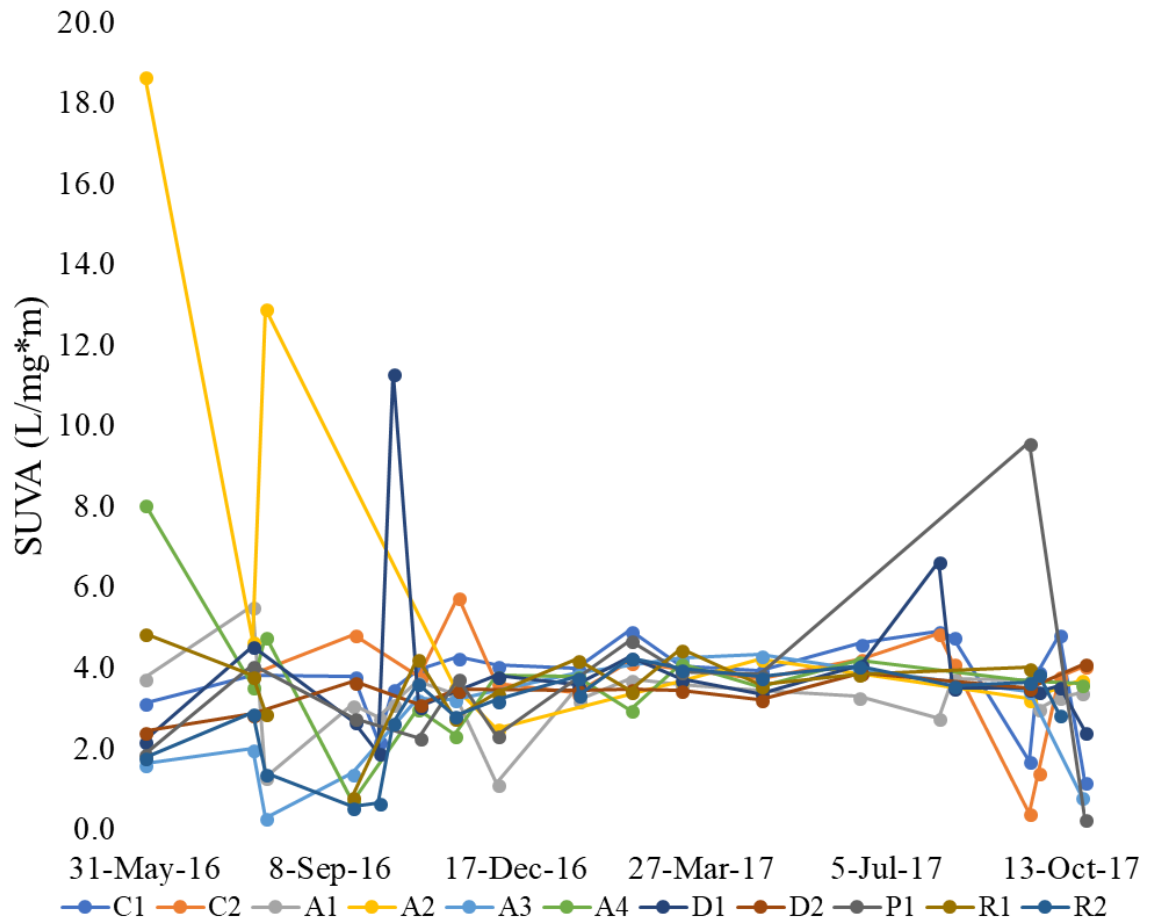


Figure 16: Time series of SUVA values for the RC group (May 2016- October 2017)

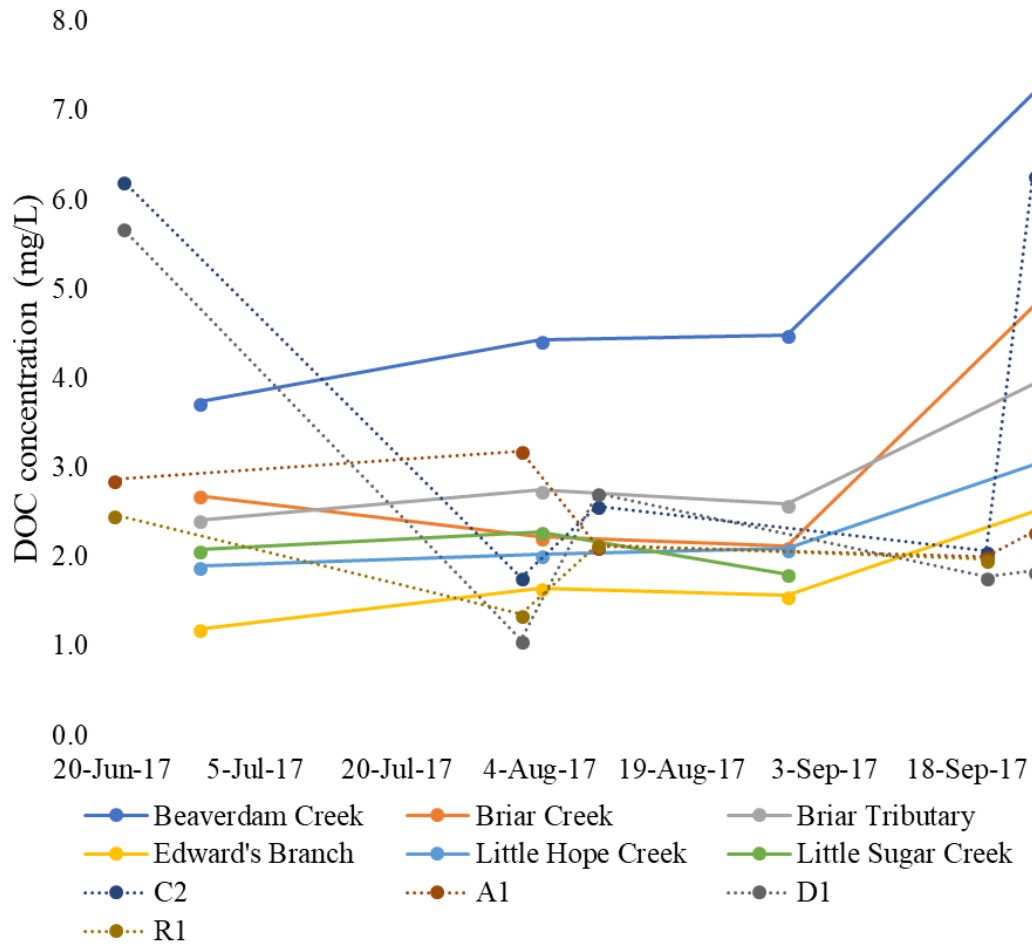


Figure 17: Time series of DOC concentration for the MC group (June 2017- September 2017). Dotted lines represent RC concentrations

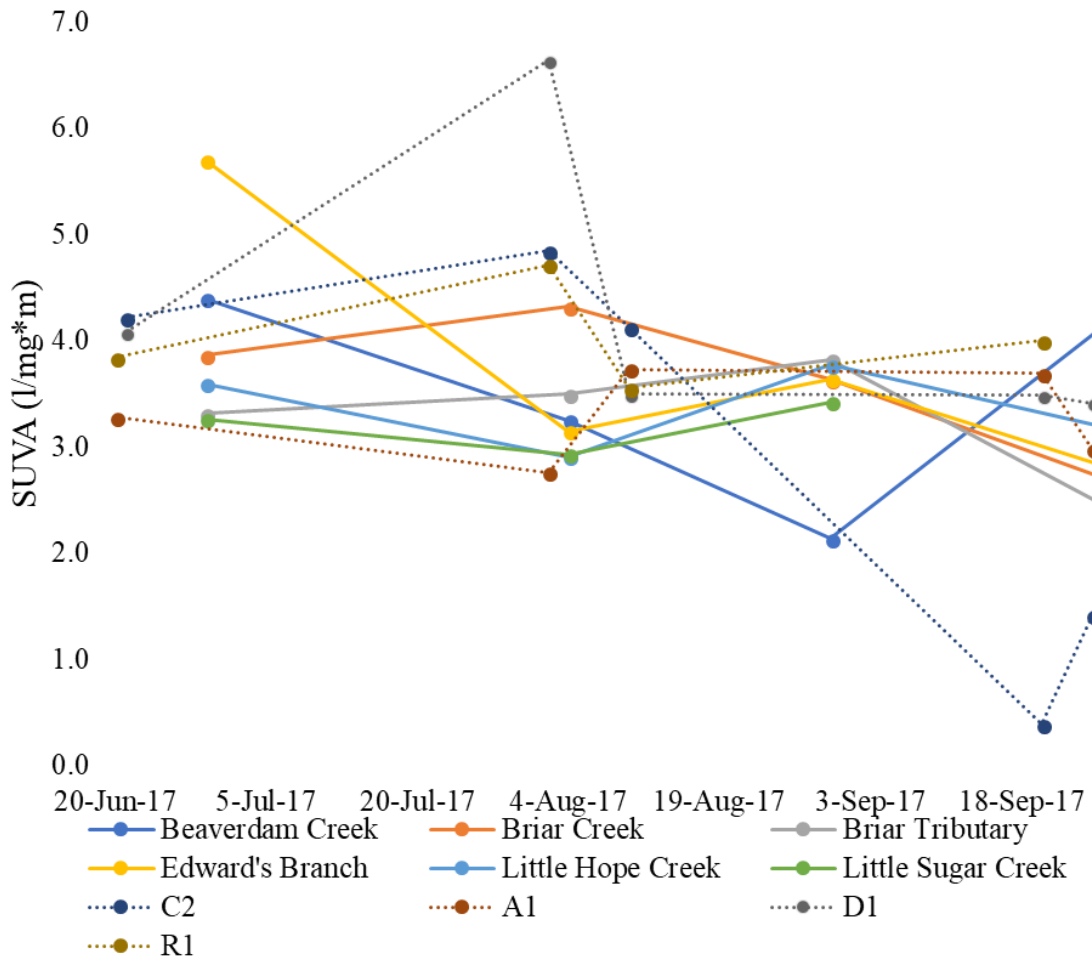


Figure 18: Time series of SUVA values for the MC group (June 2017- September 2017). Dotted lines represent RC values.

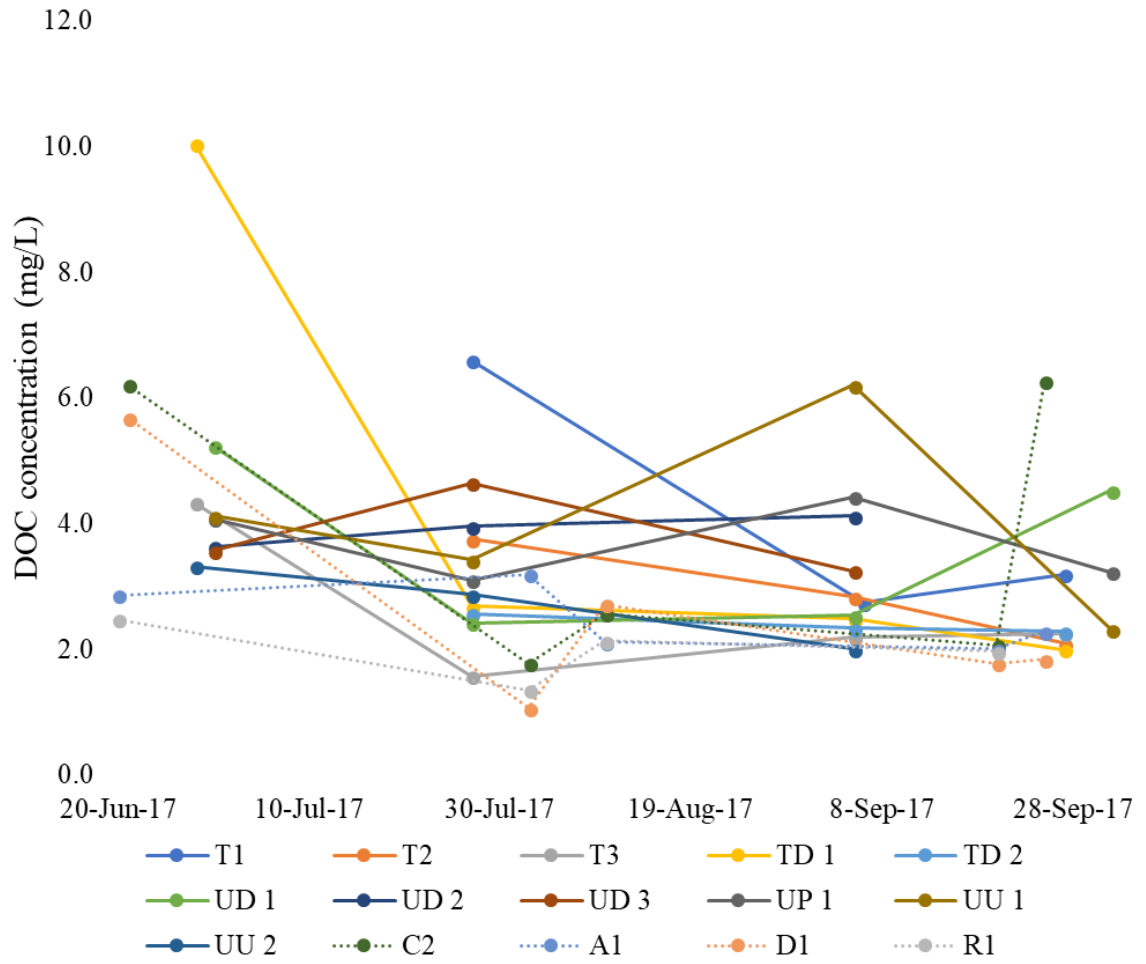


Figure 19: Time series of DOC concentration for the TC group (June 2017- October 2017). Dotted lines represent RC concentrations.

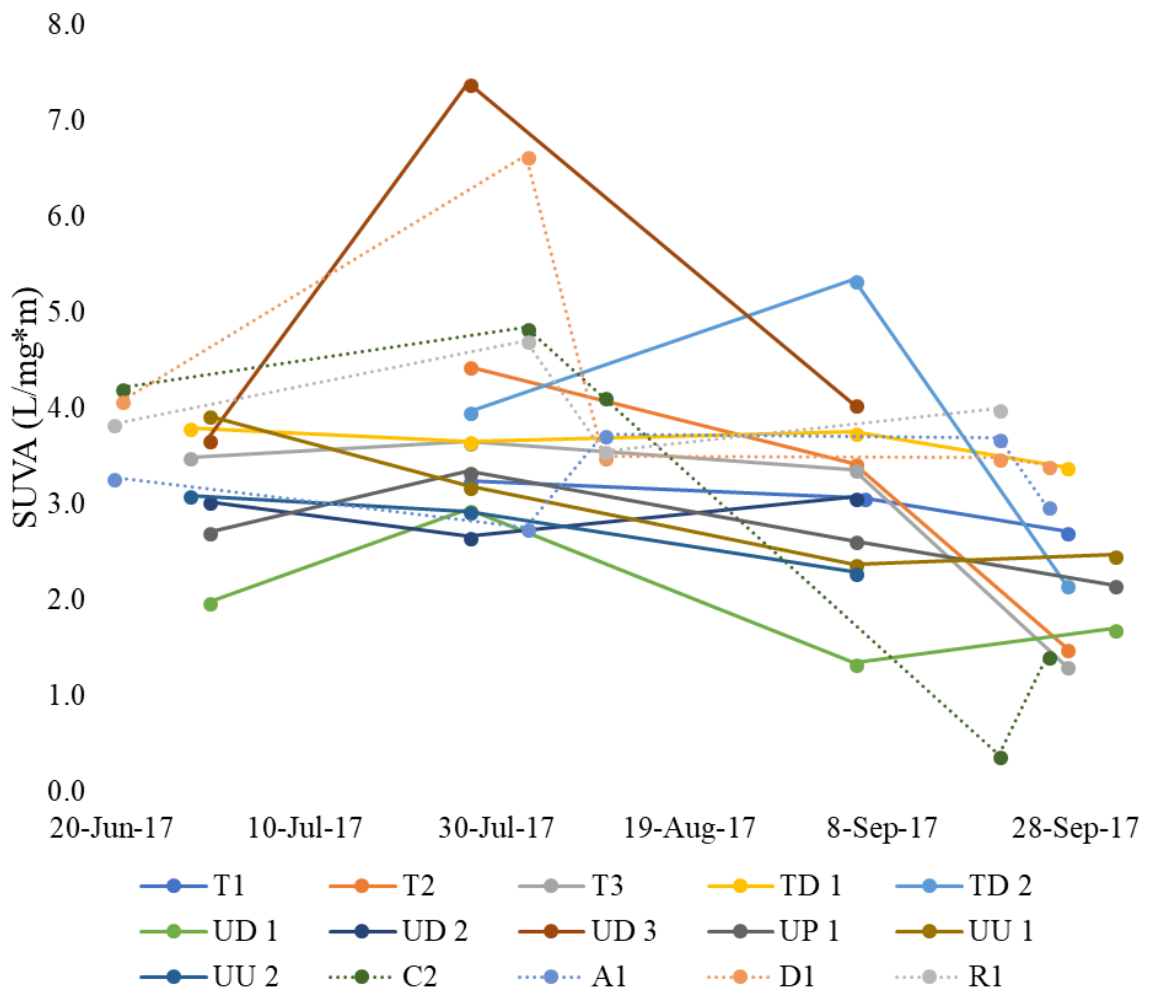


Figure 20: Time series of SUVA values for the TC group (June 2017- October 2017). Dotted lines represent RC values

4.3 Dissolved inorganic carbon, alkalinity, and pH

4.3.1 Inter-site variation

pH measurements ranged from 6.8 to 8.8 for all sites (Figure 21). Bicarbonate/ HCO_3^- was the dominant DIC/alkalinity species in this study. Little Sugar Creek had the highest pH of 8.8 and C1 had the lowest pH of 6.8. A correlation coefficient of 0.42 indicated that pH is moderately correlated with percent impervious cover; pH generally increased with increased percent impervious cover.

Control sites C1 and C2 at Reedy Creek had mean alkalinity concentrations of 0.35 and 0.38 meq/L. Agriculture sites (A1, A2, A3, and A4) had mean alkalinity concentrations ranging from 0.80 to 0.95 meq/L. C1 and C2 had the lowest alkalinity concentrations compared to all of the RC group sites. Alkalinity concentrations ranged from 0.17 meq/L to 0.57 meq/L at the control sites. The lowest alkalinity concentration of the agricultural sites was 0.36 meq/L at A1. A1 also had the highest alkalinity concentrations of the agricultural sites of 1.27 meq/L. A2, A3, and A4 alkalinity concentrations fell within the range 0.57 to 1.10 meq/L. The developed sites of the RC group had alkalinity concentrations ranging from 0.45 meq/L to 1.47 meq/L (D1 and D2). P1 had alkalinity concentrations from 0.44 meq/L to 1.33 meq/L. The main stem of Reedy (R1 and R2) had alkalinity concentrations of 0.43 to 1.08 meq/L (Figure 22 and Figure 24). RC group sites exhibited both inter-site differences and temporal variability for alkalinity and DIC concentration.

In the MC group, mean alkalinity concentrations ranged from 1.16 to 1.80 meq/L at Edward's Branch and Briar Tributary. Beaverdam Creek had alkalinity concentrations of 1.30 meq/L to 1.93 meq/L. Briar Creek ranged from 1.26 meq/L to 1.74 meq/L. Briar Creek Tributary had alkalinity concentrations of 1.56 meq/L to 2.14 meq/L. Edward's Branch alkalinity concentrations ranged from 1.14 meq/L to 1.17 meq/L. Little Hope Creek alkalinity concentrations ranged from 1.18 meq/L to 1.28 meq/L. Little Sugar Creek alkalinity concentrations were 1.44 meq/L to 1.92 meq/L (Figure 22 and Figure 24).

In the TC group, UD 3 had the highest alkalinity of 2 meq/L. T1, the outlet of Toby Creek, had alkalinity concentrations ranging from 1.56 meq/L to 1.90 meq/L. T2 alkalinity concentrations ranged from 1.52 to 2.00 meq/L. T3 had alkalinity concentrations ranging from 1.30 meq/L to 2.13 meq/L. TD 1 and TD 2 alkalinity concentrations ranged from 1.24 to 2.16 meq/L. UD 1 and UD 2 alkalinity concentrations ranged from 1.40 meq/L to 3.12 meq/L. UD 3 alkalinity concentrations ranged from 0.6 meq/L to 3.76 meq/L. UP 1 alkalinity concentrations were 1.23 to 2.14 meq/L. UU 1 and UU 2 alkalinity concentrations ranged from 1.30 to 2.47 meq/L (Figure 22 and Figure 24).

Within the RC group, control sites C1 and C2 had mean DIC concentrations of 0.54 and 0.51 mM. A1, A2, A3, and A4 had mean DIC concentrations of 1.13, 0.94, 1.13, and 1.07 mM respectively. DIC concentrations of C1 and C2 ranged from 0.29 mM to 0.87 mM. A2 had the lowest DIC concentration of the agricultural sites of 0.33 mM. A3 had the highest DIC concentration of 1.90 mM. D2 had the lowest and highest DIC concentrations of 0.49 mM and 1.78 mM for the developed RC sites. D1 DIC concentrations were less variable and ranged from 0.65 mM to 1.19 mM. P1 DIC concentrations ranged from 0.57 mM to 1.60 mM. The main stem of Reedy (R1 and R2) had DIC concentrations ranging from 0.70 mM (R1) to 1.27 mM (R2) (Figure 23 and Figure 26).

MC group had mean DIC concentrations ranging from 1.33 mM at Edward's and 2.12 mM at Beaverdam Creek. Beaverdam Creek had DIC concentrations ranging from 1.47 mM to 2.79 mM. Briar Creek and Briar Creek Tributary had DIC concentrations of 1.37 mM to 1.94 mM. Edward's DIC concentrations ranged from 1.27 mM to 1.37 meq/L. Little Hope Creek DIC concentrations ranged from 1.34 mM to 1.52 mM. DIC concentrations of Little Sugar Creek were 1.58 mM to 1.97 mM (Figure 23 and Figure 26).

TC group had DIC concentrations ranging from 1.50 mM at UP 1 and 2.28 mM at UD 1. DIC concentrations of T1 ranged from 1.77 mM to 2.20 mM. T2 and T3 DIC concentrations were 1.70 mM to 2.30 mM. TD 1 and TD 2 had DIC concentrations ranging from 1.55 mM to 2.27

mM. UD 1 and UD 2 DIC concentrations ranged from 1.73 mM to 2.84 mM. UD 3 DIC concentrations ranged from 0.67 mM to 3.76 mM. UP 1 had DIC concentrations of 0.96 mM to 1.92 mM. UU1 and UU 2 had DIC concentrations ranging from 1.42 mM to 2.41 mM (Figure 23 and Figure 26).

As percent impervious cover increases, there was an observable increase in alkalinity (Figure 24 and Figure 25). UD 3 (TC group) had the highest alkalinity of 3.76 meq/L. C1 (RC group) had the lowest alkalinity of 0.20 meq/L. Also, DIC concentrations generally increase as percent impervious cover increases (Figure 26 and Figure 27). DIC concentration is highest for UD 3 (MC group) at 3.76 mM. C2 and R1 (RC group) had the lowest DIC concentrations of 0.29 mM and 0.27 mM, respectively.

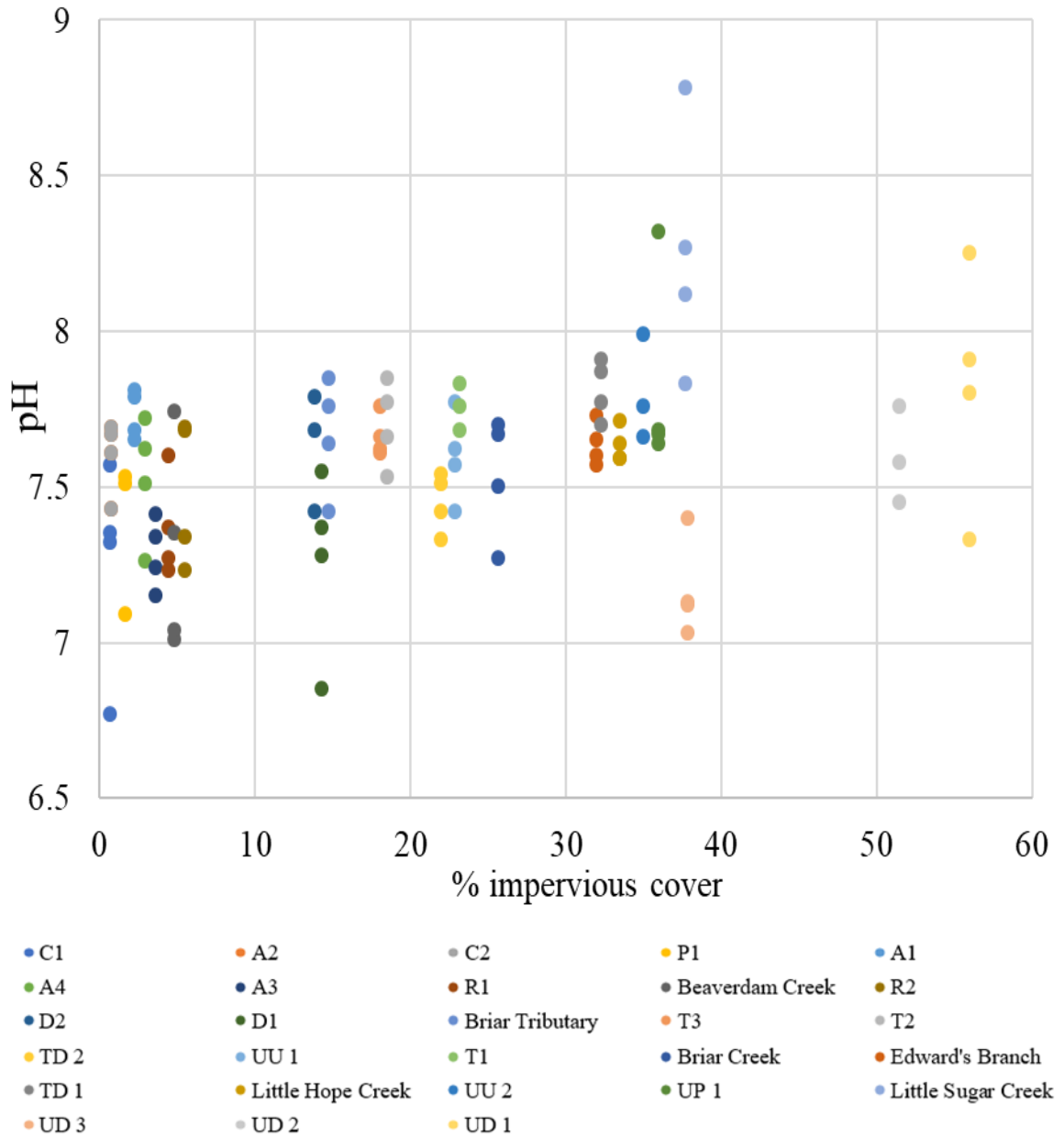


Figure 21: pH vs. percent impervious cover (June 2017- October 2017)

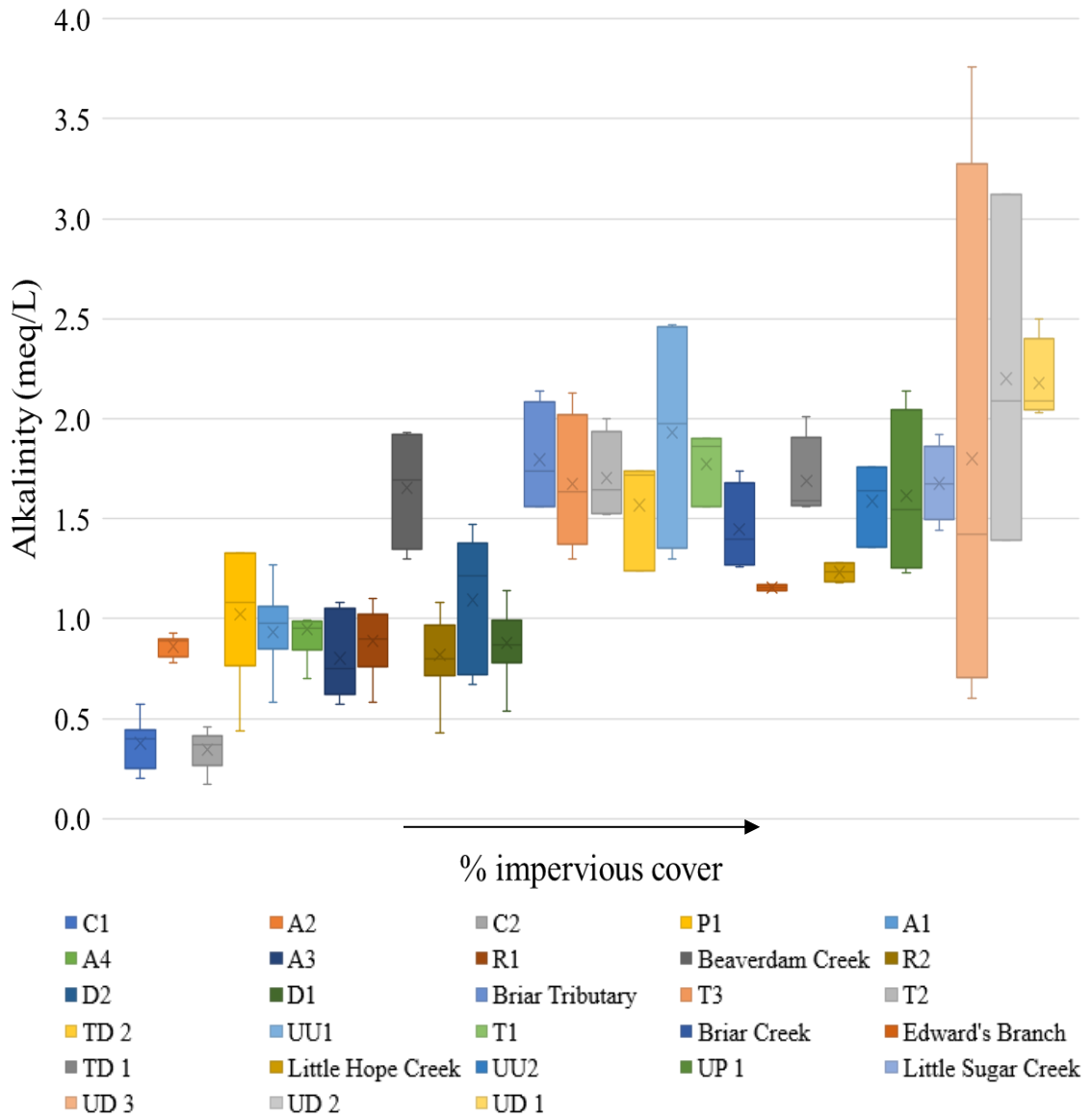


Figure 22: Box plots of alkalinity concentration vs. percent impervious cover

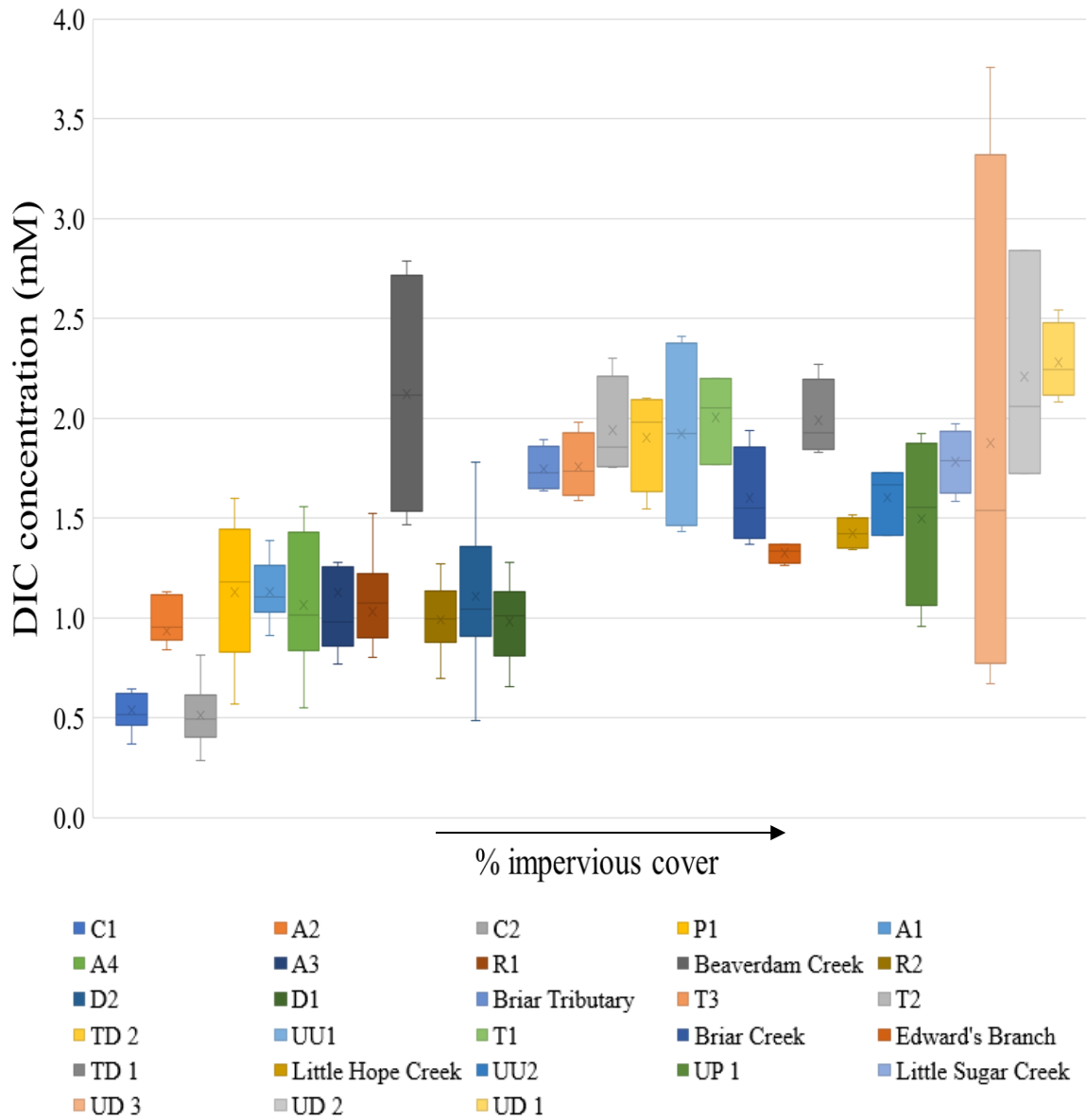


Figure 23: Box plot of DIC concentration vs. increasing percent impervious cover

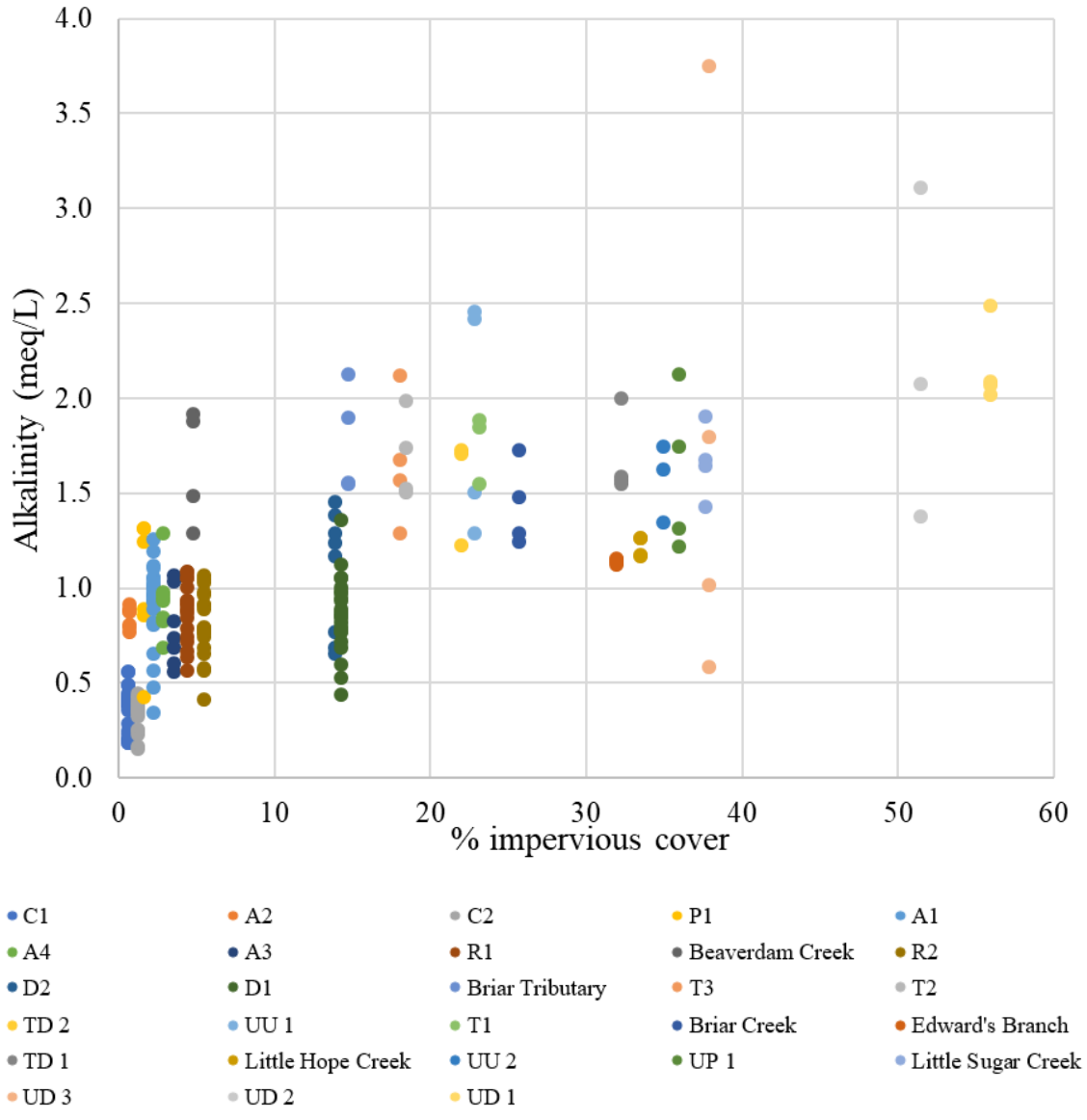


Figure 24: Alkalinity concentration vs. percent impervious cover (May 2016- October 2017)

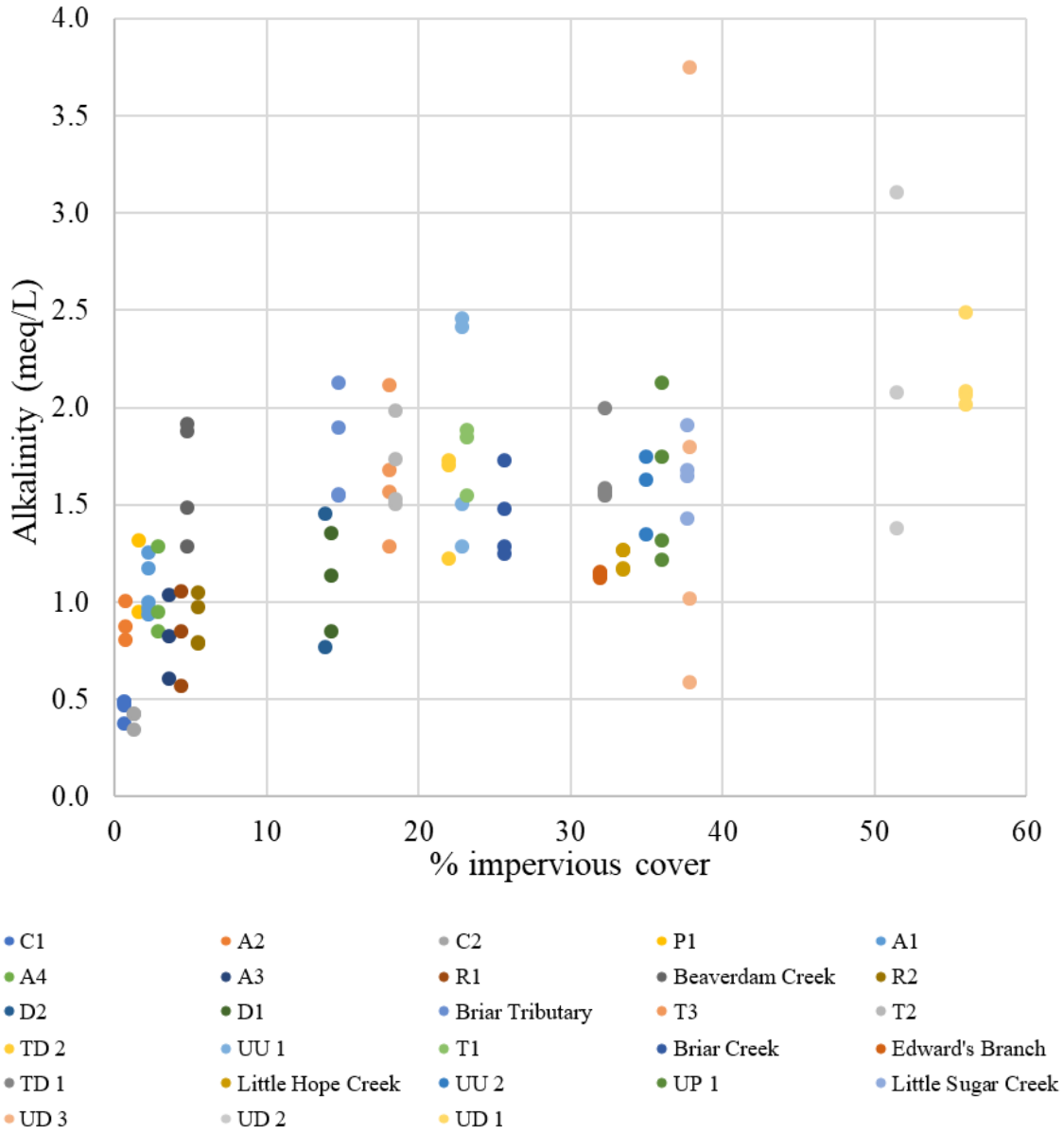


Figure 25: Alkalinity concentration vs. percent impervious cover (June 2017- October 2017)

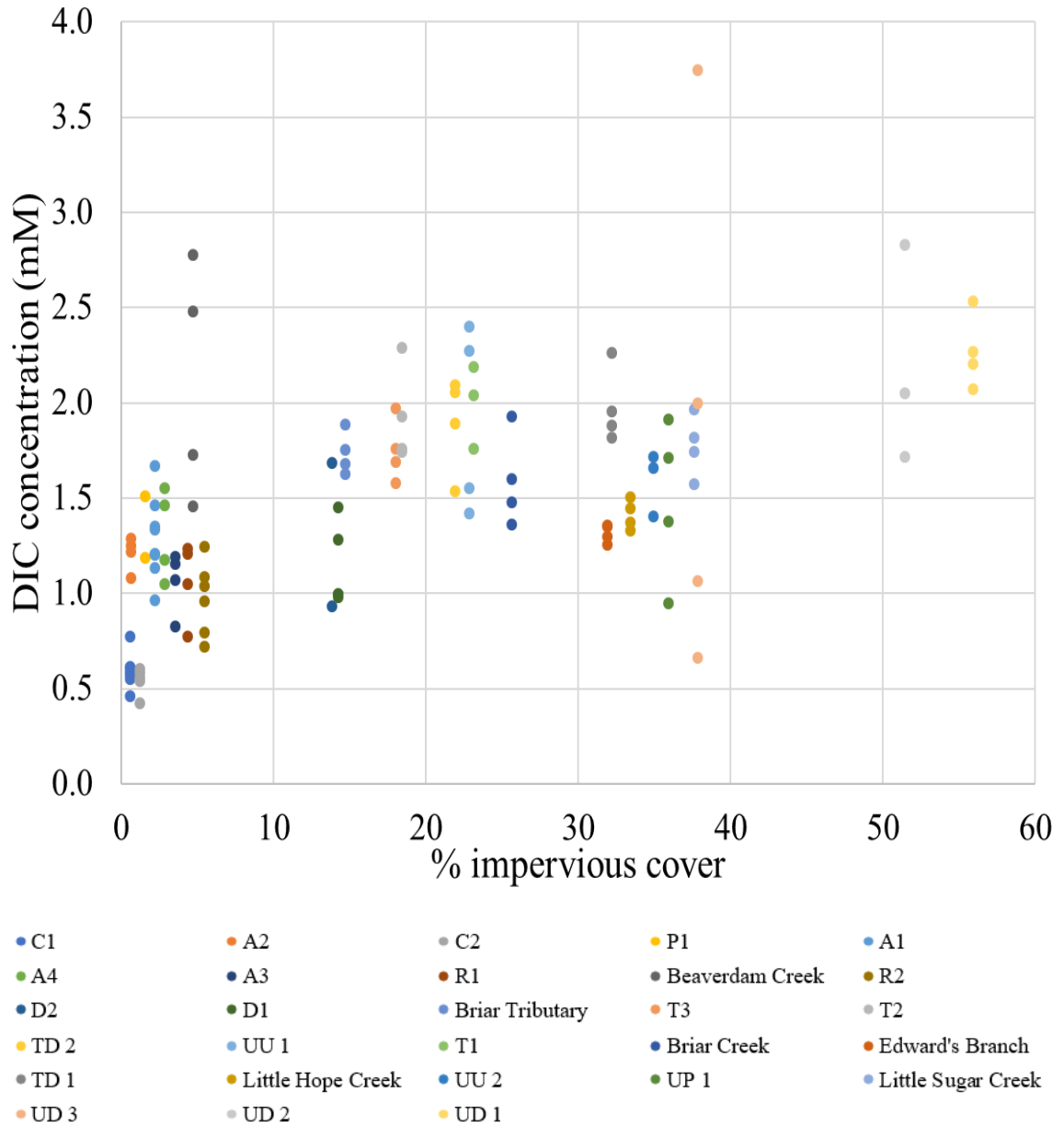


Figure 27: DIC concentration vs. percent impervious cover (June 2017- October 2017)

4.3.2 Temporal variation

In the RC group, alkalinity concentration reached a maximum of 2.2 meq/L at A1 during summer 2016. Autumn 2016 also produced high alkalinity. Alkalinity decreased in March 2017 and then increased towards September 2017 (Figure 28). DIC concentrations of the RC group were highest during autumn months of 2016 and 2017. A3 had the highest DIC concentration of 1.93 mM on 9/20/2016. D2 had a peak DIC concentration of 1.78 mM on 11/16/2016 and 1.69 mM on 9/20/2017. C1 and C2 DIC concentration reached 0.87 mM and 0.81 mM on 9/21/2016 (Figure 29), again reflecting the fall autumn maximums. DIC concentrations and alkalinity exhibited more variability/range at the agriculture and developed sites of the RC group, compared to the controls (Figure 28 and Figure 29).

Edward's branch alkalinity was uniform on all four sampling dates (1.14-1.17 meq/L). Little Hope Creek was also fairly uniform on all four sampling dates (1.18-1.28 meq/L). Briar Creek and Beaverdam Creek both increased between 8/4/2017 and 8/30/2017, then decreased on 9/26/2017. Briar Tributary and Little Sugar Creek both had their highest alkalinities on 9/26/2017 of 2.14 meq/L and 1.92 meq/L, respectively (Figure 30). DIC concentrations were fairly consistent on all four sampling dates for Edward's, Little Hope Creek and Briar Tributary. Beaverdam Creek had a sharp increase from 6/29/2017 to 8/4/2017 and 8/30/2017 (1.47 mM to 2.79 mM). DIC concentration then decreased from 2.79 mM to 1.74 mM on 9/26/2017 at Beaverdam Creek. Briar Creek exhibited a small increase from 1.37 to 1.61 then to 1.94 from 6/29/2017 to 8/4/2017 to 8/30/2017. Little Sugar Creek decreased to 1.58 mM on 8/30/2017 (Figure 31).

Alkalinity and DIC concentration followed the same pattern for the TC group (Figure 32 and Figure 33). UP 1, TD 2, UU 1, and UD 2 had peak alkalinity and DIC concentration on 7/27/2017. UD 3 had the highest alkalinity of 3.76 meq/L and DIC concentration of 3.76 mM on 10/2/2017 for all of the TC group.

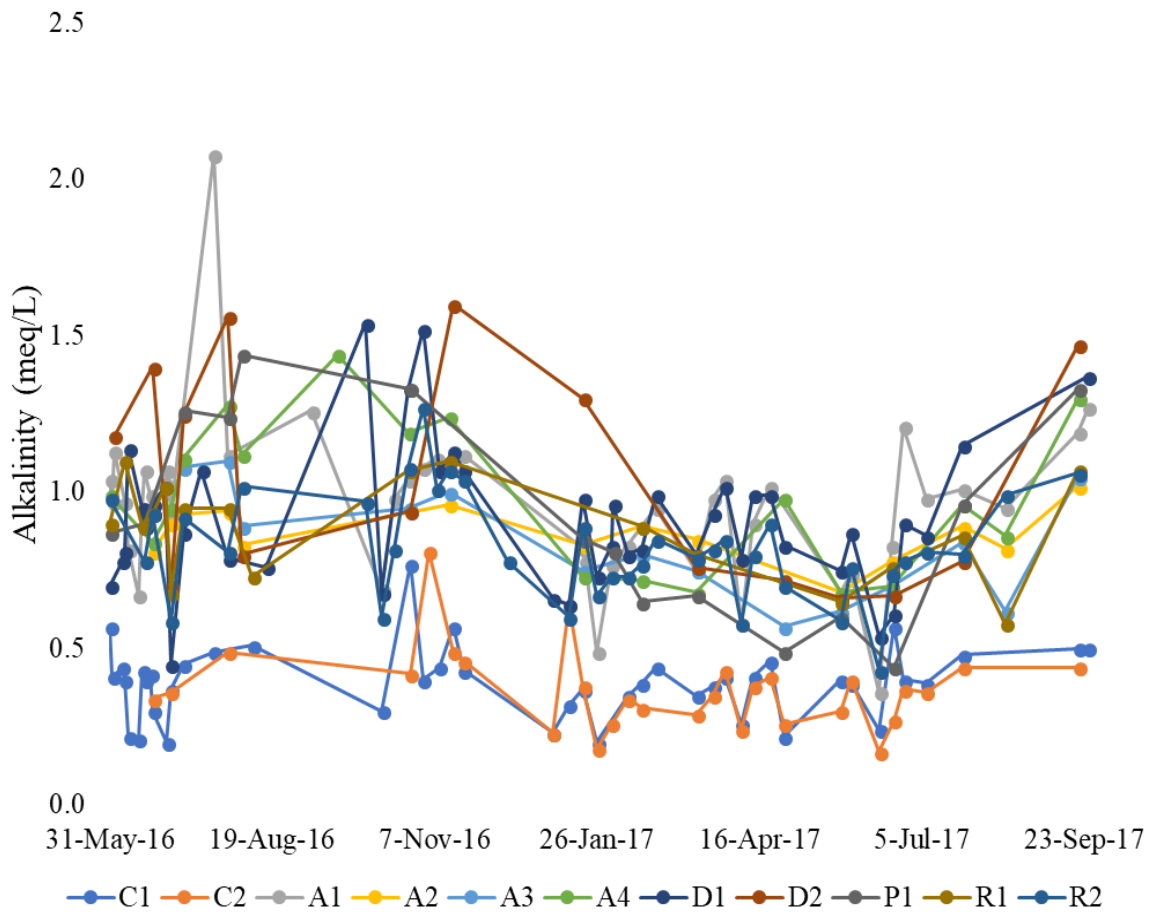


Figure 28: Time series of alkalinity concentration for the RC group (May 2016- September 2017)

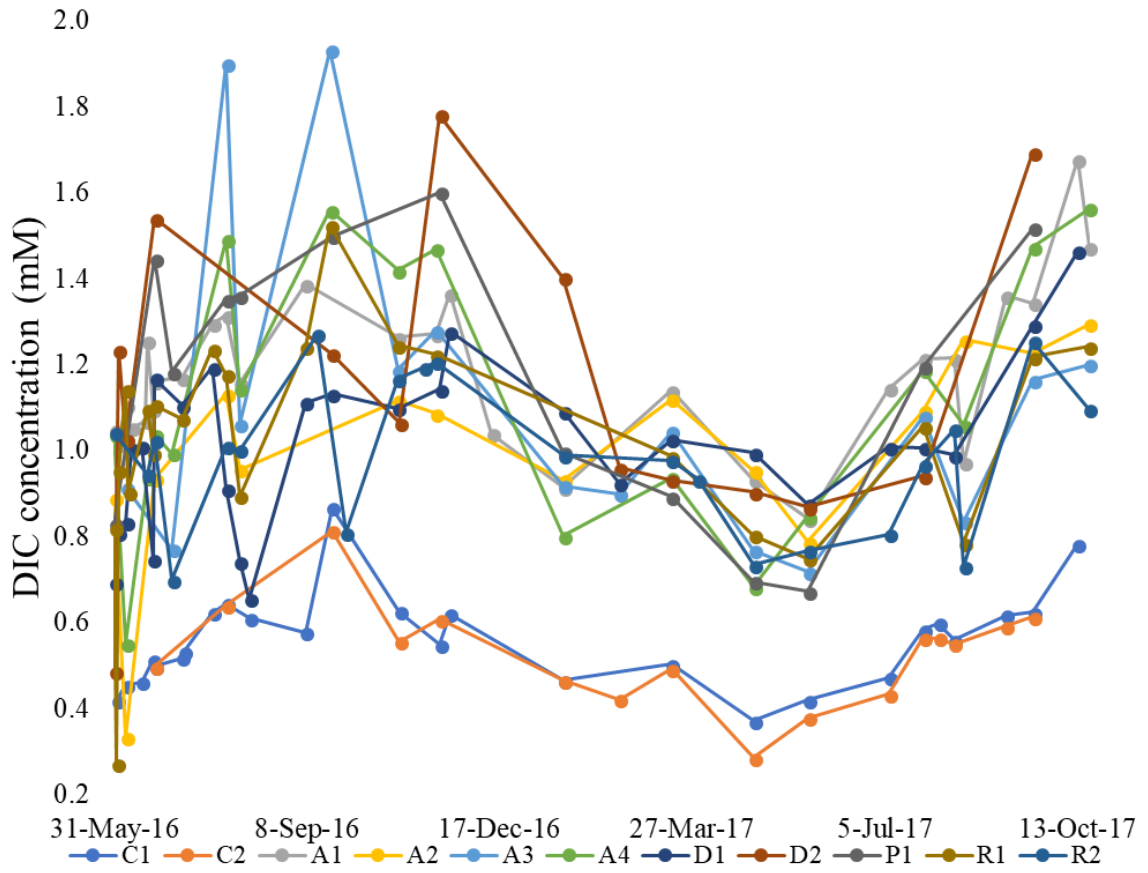


Figure 29: Time series of DIC concentration for the RC group (May 2016- October 2017)

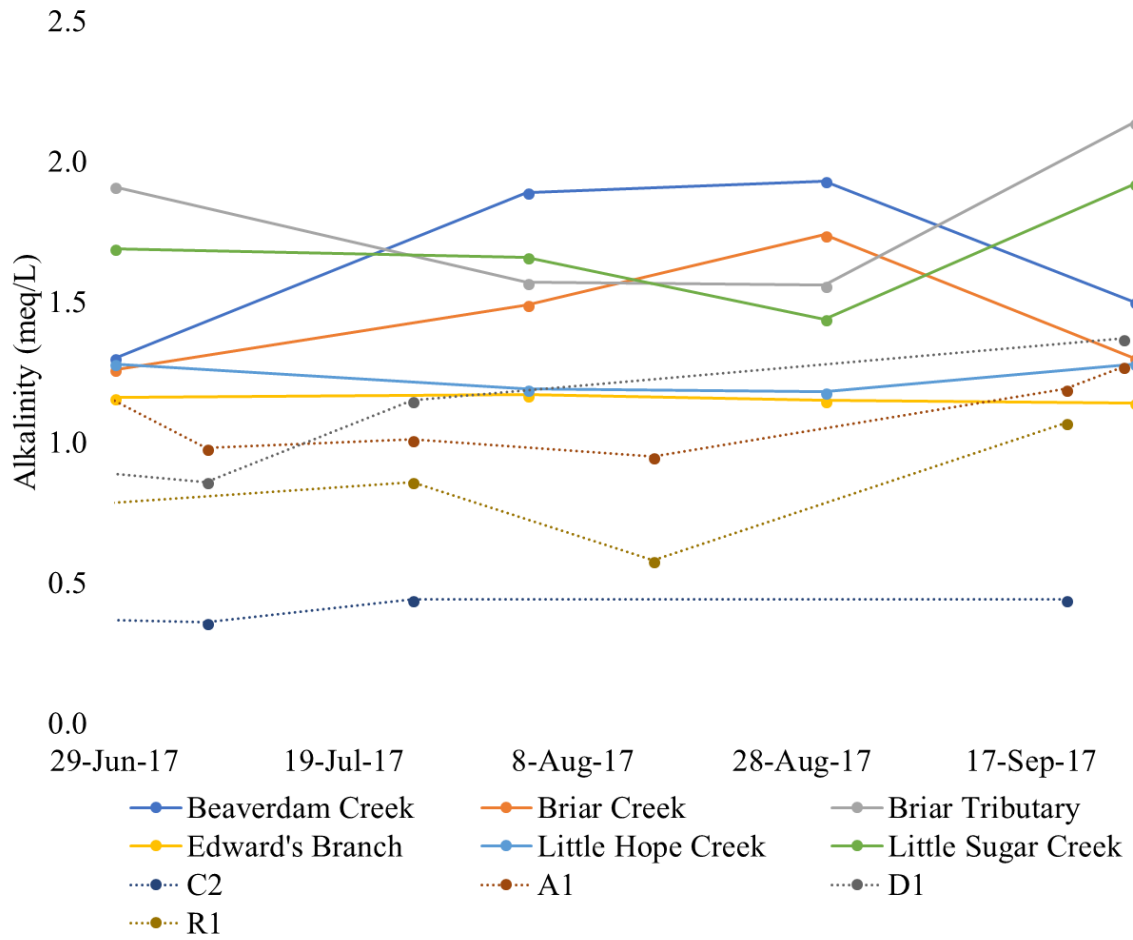


Figure 30: Time series of alkalinity concentration for the MC group (June 2017- September 2017). Dotted lines represent RC concentrations.

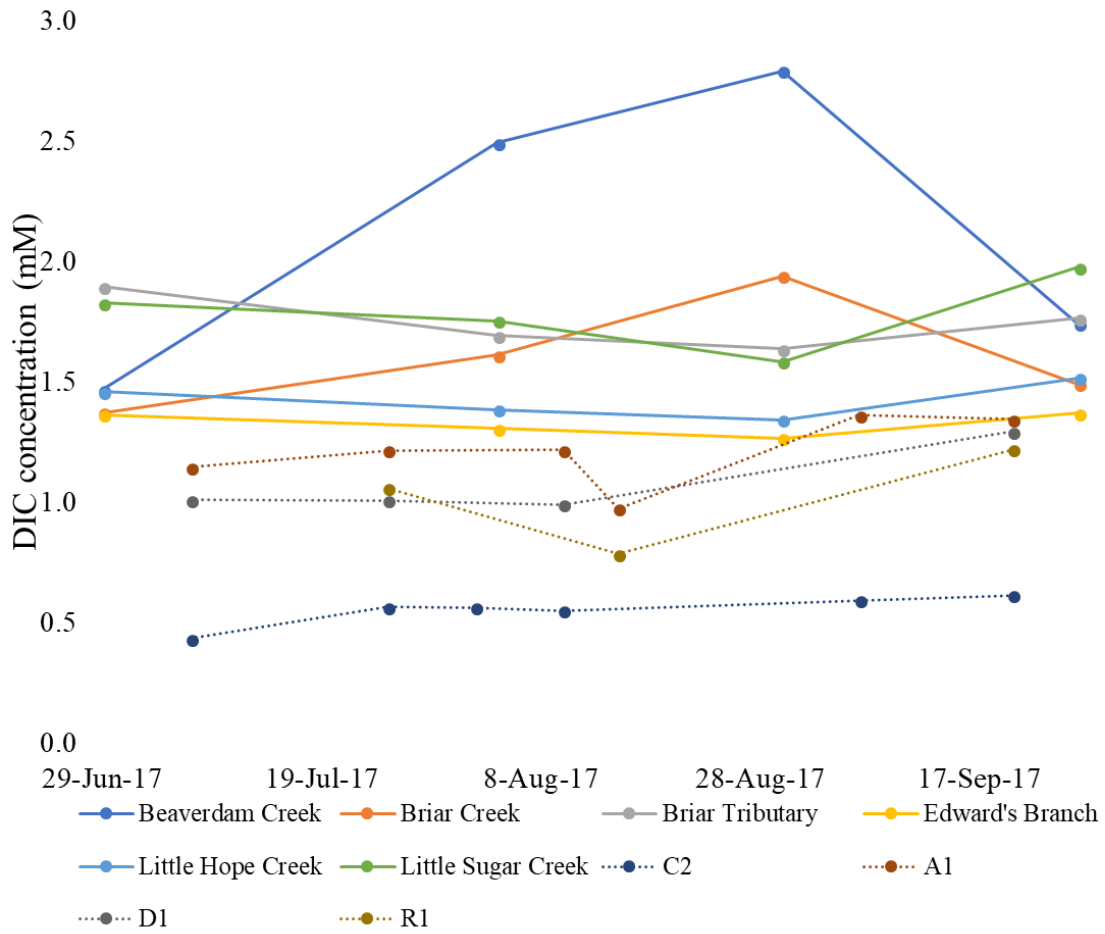


Figure 31: Time series of DIC concentration for the MC group (June 2017- September 2017). Dotted lines represent RC concentrations

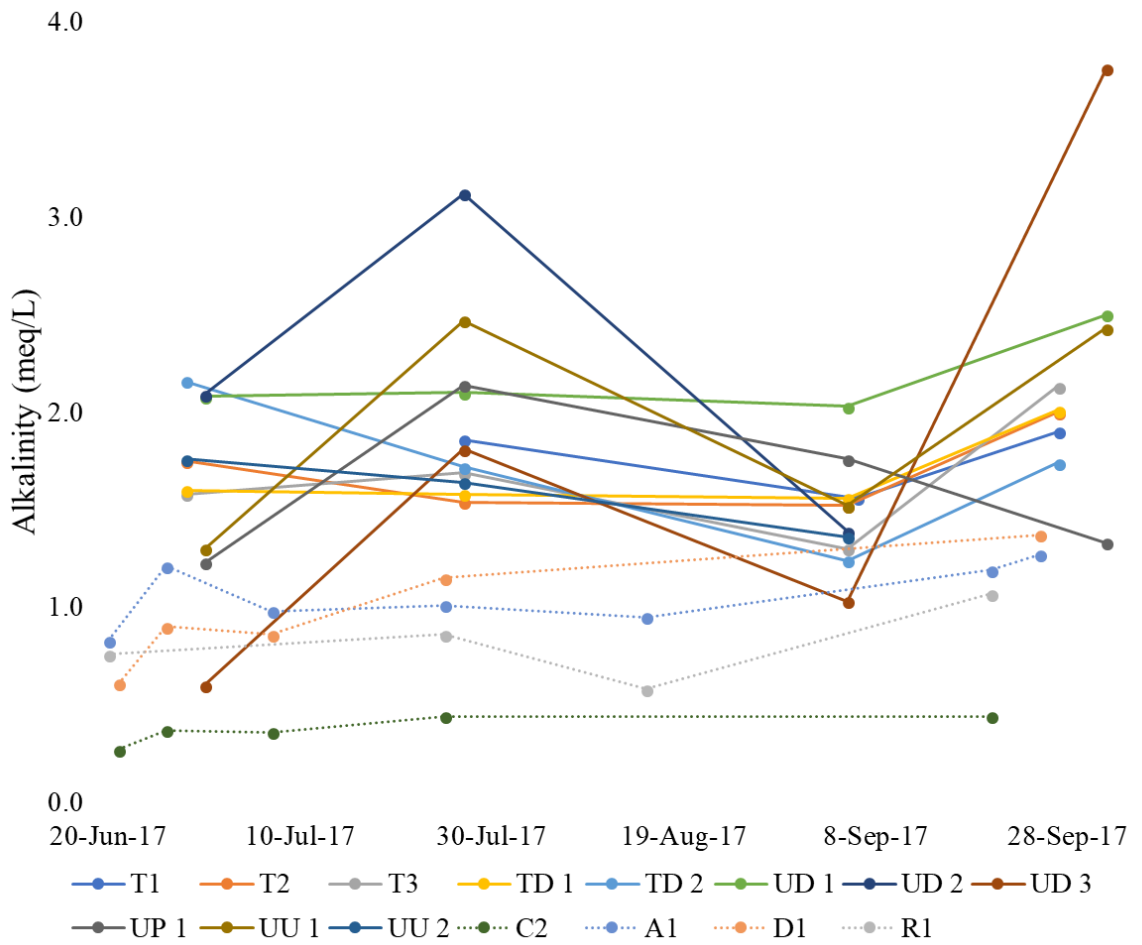


Figure 32: Time series of alkalinity concentration for the TC group (June 2017- October 2017). Dotted lines represent RC concentrations

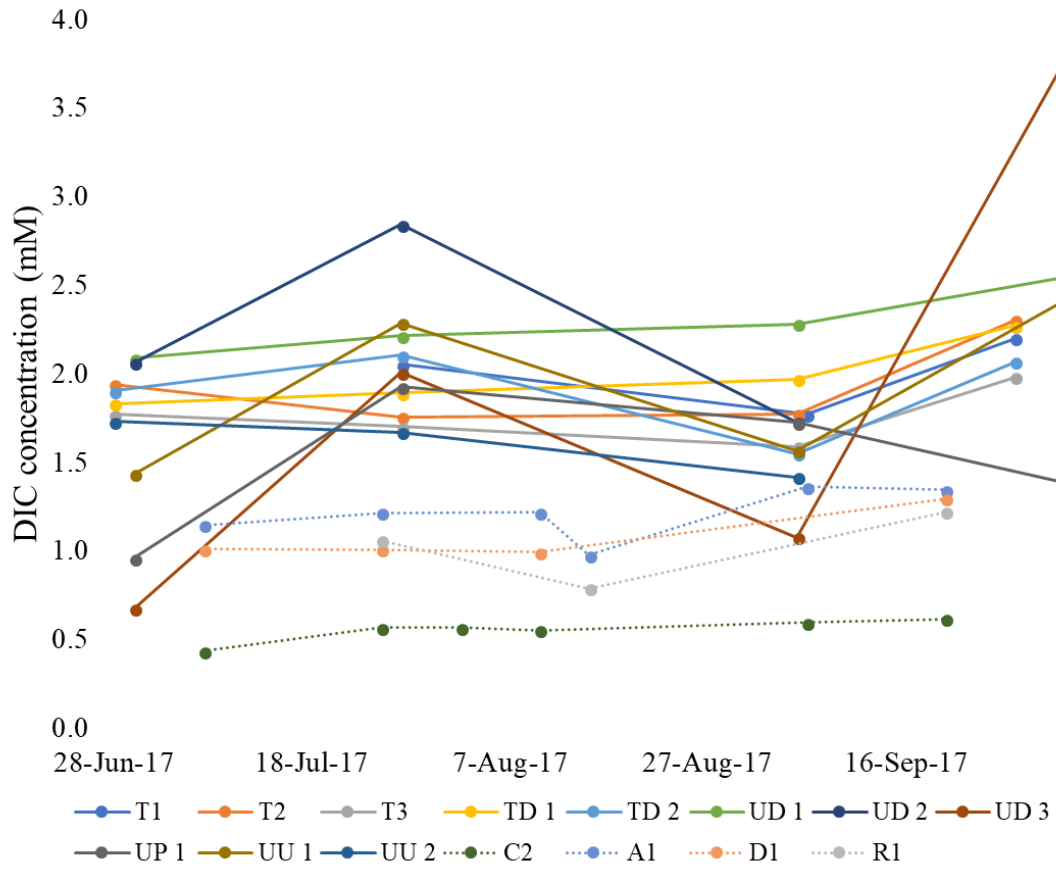


Figure 33: Time series of DIC concentration for the TC group (June 2017- October 2017). Dotted lines represent RC concentrations

4.4 $\delta^{13}\text{C}$ -DIC

4.4.1 Inter-site variation

C1 and C2 had mean $\delta^{13}\text{C}$ -DIC values of -14.8 and -15.3 ‰, respectively. Agriculture mean $\delta^{13}\text{C}$ -DIC values ranged from -15.5 to -14.9 ‰. C1 and C2 had $\delta^{13}\text{C}$ -DIC values ranging from -17.4 to -10.0. Agricultural sites had $\delta^{13}\text{C}$ -DIC values ranging from -17.9‰ at A3 to -12.3‰ at A2. D1 and D2 had $\delta^{13}\text{C}$ -DIC values of -16.5‰ at D1 to -9.4‰ at D2. P1 $\delta^{13}\text{C}$ -DIC values ranged from -16.7‰ to -11.2‰. The main stem of Reedy Creek had $\delta^{13}\text{C}$ -DIC values of -16.5‰ at R1 to -12.3‰ at R2. Overall at RC, the most positive values of $\delta^{13}\text{C}$ -DIC were found at D2 (Figure 35).

Streams in the MC group exhibited mean $\delta^{13}\text{C}$ -DIC values ranging from -15.8 (Beaverdam Creek) to -13.0 ‰ (Little Sugar Creek). Beaverdam Creek $\delta^{13}\text{C}$ -DIC values ranged from -16.5‰ to -15.1‰. Briar Creek and Briar Creek Tributary $\delta^{13}\text{C}$ -DIC values ranged from -14.4‰ to -12.6‰. Edwards Branch had $\delta^{13}\text{C}$ -DIC values of -15.7‰ to -14.5‰. Little Hope Creek $\delta^{13}\text{C}$ -DIC values ranged from -15.1‰ to -13.6‰. Little Sugar Creek had $\delta^{13}\text{C}$ -DIC values of -13.2‰ to -12.7‰. Overall within the MC group, the most positive values of $\delta^{13}\text{C}$ -DIC were found at Briar Creek, Little Sugar Creek, and Briar Tributary (Figure 35).

Within the TC group, UD 2 had the most negative mean $\delta^{13}\text{C}$ -DIC value of -15.0‰ and UD 3 had the least negative mean $\delta^{13}\text{C}$ -DIC value of -10.7‰. T1 had $\delta^{13}\text{C}$ -DIC values of -13.6‰ to -13.2‰. T2 and T3 $\delta^{13}\text{C}$ -DIC values ranged from -15.0‰ to -13.3‰. TD 1 and TD 2 $\delta^{13}\text{C}$ -DIC values ranged from -14.0‰ to -13.6‰. UD 1 and UD 2 had $\delta^{13}\text{C}$ -DIC values of -15.4‰ to -12.5‰. UD 3 $\delta^{13}\text{C}$ -DIC values ranged from -12.5‰ to -7.4‰. UP 1 $\delta^{13}\text{C}$ -DIC values ranged from -12.4‰ to -11.4‰. UU 1 and UU 2 had $\delta^{13}\text{C}$ -DIC values of -12.8‰ to -11.8‰. Overall in the TC group, the most positive values of $\delta^{13}\text{C}$ -DIC were found at UD 3 and UP 1 (Figure 35).

When all data are used, it looks like there is a clear increase in $\delta^{13}\text{C}$ -DIC with increased percent impervious cover (Figure 34 and Figure 35). However, Figure 36 only looks at $\delta^{13}\text{C}$ -DIC from June 2017- October 2017 and there is no observable trend.

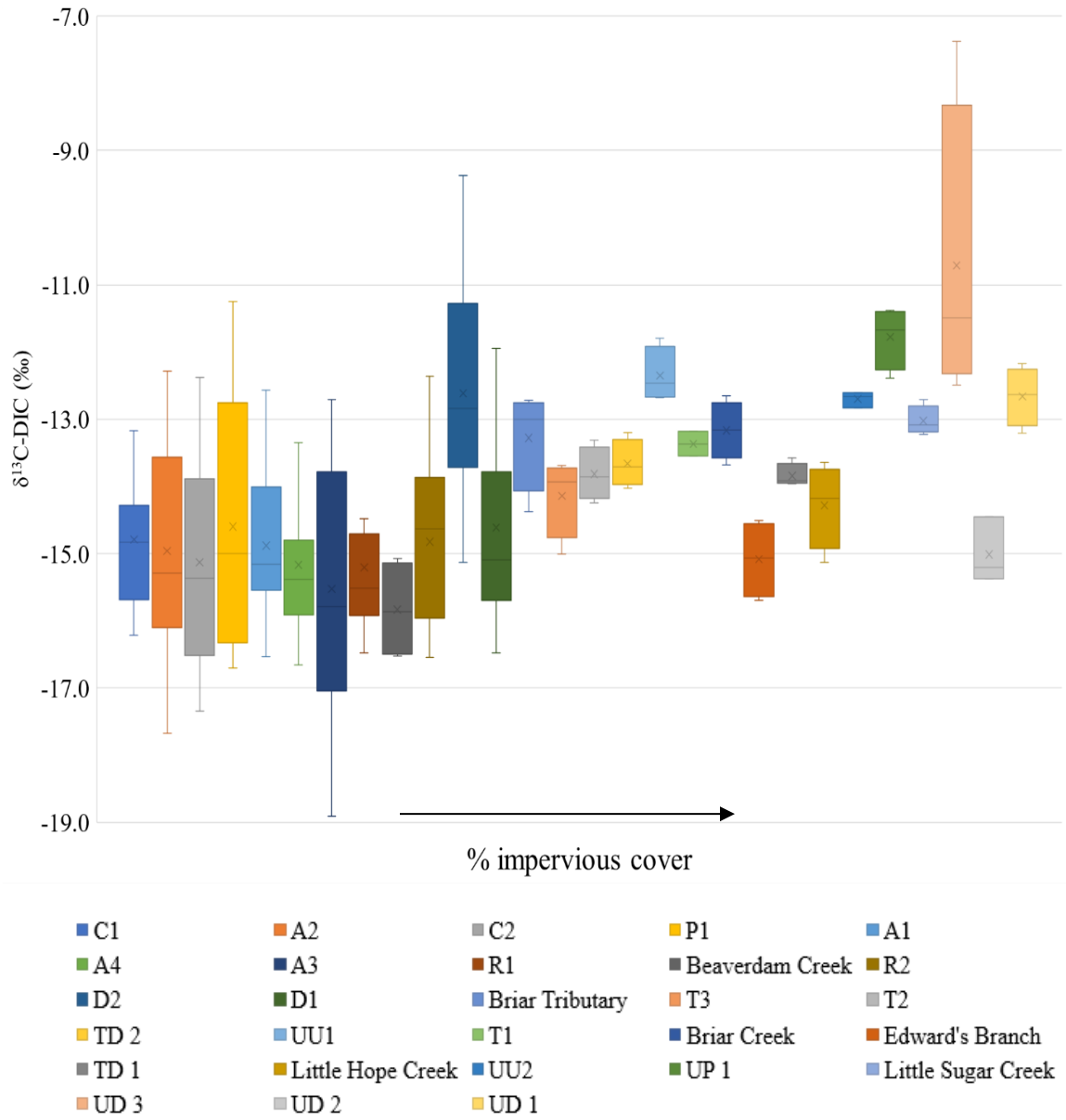


Figure 34: Box plot of $\delta^{13}\text{C-DIC}$ vs. increasing percent impervious cover

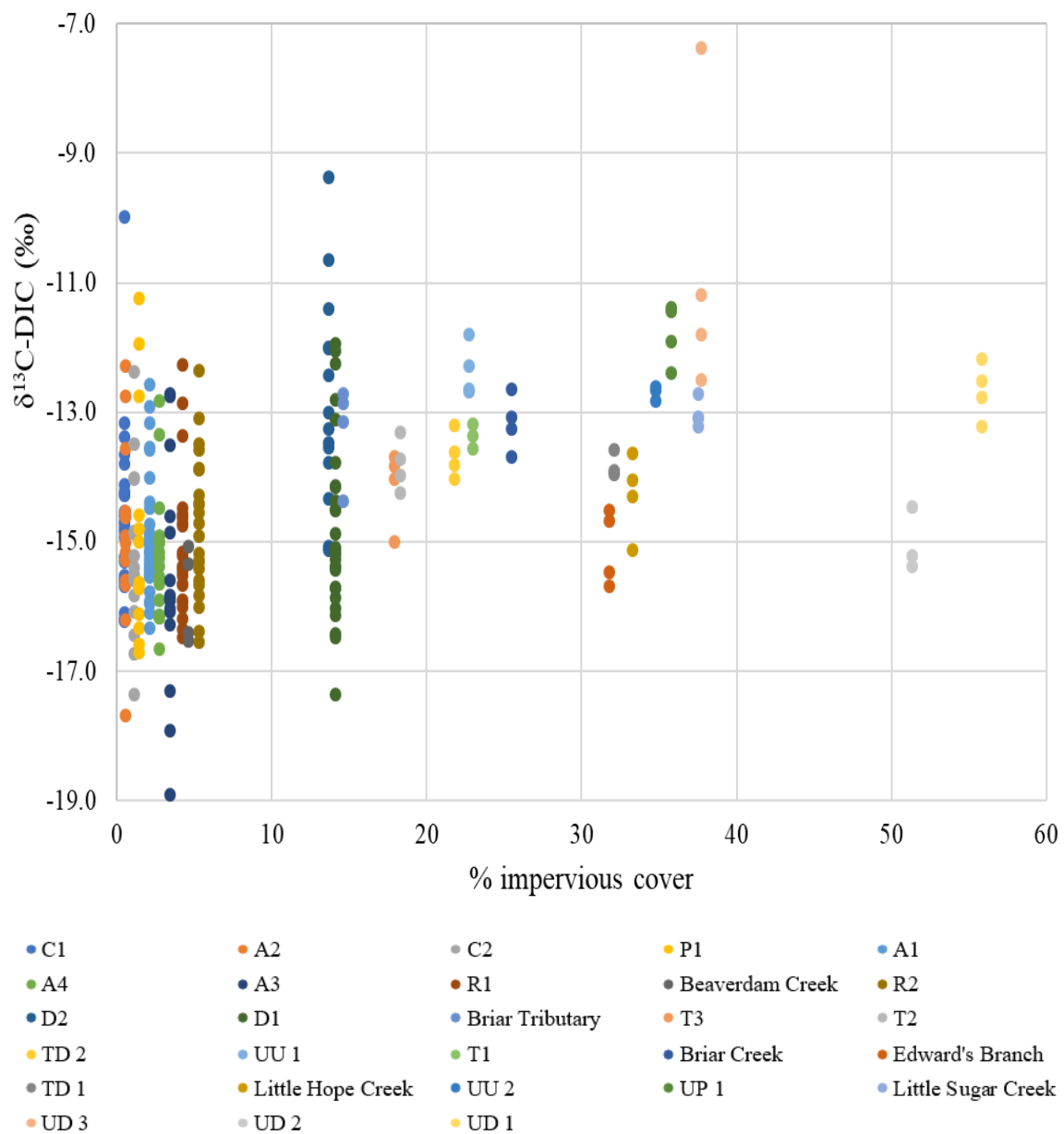


Figure 35: δ¹³C-DIC vs. percent impervious cover (May 2016- October 2017)

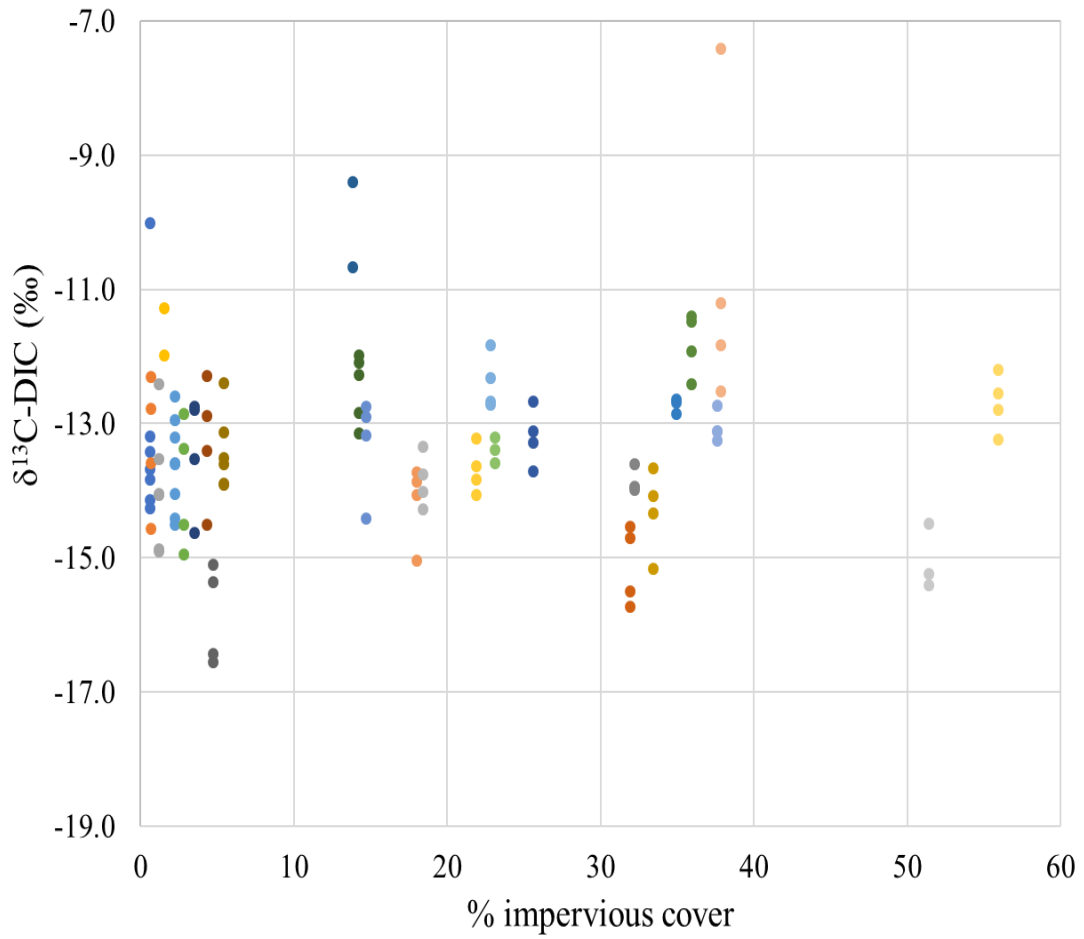


Figure 36: $\delta^{13}\text{C-DIC}$ vs. percent impervious cover (June 2017-October 2017)

4.4.2 Temporal variation

$\delta^{13}\text{C-DIC}$ reached the most positive values on 3/16/2017 for the RC group (Figure 37). D2 had the most positive $\delta^{13}\text{C-DIC}$ value of -9.4‰ on 3/16/2017. A3 had the most negative $\delta^{13}\text{C-DIC}$ value of -18.9‰ on 7/28/2016. The RC group is experiencing some seasonal trends of $\delta^{13}\text{C-DIC}$. More negative $\delta^{13}\text{C-DIC}$ values are occurring in later summer 2016 and rising to the highest $\delta^{13}\text{C-DIC}$ values March 2017. $\delta^{13}\text{C-DIC}$ values are then decreasing from March 2017 to October 2017, with a slight peak at D1 and A3 during summer 2017. Little Sugar Creek $\delta^{13}\text{C-DIC}$ values were consistent for the four sampling dates, ranging from -13.2‰ to -12.7‰. Beaverdam Creek had the most negative $\delta^{13}\text{C-DIC}$ values of the MC group on 8/4/2017 and 8/30/2017 of -16.4‰ and -16.5‰, respectively. Briar Creek and Briar Tributary had the most positive $\delta^{13}\text{C-DIC}$ values of -12.6‰ and -12.7‰ on 8/4/2017 (Figure 38). UD 3 had the most positive $\delta^{13}\text{C-DIC}$ value of -7.4‰ on 9/5/2017. Overall, $\delta^{13}\text{C-DIC}$ values were fairly uniform for all four sampling dates at all TC sites (except for UD 3). UD 2 had the most negative $\delta^{13}\text{C-DIC}$ values ranging from -15.4‰ to -14.5 ‰ (Figure 39). $\delta^{13}\text{C-DIC}$ values varied more at Reedy Creek, due to the sampling period being longer (May 2016- 2017). The summer TC and MC group sampling might not have been able to capture the true seasonal variation of $\delta^{13}\text{C-DIC}$ between all sites.

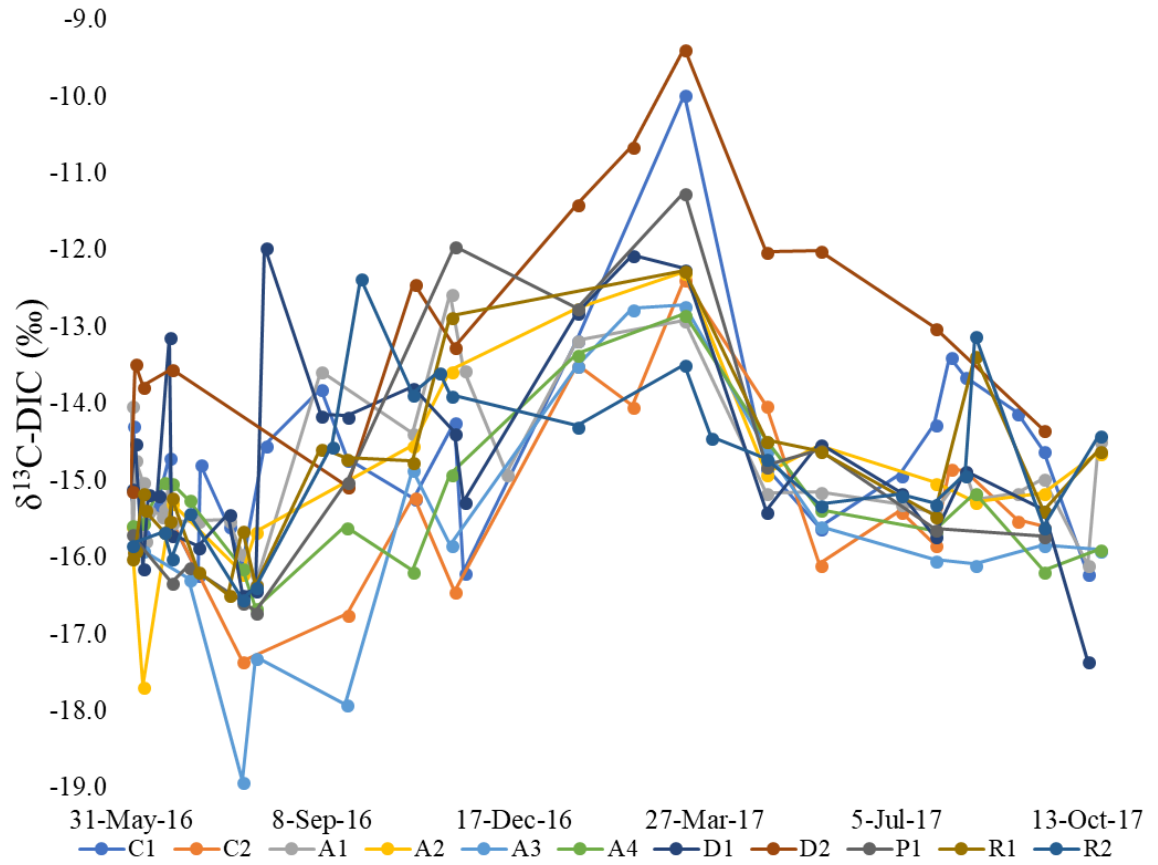


Figure 37: Time series of $\delta^{13}\text{C-DIC}$ for the RC group (May 2016- October 2017)

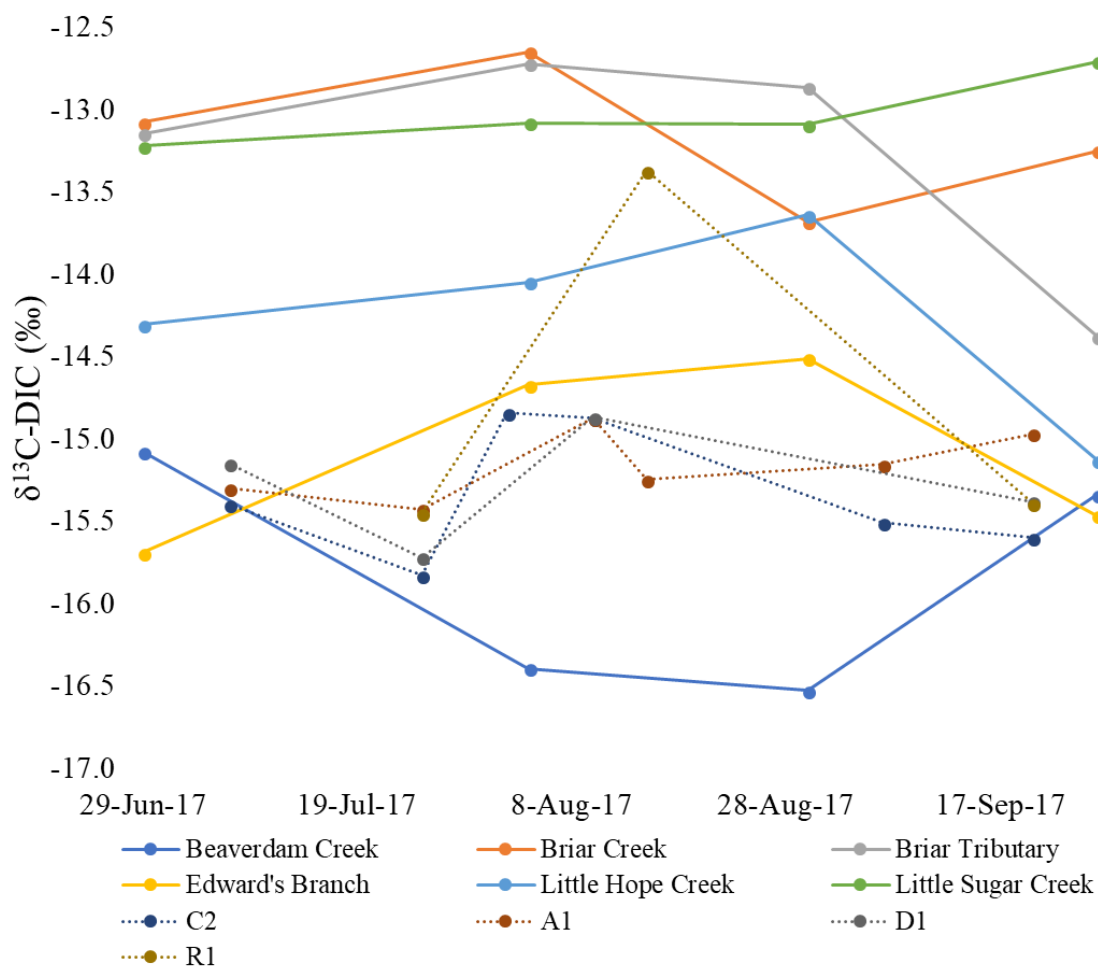


Figure 38: Time series of $\delta^{13}\text{C-DIC}$ for the MC group (June 2017- September 2017). Dotted lines represent RC values

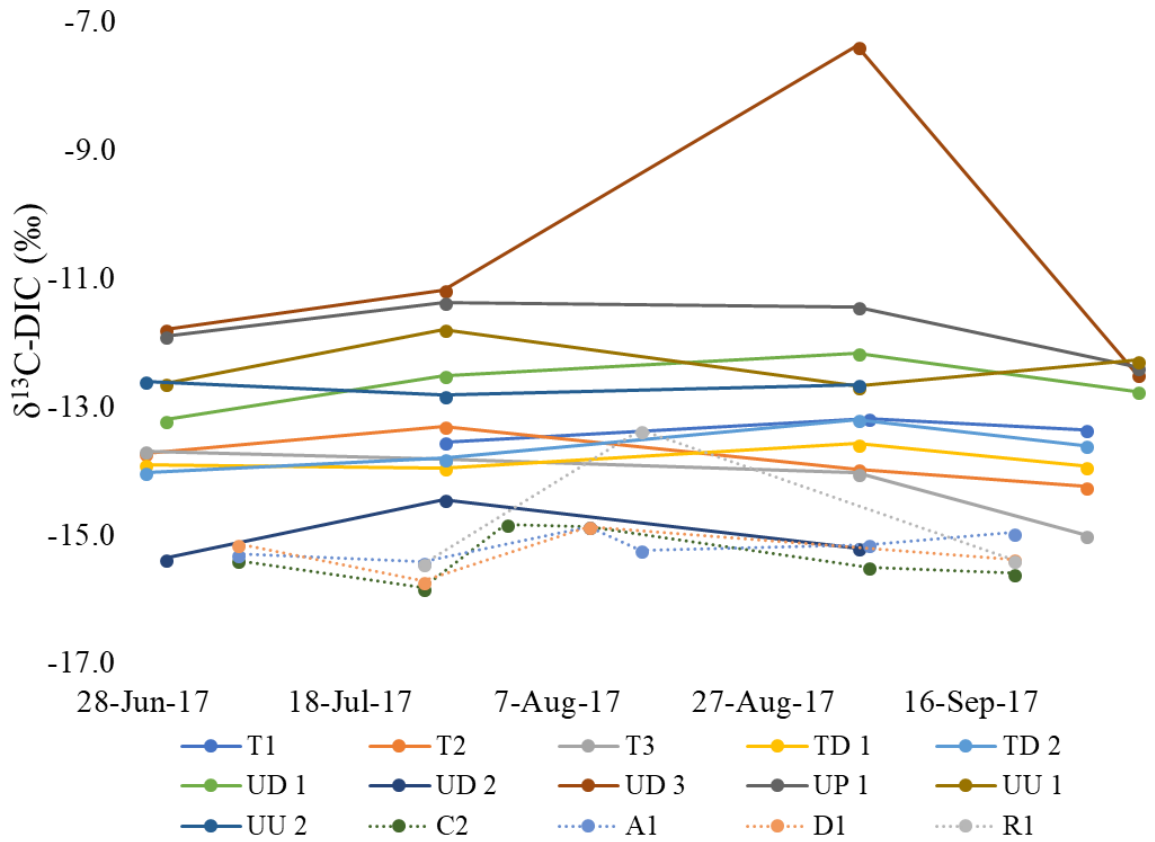


Figure 39: Time series of $\delta^{13}\text{C-DIC}$ for the TC group (June 2017- October 2017). Dotted lines represent RC values

Mean DOC, SUVA, alkalinity, DIC, and $\delta^{13}\text{C}$ -DIC are listed below (Table 6).

Table 6: Means and standard deviations of DOC and DIC concentrations, alkalinity, SUVA, and $\delta^{13}\text{C}$ -DIC for all 28 sampling sites (green highlight= undeveloped/forest, orange highlight=agriculture, purple highlight= urban/developed, unshaded=watershed outlet or mixed uses)

Group	Site	Mean DOC (mg/L)	Mean SUVA (L/mg*m)	Mean alkalinity (meq/L)	Mean DIC (mM)	Mean $\delta^{13}\text{C}$ -DIC (‰)
RC	C1	2.89±1.00	3.85±0.69	0.38±0.11	0.54±0.12	-14.8±1.41
RC	C2	2.83±1.44	4.16±0.78	0.35±0.09	0.51±0.14	-15.3±1.65
RC	A1	2.49±0.62	3.01±0.89	0.93±0.22	1.13±0.14	-14.9±1.10
RC	A2	2.48±1.55	8.26±7.19	0.86±0.06	0.94±0.22	-15.0±1.59
RC	A3	4.70±7.57	2.48±1.37	0.80±0.20	1.13±0.40	-15.5±1.96
RC	A4	3.75±4.92	3.70±1.90	0.95±0.17	1.07±0.31	-15.2±1.06
RC	R1	2.33±0.53	3.48±1.16	0.79±0.17	1.03±0.26	-15.2±1.11
RC	R2	3.00±1.72	2.68±1.23	0.82±0.17	0.99±0.17	-14.8±1.22
RC	D1	2.93±1.35	4.04±2.55	0.88±0.20	0.98±0.19	-14.6±1.39
RC	D2	4.00±1.00	3.23±0.42	1.09±0.33	1.11±0.35	-12.6±1.76
RC	P1	2.82±1.37	3.20±1.02	1.02±0.35	1.13±0.35	-14.7±1.91
MC	Beaverdam Creek	4.99±1.58	3.48±1.02	1.66±0.31	2.12±0.62	-15.8±0.73
MC	Briar Creek	2.98±1.31	3.63±0.68	1.45±0.22	1.60±0.25	-13.2±0.43
MC	Briar Tributary	2.93±0.71	3.27±0.58	1.80±0.28	1.75±0.11	-13.3±0.75
MC	Edward's Branch	1.74±0.57	3.83±1.29	1.16±0.013	1.33±0.049	-15.1±0.58
MC	Little Hope Creek	2.27±0.54	3.37±0.39	1.23±0.06	1.42±0.078	-14.3±0.63
MC	Little Sugar Creek	3.20±2.28	3.21±0.25	1.68±0.20	1.78±0.16	-13.0±0.22
TC	T1	3.23±0.51	3.01±0.27	1.77±0.19	2.01±0.18	-13.4±0.19
TC	T2	3.09±1.14	3.12±1.50	1.70±0.22	1.94±0.25	-13.8±0.39
TC	T3	4.02±4.03	2.96±1.10	1.68±0.35	1.76±0.17	-14.1±0.59
TC	TD 1	2.43±0.30	3.65±0.18	1.69±0.22	1.99±0.19	-13.8±0.18
TC	TD 2	3.29±1.69	3.82±1.60	1.57±0.28	1.90±0.25	-13.7±0.35
TC	UD 1	3.28±1.00	2.00±0.69	2.18±0.22	2.28±0.19	-12.7±0.44
TC	UD 2	3.89±0.28	2.93±0.23	2.20±0.87	2.21±0.57	-15.0±0.49
TC	UD 3	3.77±0.73	5.04±2.05	1.80±1.40	1.88±1.37	-10.7±2.29
TC	UP 1	3.80±0.57	2.71±0.49	1.62±0.42	1.50±0.42	-11.8±0.47
TC	UU 1	3.68±1.73	2.99±0.72	1.93±0.61	1.92±0.49	-12.4±0.41
TC	UU 2	2.70±0.66	2.77±0.42	1.59±0.21	1.60±0.17	-12.7±0.12

4.5 Cation and anion concentrations

4.5.1 Cations

Major cation and anion concentrations were sampled as additional measures of water quality along an urbanization gradient. R1 and R2 (RC group) had the lowest Na⁺ concentration of 1.9 ppm. Of the RC group, A1 and D2 had the highest Na⁺ concentrations of 12.1 and 12.2 ppm. Control sites (C1 and C2) Na⁺ concentration ranged from 2.5 ppm to 8.8 ppm. UU1, UP 1, and UD 3 (TC group) had the highest Na⁺ concentrations of 22.2 ppm, 22.9 ppm, and 23.5 ppm, respectively (Figure 40). In general, Na⁺ concentration increases as percent impervious cover increases. K⁺ concentration was lowest at R2 and R1 (RC group) at 0.5 ppm. UU1 (TC group) had the highest K⁺ concentration of 6.5 ppm. The control sites had K⁺ concentrations ranging from 0.49 ppm to 1.09 ppm. UD 2 and UD 1 had some of the highest K⁺ concentrations of 5.4 ppm and 4.9 ppm, respectively (Figure 41). Overall, K⁺ concentrations are increasing with increasing percent impervious cover. Control sites (C1 and C2) had the lowest Mg²⁺ concentrations of 0.8 ppm and 1.0 ppm. UP 1, UU 1, and UD 3 (TC group) had the highest Mg²⁺ concentrations of 16.1 ppm, 16.4 ppm, and 16.8 ppm, respectively. Control sites Mg²⁺ concentrations ranged from 0.8 ppm (C1) to 7.8 ppm (C2). There appears to be an increase in Mg²⁺ concentration as percent impervious cover increases (Figure 42). C2 and C1 (control sites) had the lowest Ca²⁺ concentrations of 2.4 ppm and 2.5 ppm. UD 2 and UD 3 (TC group) had the highest Ca²⁺ concentrations of 37.8 ppm and 37.9 ppm. Ca²⁺ concentrations ranged from 2.4 ppm to 16.2 at the control sites. Overall, Ca²⁺ concentrations are increasing with increasing percent impervious cover (Figure 43).

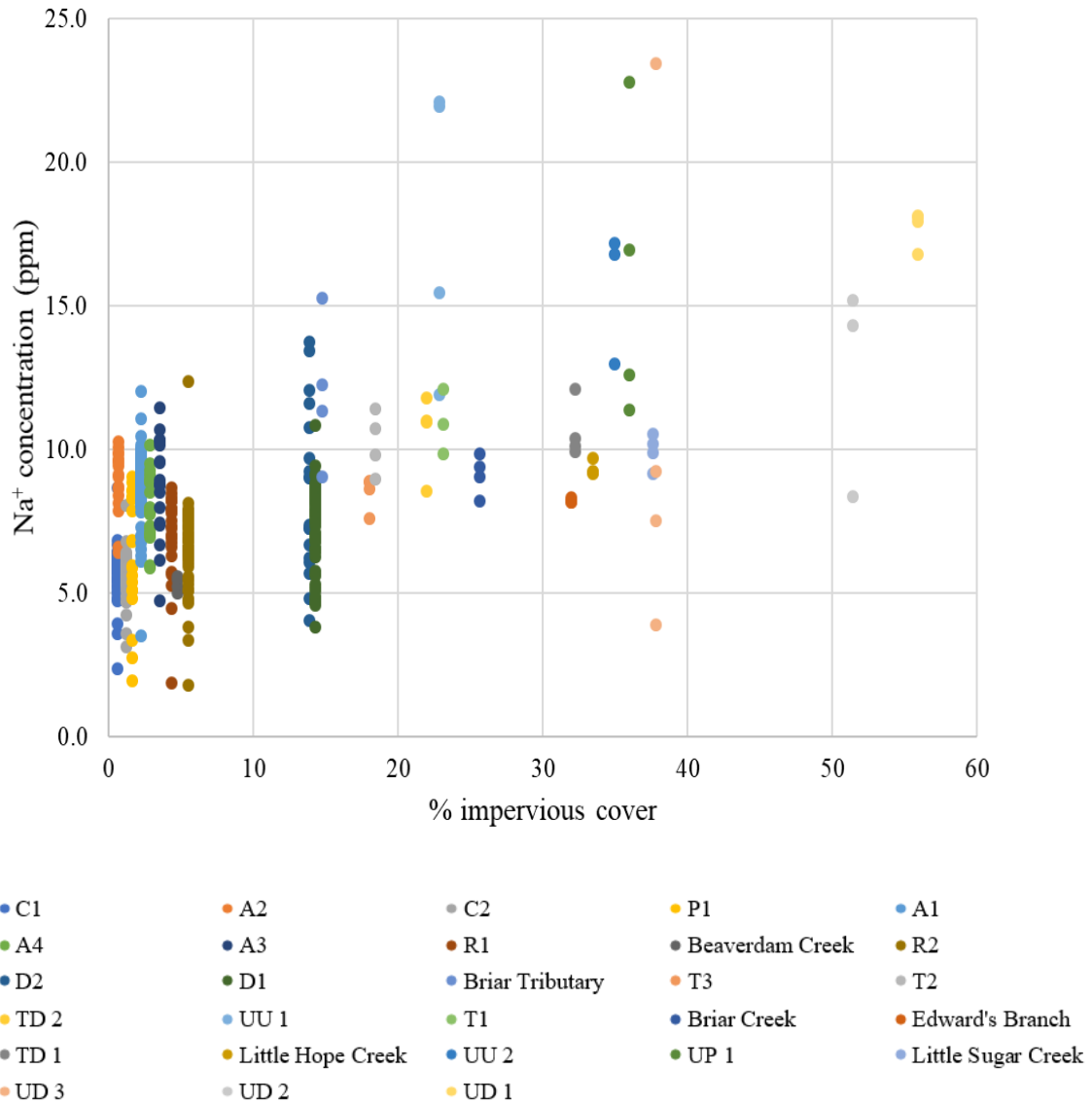


Figure 40: Sodium (Na⁺) concentration vs. percent impervious cover (May 2016- October 2017)

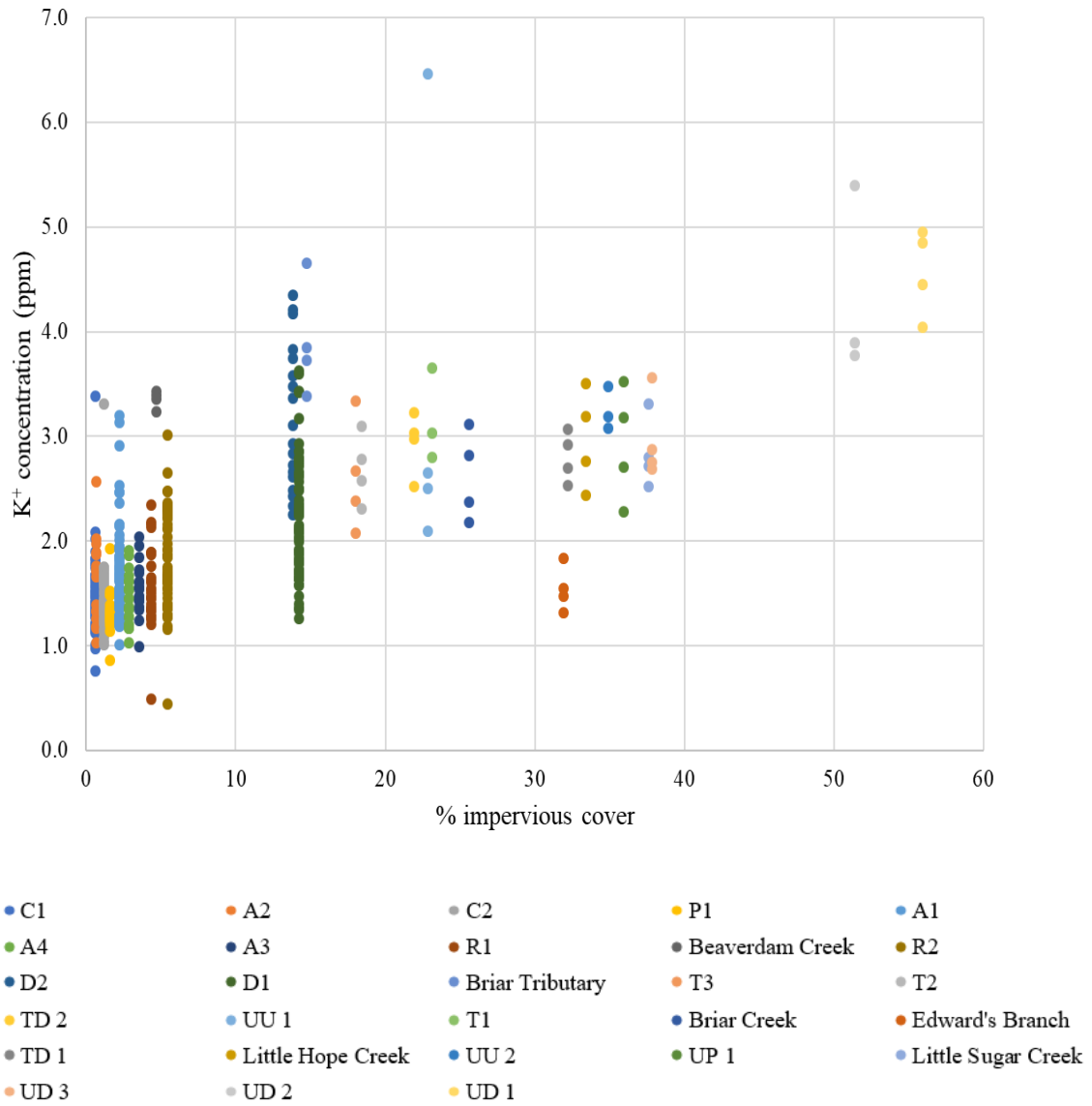


Figure 41: Potassium (K^+) concentration vs. percent impervious cover (May 2016- October 2017)

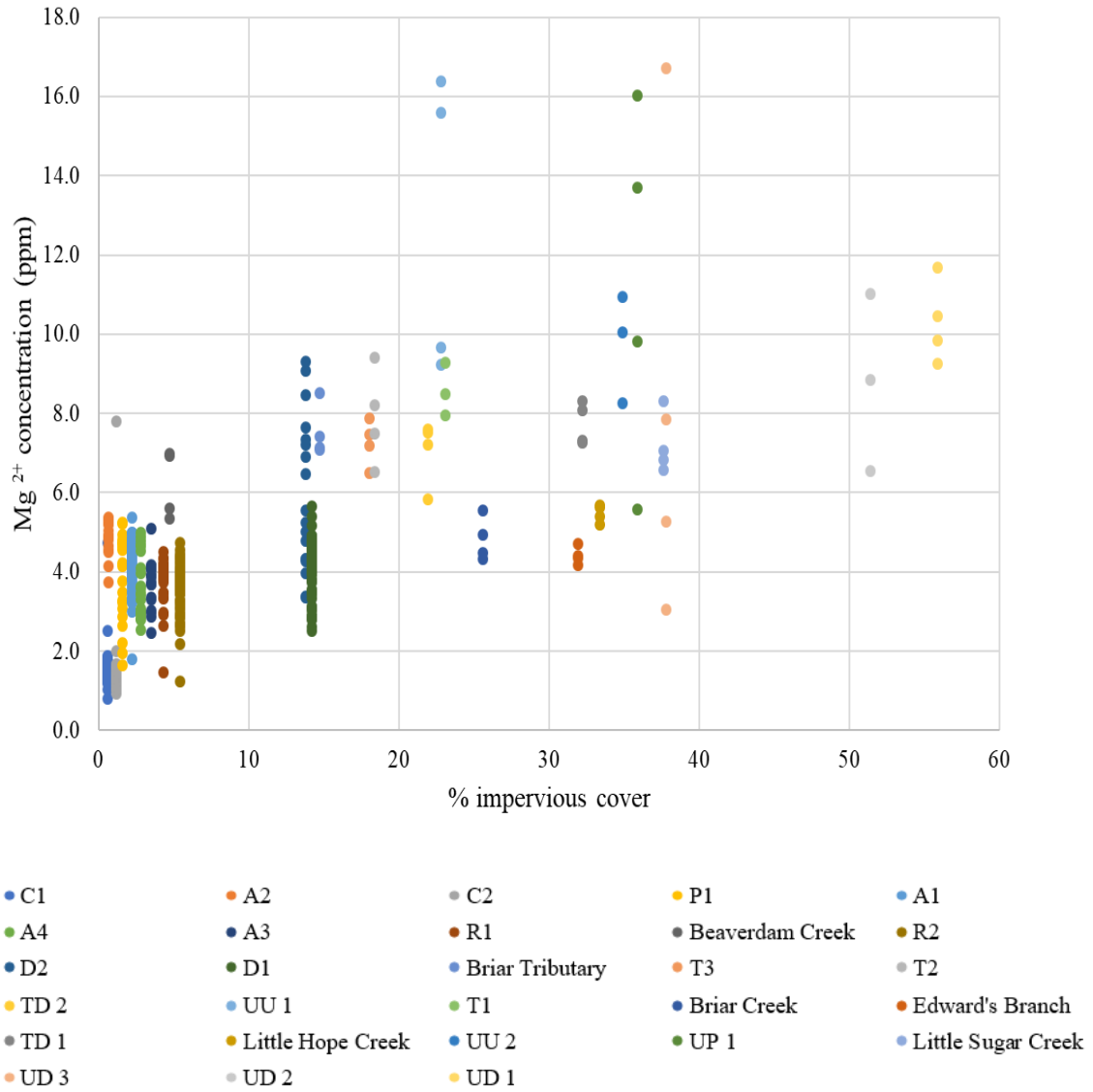


Figure 42: Magnesium (Mg²⁺) concentration vs. percent impervious cover (May 2016- October 2017)

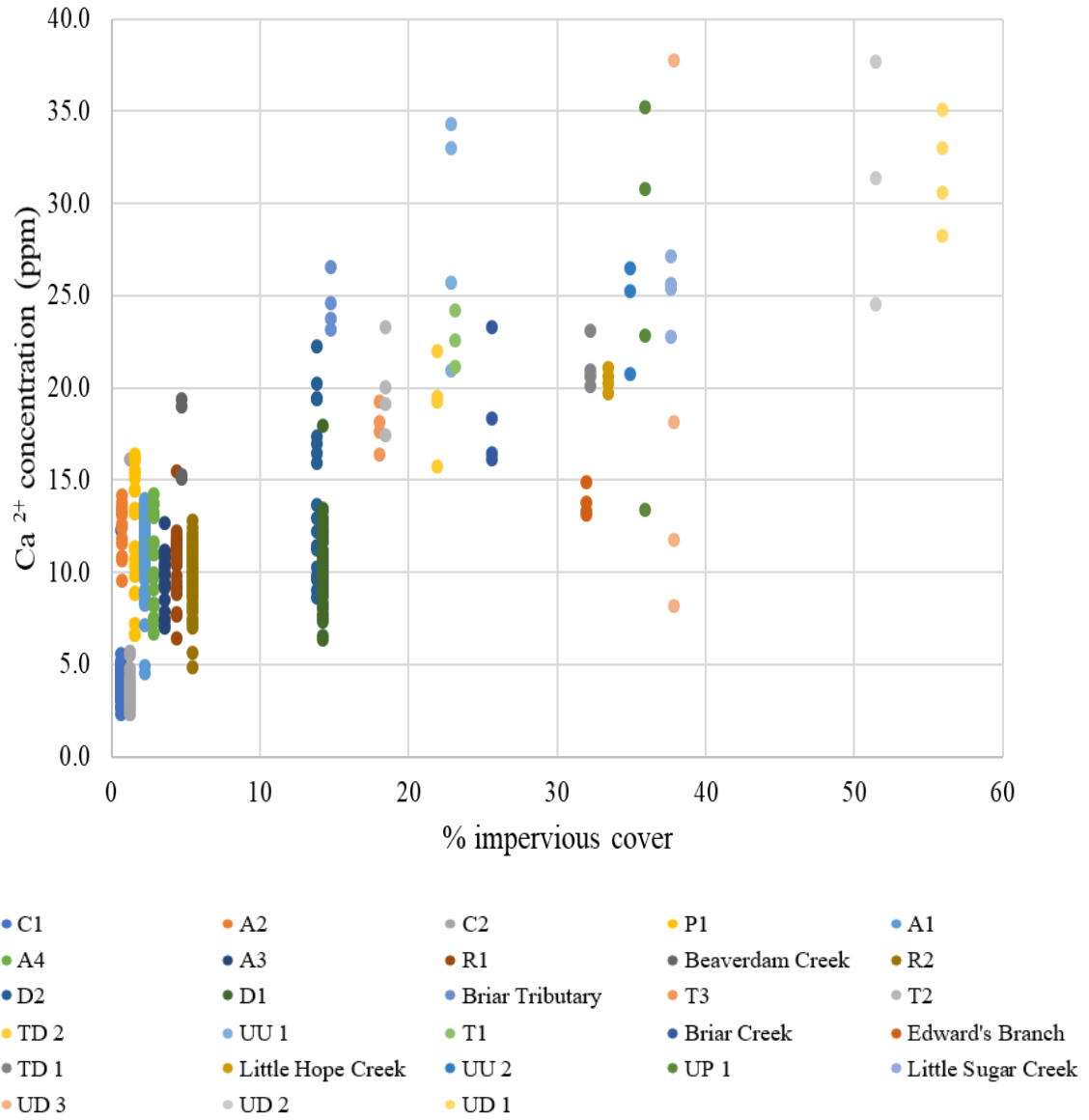
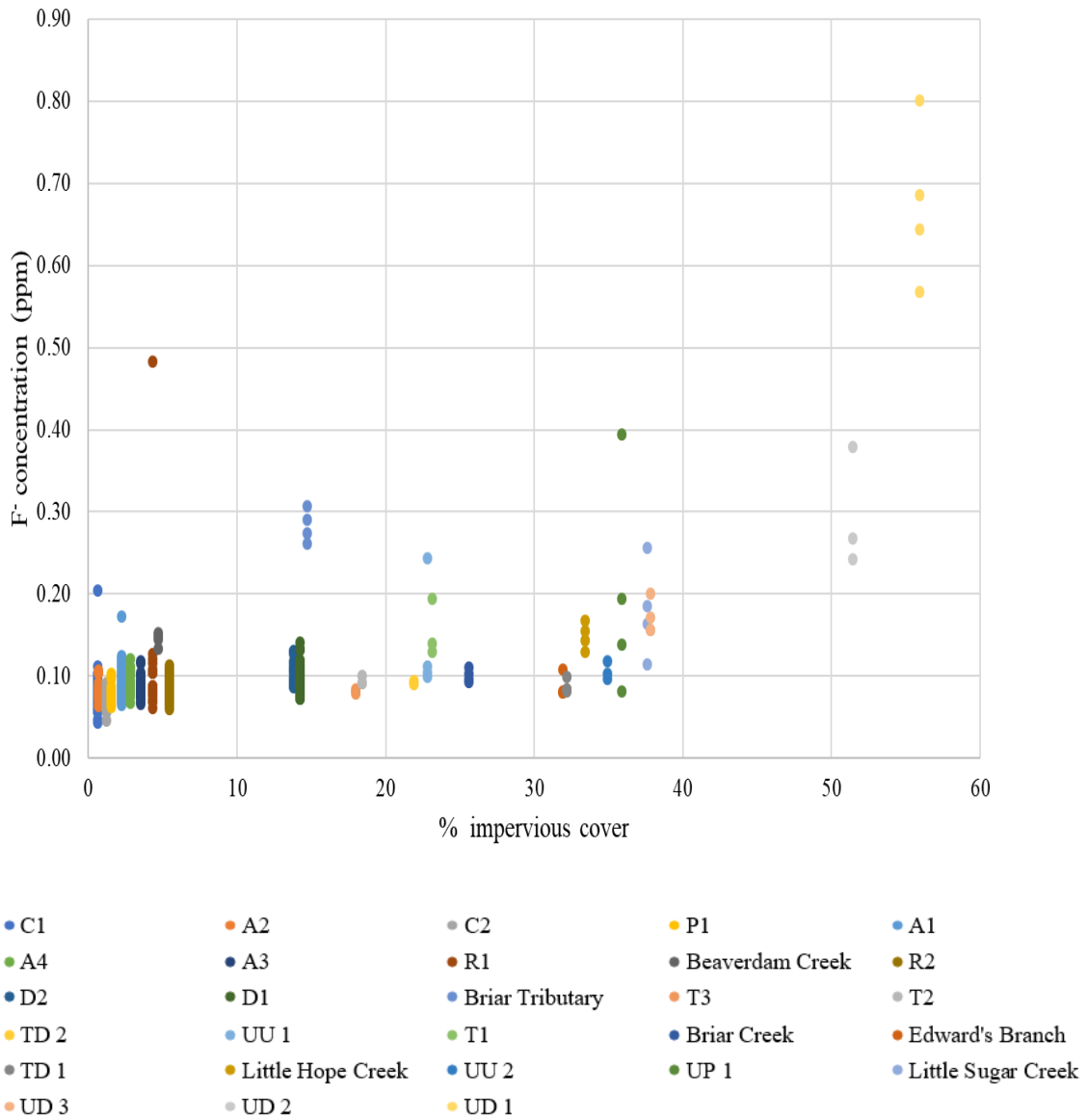


Figure 43: Calcium (Ca^{2+}) concentration vs. percent impervious cover (May 2016- October 2017)

4.5.2 Anions

Control sites, C1 and C2, had the lowest F^- concentration of 0.05 ppm. UD 1 (TC group) had the highest F^- concentration of 0.80 ppm. F^- concentration is increasing as percent impervious cover increases (Figure 44). P1 (RC group) had the lowest Cl^- concentration of 1.81 ppm. UP 1 had the highest Cl^- concentrations of 42.1 ppm and 51.9 ppm. Control sites, C1 and C2, had Cl^- concentrations ranging from 2.76 ppm to 6.51. There is an observable pattern of Cl^- concentrations increasing as percent impervious cover increases (Figure 45). A3 (RC group) had the highest NO_3^- concentration of 5.93 ppm. A2 had high NO_3^- concentrations of 2.90 ppm, 2.88 ppm, and 2.86 ppm. UP 1 had the lowest NO_3^- concentration of 0.02 ppm (Figure 46). Briar Tributary (MC group) had the highest PO_4^{3-} concentration of 0.43 ppm. Control sites (C1 and C2) had PO_4^{3-} concentrations ranging from 0.0 ppm to 0.29 ppm. There appears to be a slight negative correlation between PO_4^{3-} concentration and percent impervious cover. Overall, PO_4^{3-} concentration is decreasing with increasing percent impervious cover (Figure 47). UD 1 (TC group) had the highest SO_4^{2-} concentrations of 32.9 ppm, 29.8 ppm, and 26.8 ppm. C1 and C2 (control sites) had the lowest SO_4^{2-} concentrations of 0.90 ppm and 0.91 ppm. Overall, SO_4^{2-} concentration is increasing as percent impervious cover is increasing (Figure 48). There is no trend in fluoride/chloride ratios (Figure 49).



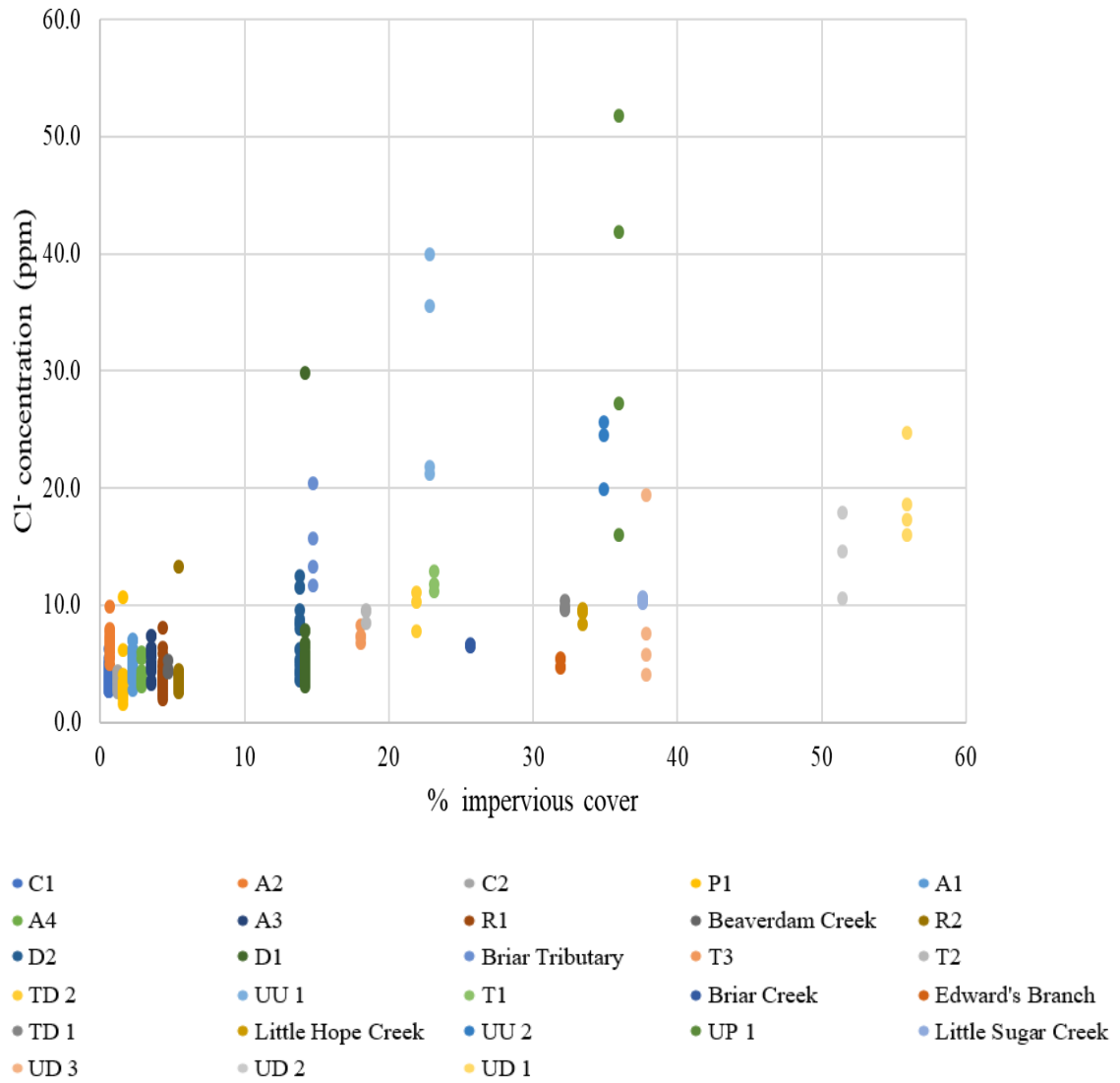


Figure 45: Chloride (Cl⁻) concentration vs. percent impervious cover (May 2016- October 2017)

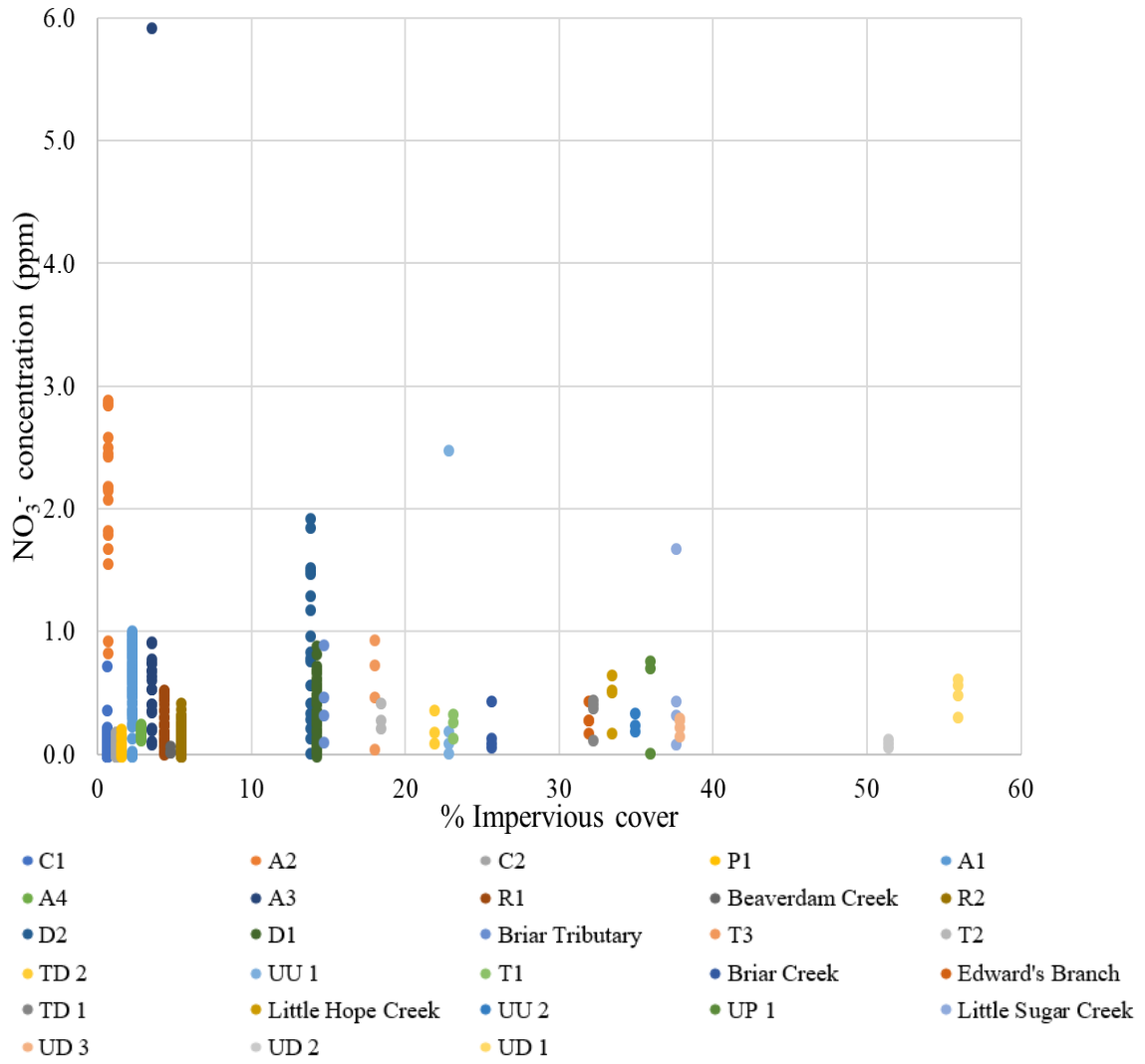
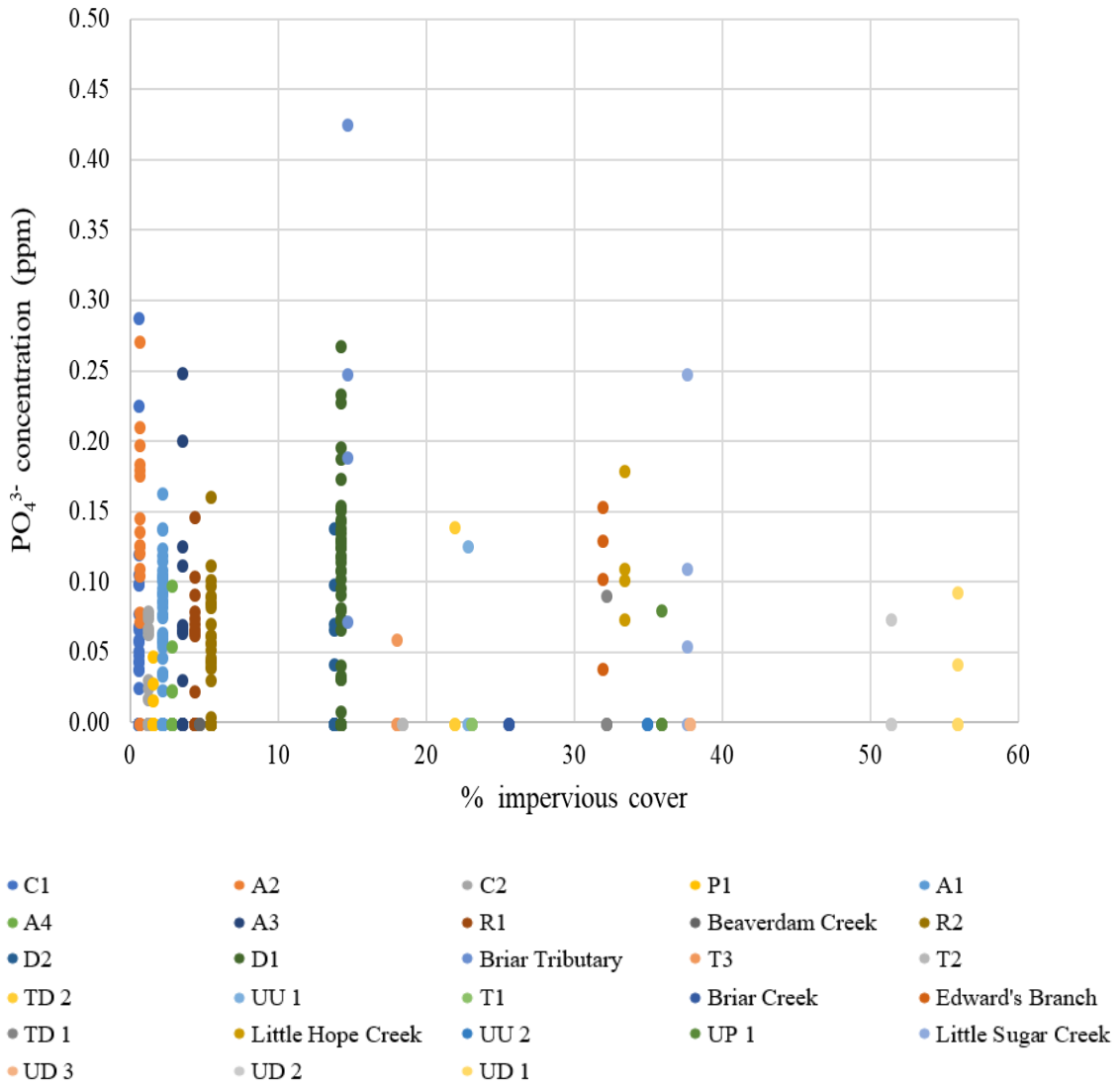


Figure 46: Nitrate concentration (NO₃⁻) vs. percent impervious cover (May 2016- October 2017). Nondetectable concentrations are plotted as zero.



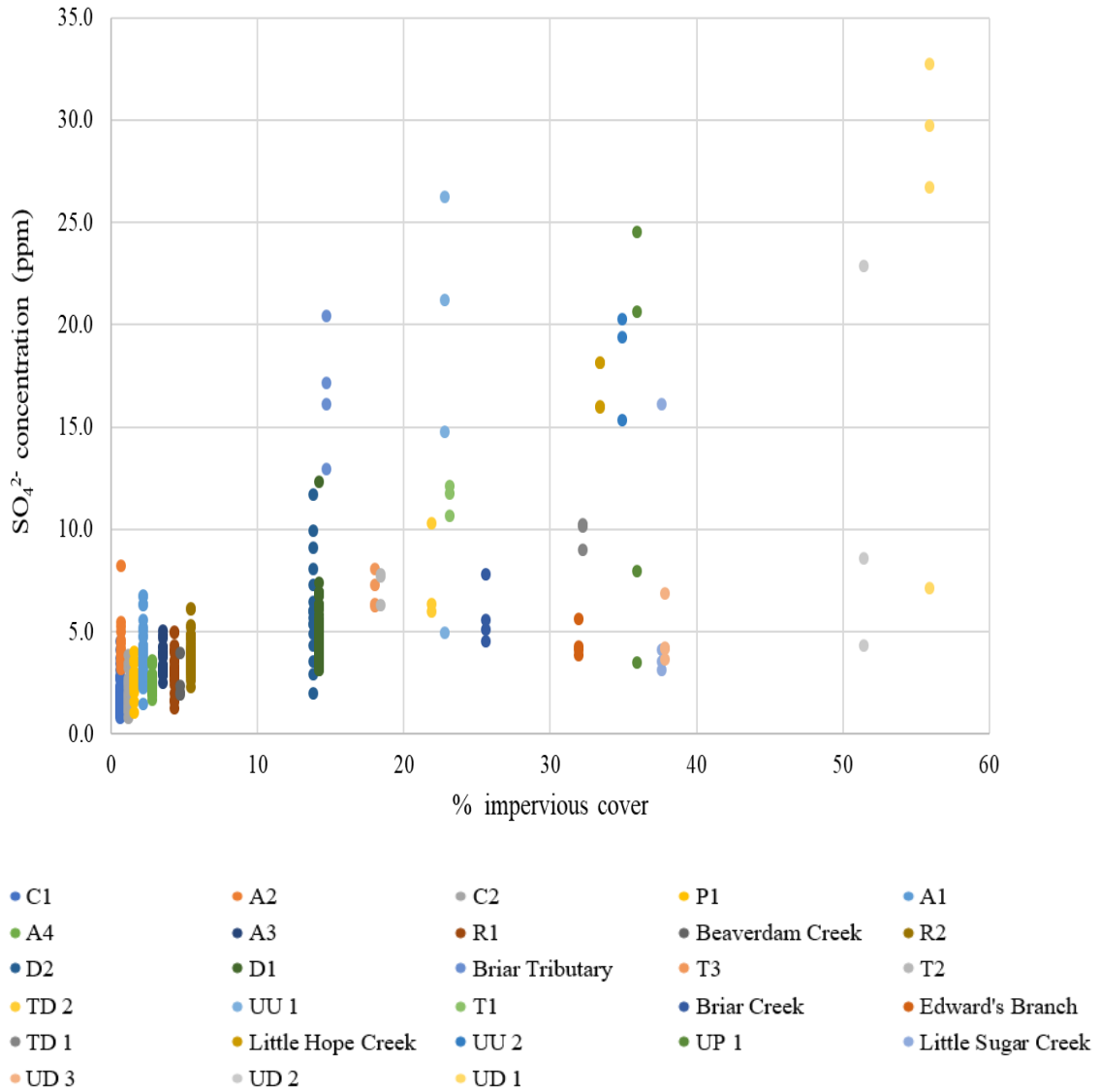


Figure 48: Sulfate (SO_4^{2-}) concentration (in ppm) vs. percent impervious cover (May 2016-October 2017)

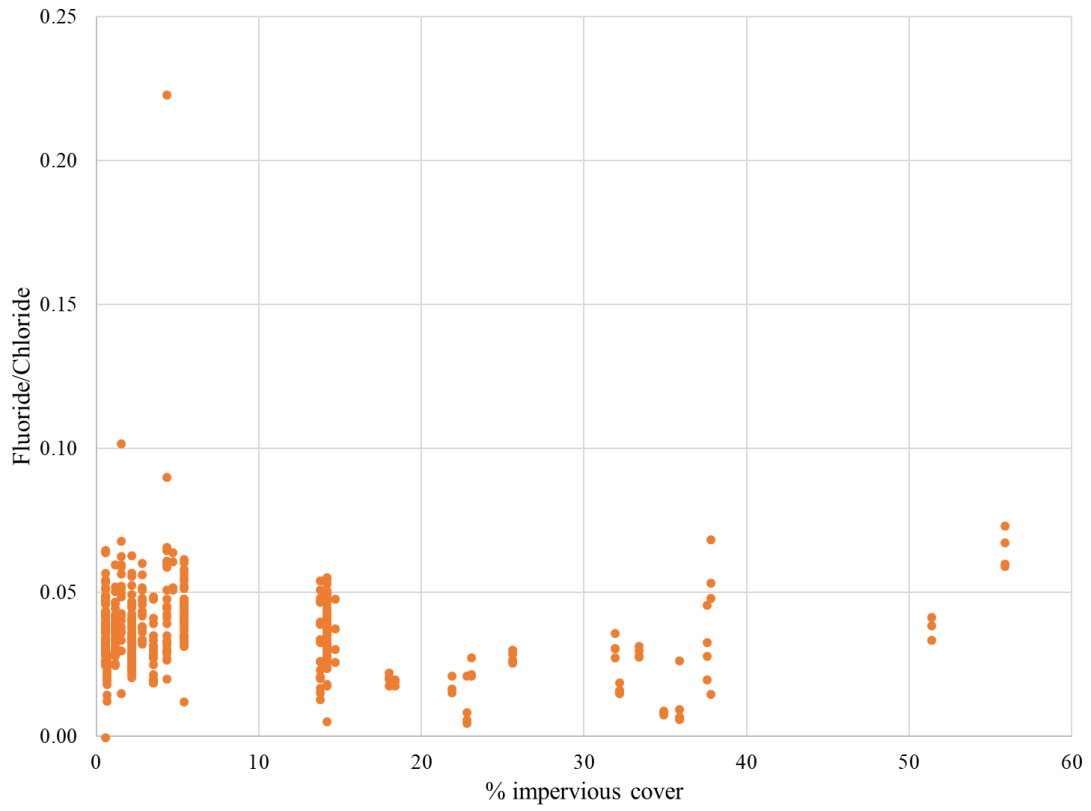


Figure 49: Fluoride/Chloride ratio vs. percent impervious cover (May 2016- October 2017)

Mean cation and anion concentrations are listed below in Table 7 and Table 8.

Table 7: Means and standard deviations of cation concentrations (Na, K⁺, Mg²⁺, and Ca²⁺) for the 28 sampling sites (green highlight= undeveloped/forest, orange highlight=agriculture, purple highlight= urban/developed, unshaded=watershed outlet or mixed uses)

Group	Site	Mean Na ⁺ (ppm)	Mean K ⁺ (ppm)	Mean Mg ²⁺ (ppm)	Mean Ca ²⁺ (ppm)
RC	C1	5.64±1.32	1.36±0.48	2.07±1.30	5.41±3.40
RC	C2	5.63±0.71	1.47±0.33	1.40±0.21	3.70±0.73
RC	A1	8.73±2.27	1.47±0.67	3.92±0.93	10.6±2.70
RC	A2	8.98±1.13	1.61±0.41	4.92±0.44	12.7±1.28
RC	A3	8.83±1.68	1.56±0.24	3.74±0.59	9.58±1.60
RC	A4	8.01±1.16	1.48±0.24	3.72±0.81	10.2±2.45
RC	R1	7.19±1.46	1.59±0.37	3.80±0.64	10.9±1.78
RC	R2	7.03±1.76	1.69±0.55	4.29±1.62	11.3±3.58
RC	D1	7.29±2.15	2.08±0.66	3.84±0.89	10.2±2.43
RC	D2	8.40±2.99	3.25±0.71	5.84±1.96	14.1±4.39
RC	P1	7.44±4.11	1.36±0.52	3.84±1.47	11.5±4.50
MC	Beaverdam Creek	5.39±0.26	3.37±0.08	6.27±0.86	17.3±2.33
MC	Briar Creek	9.20±0.69	2.64±0.42	4.88±0.56	18.7±3.31
MC	Briar Tributary	12.1±2.58	3.92±0.54	7.59±0.67	24.6±1.48
MC	Edwards Branch	8.31±0.07	1.56±0.22	4.46±0.22	13.9±0.80
MC	Little Hope Creek	9.42±0.25	2.99±0.47	5.52±0.22	20.6±0.57
MC	Little Sugar Creek	10.0±0.58	2.86±0.33	7.24±0.77	25.4±1.81
TC	T1	11.02±1.11	3.18±0.44	8.62±0.66	22.8±1.55
TC	T2	10.31±1.07	2.71±0.33	7.96±1.21	20.11±2.46
TC	T3	8.57±5.55	2.63±5.73	7.30±6.03	17.99±6.39
TC	TD 1	10.72±1.01	2.82±0.24	7.79±0.53	21.33±1.30
TC	TD 2	10.66±1.41	2.96±0.29	7.09±0.82	19.25±2.58
TC	UD 1	17.82±0.63	4.59±0.42	10.36±1.04	31.87±2.96
TC	UD 2	12.70±3.72	4.38±0.90	8.85±2.24	31.32±6.59
TC	UD 3	11.12±8.57	2.99±0.40	8.27±5.98	19.11±13.20
TC	UP 1	16.01±5.17	2.94±0.54	11.33±4.58	25.71±9.58
TC	UU 1	17.93±5.02	3.45±2.03	12.77±3.79	28.62±6.29
TC	UU 2	15.74±2.32	3.27±0.21	9.81±1.37	24.31±3.01

Table 8: Means and standard deviations of anion concentrations (F⁻, Cl⁻, NO₃⁻, PO₄³⁻, SO₄²⁻) for the 28 sampling sites. Where a peak was not detected, a concentration of 0 was used to calculate means. (green highlight= undeveloped/forest, orange highlight=agriculture, purple highlight= urban/developed, unshaded=watershed outlet or mixed uses)

Group	Site	Mean F ⁻ (ppm)	Mean Cl ⁻ (ppm)	Mean NO ₃ ⁻ (ppm as N)	Mean PO ₄ ³⁻ (ppm)	Mean SO ₄ ²⁻ (ppm)
RC	C1	0.08± 0.02	3.56± 0.79	0.11±0.18	0.02±0.05	5.01±8.20
RC	C2	0.07± 0.01	3.52± 0.36	0.08±0.05	0.01±0.03	1.77±0.67
RC	A1	0.09± 0.02	4.83±1.13	0.56±0.3	0.08±0.1	3.82±1.17
RC	A2	0.09± 0.01	7.05±1.15	2.12±0.59	0.13±0.07	4.46±1.16
RC	A3	0.09± 0.01	5.66±1.06	0.74±1.16	0.05±0.07	3.69±0.69
RC	A4	0.09± 0.01	4.04± 0.74	0.19±0.04	0.01±0.03	2.65±0.57
RC	R1	0.11± 0.07	4.09±1.26	0.26±0.16	0.03±0.04	3.25±0.86
RC	R2	0.09± 0.02	3.88±1.26	0.13±0.11	0.04±0.06	3.83±1.25
RC	D1	0.09± 0.02	4.88±3.19	0.32±0.23	0.06±0.07	4.88±1.71
RC	D2	0.11± 0.14	7.05±2.92	0.87±0.59	0.02±0.4	6.22±2.43
RC	P1	0.09± 0.27	3.28±1.74	0.07±0.06	0.003±0.01	4.23±2.27
MC	Beaverdam Creek	0.15± 0.01	4.78± 0.48	0.05±0.03	<0.01	2.67±0.95
MC	Briar Creek	0.10± 0.01	6.78± 0.07	0.19±0.18	<0.01	5.85±1.42
MC	Briar Tributary	0.29± 0.02	15.5±3.8	0.46±0.3	0.23±0.15	16.8±3.07
MC	Edward's Branch	0.09± 0.01	5.27± 0.36	0.31±0.11	0.11±0.05	4.56±0.79
MC	Little Hope Creek	0.15± 0.02	9.42± 0.58	0.48±0.20	0.12±0.05	17.2±1.3
MC	Little Sugar Creek	0.18± 0.06	10.6± 0.23	0.64±0.71	0.10±0.11	6.83±6.27
TC	T1	0.16±0.04	12.2±0.9	0.25±0.10	<0.01	11.6±0.7
TC	T2	0.10±0.01	9.40±0.63	0.32±0.11	<0.01	7.38±0.83
TC	T3	0.08±3.50	7.62±3.64	0.55±3.40	0.02±3.83	7.10±0.87
TC	TD 1	0.09±0	10.1±0.4	0.35±0.15	0.02±0.05	10.0±0.6
TC	TD 2	0.09±0	9.95±1.72	0.22±0.14	0.05±0.08	7.66±2.40
TC	UD 1	0.68±0.10	19.3±3.9	0.51±0.14	0.03±0.05	24.2±11.6
TC	UD 2	0.30±0.07	14.6±3.7	0.10±0.04	0.02±0.04	12.0±9.7
TC	UD 3	0.17±0.02	9.40±6.97	0.25±0.07	<0.01	4.82±1.45

Group	Site	Mean F ⁻ (ppm)	Mean Cl ⁻ (ppm)	Mean NO ₃ ⁻ (ppm as N)	Mean PO ₄ ³⁻ (ppm)	Mean SO ₄ ²⁻ (ppm)
TC	UP 1	0.21±0.14	34.4±15.8	0.41±0.39	0.02±0.04	14.3±10.0
TC	UU 1	0.14±0.07	29.8±9.6	0.70±1.19	0.03±0.06	16.9±9.2
TC	UU 2	0.11±0.01	23.5±3.0	0.27±0.07	<0.01	18.4±2.6

4.6 Correlation coefficients

From Table 8, pH, DIC concentration, $\delta^{13}\text{C}$ -DIC (‰), alkalinity, DOC flux, DIC flux Na⁺, K⁺, Mg²⁺, Ca²⁺, F⁻, Cl⁻, and SO₄²⁻ have strong positive correlations with percent impervious cover. This means that as percent impervious cover increases, those parameters also increase. DOC concentration and SUVA have weak negative correlations with percent impervious cover. F/Cl ratio also has a weak negative correlation with percent impervious cover. NO₃⁻ and PO₄³⁻ are not significantly correlated with percent impervious cover (correlation coefficient is close to 0).

Table 9: Correlation coefficient of multiple parameters versus percent impervious cover. Green shading indicates there is an association between the two parameters and red shading indicates there is no association.

Percent impervious cover versus:	Correlation coefficient
DOC concentration (mg/L)	-0.17
SUVA (L/mg*m)	-0.15
pH	0.42
DIC concentration (mM)	0.62
$\delta^{13}\text{C}$ -DIC (‰)	0.60
Alkalinity (meq/L)	0.71
DOC flux (kg C/ha/yr)	0.67
DIC flux (kg C/ha/yr)	0.72
Na ⁺ (ppm)	0.56
K ⁺ (ppm)	0.69
Mg ²⁺ (ppm)	0.68
Ca ²⁺ (ppm)	0.74
F ⁻ (ppm)	0.61
Cl ⁻ (ppm)	0.60
SO ₄ ²⁻ (ppm)	0.71
NO ₃ ⁻ (ppm)	0.01
PO ₄ ³⁻ (ppm)	0.09
Fluoride/Chloride	-0.13

4.7 Percent forest cover

In addition to impervious cover, forest cover was used to better understand trends in the data. DOC concentration, SUVA, DIC concentration, alkalinity, and $\delta^{13}\text{C}$ -DIC were plotted against percent forest cover (Figure 50, Figure 51, Figure 52, Figure 53, and Figure 54). The expectation is the opposite trend when percent impervious cover is used. Figure 50, DOC concentration weakly increased with increased percent forest cover (correlation coefficient 0.2). Figure 51, there is no obvious trend between percent forest cover and SUVA values. The correlation coefficient is 0.06, suggesting that there is no significant correlation between the two. Both DIC concentration and alkalinity concentration decreased with increased percent forest cover (Figure 52 and Figure 53). Both have correlation coefficients of -0.6: DIC concentration and alkalinity concentration have a strong negative relationship with percent forest cover. $\delta^{13}\text{C}$ -DIC also has a strong negative relationship with percent forest cover (correlation coefficient -0.55). As percent forest cover increases, $\delta^{13}\text{C}$ -DIC becomes more negative (Figure 54).

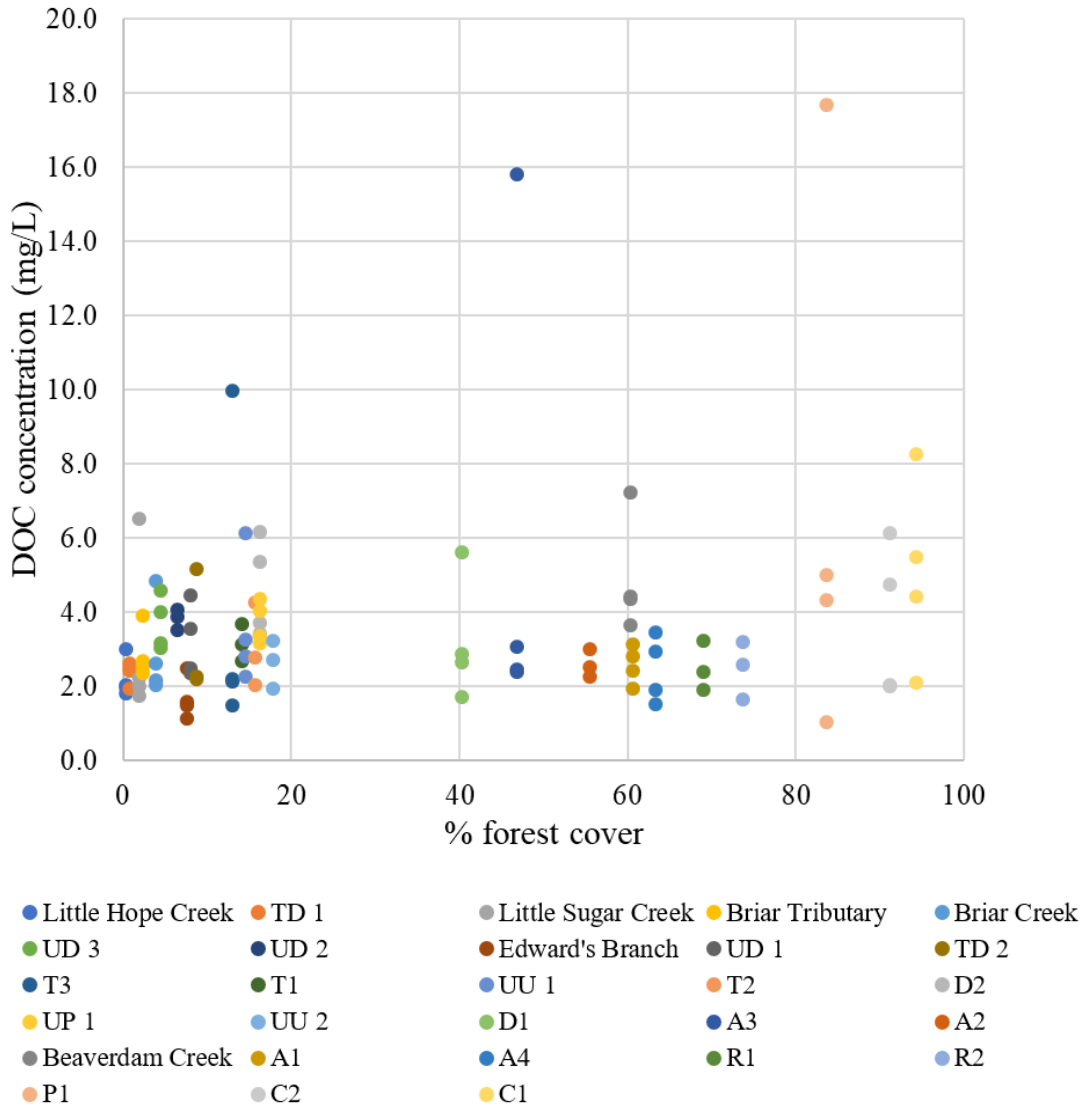


Figure 50: Percent forest cover vs. DOC concentration (June 2017- October 2017)

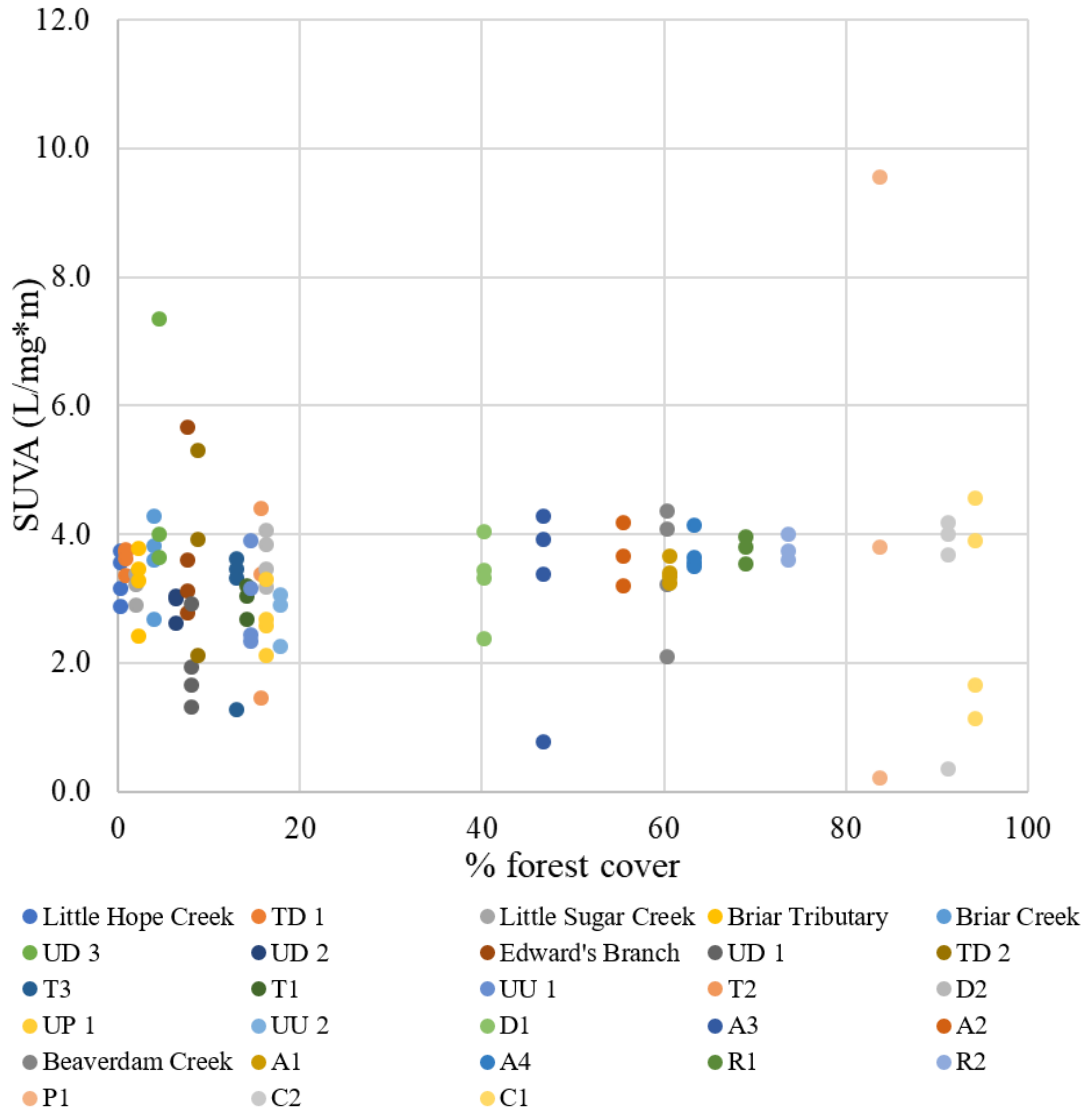
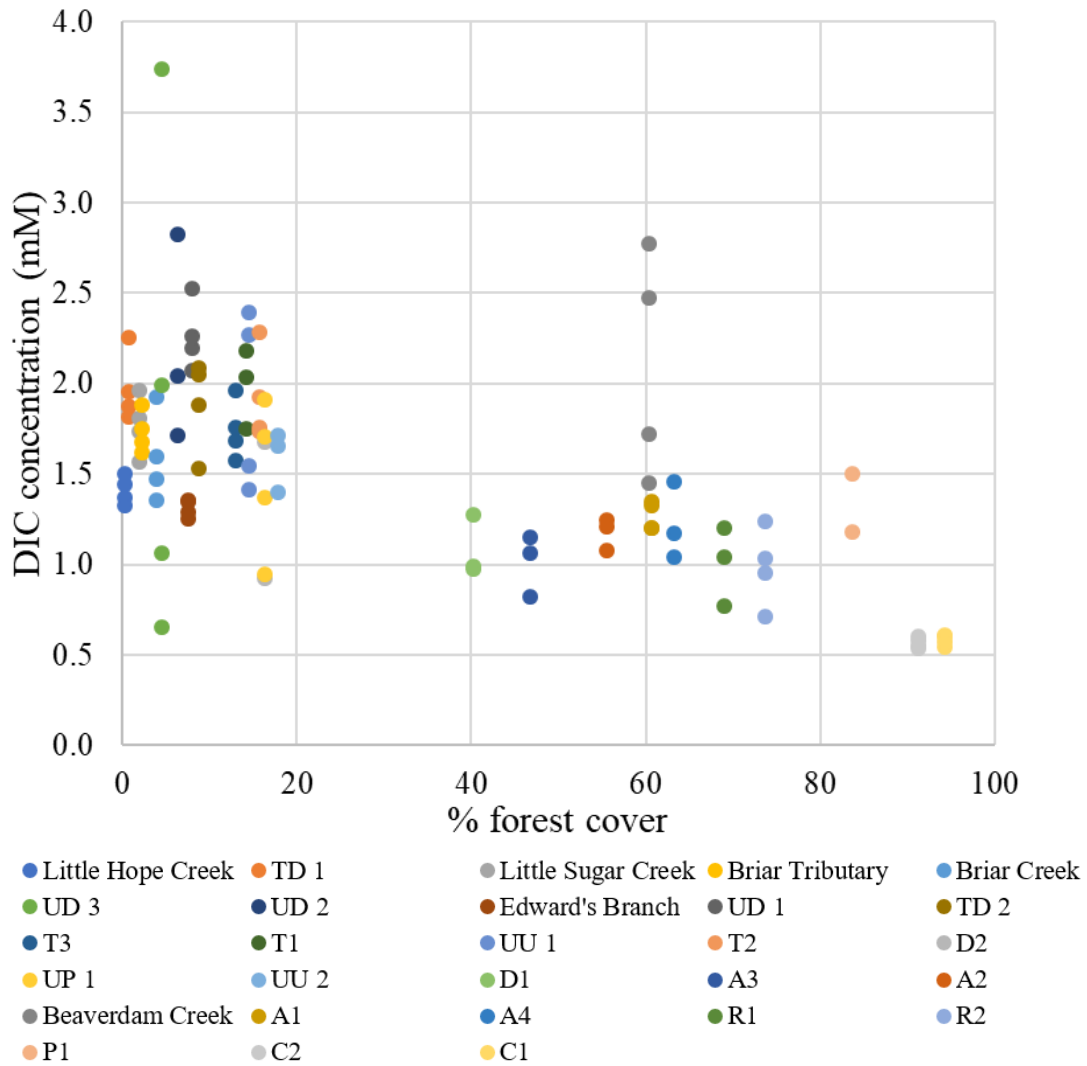


Figure 51: Percent forest cover vs. SUVA (June 2017- October 2017)



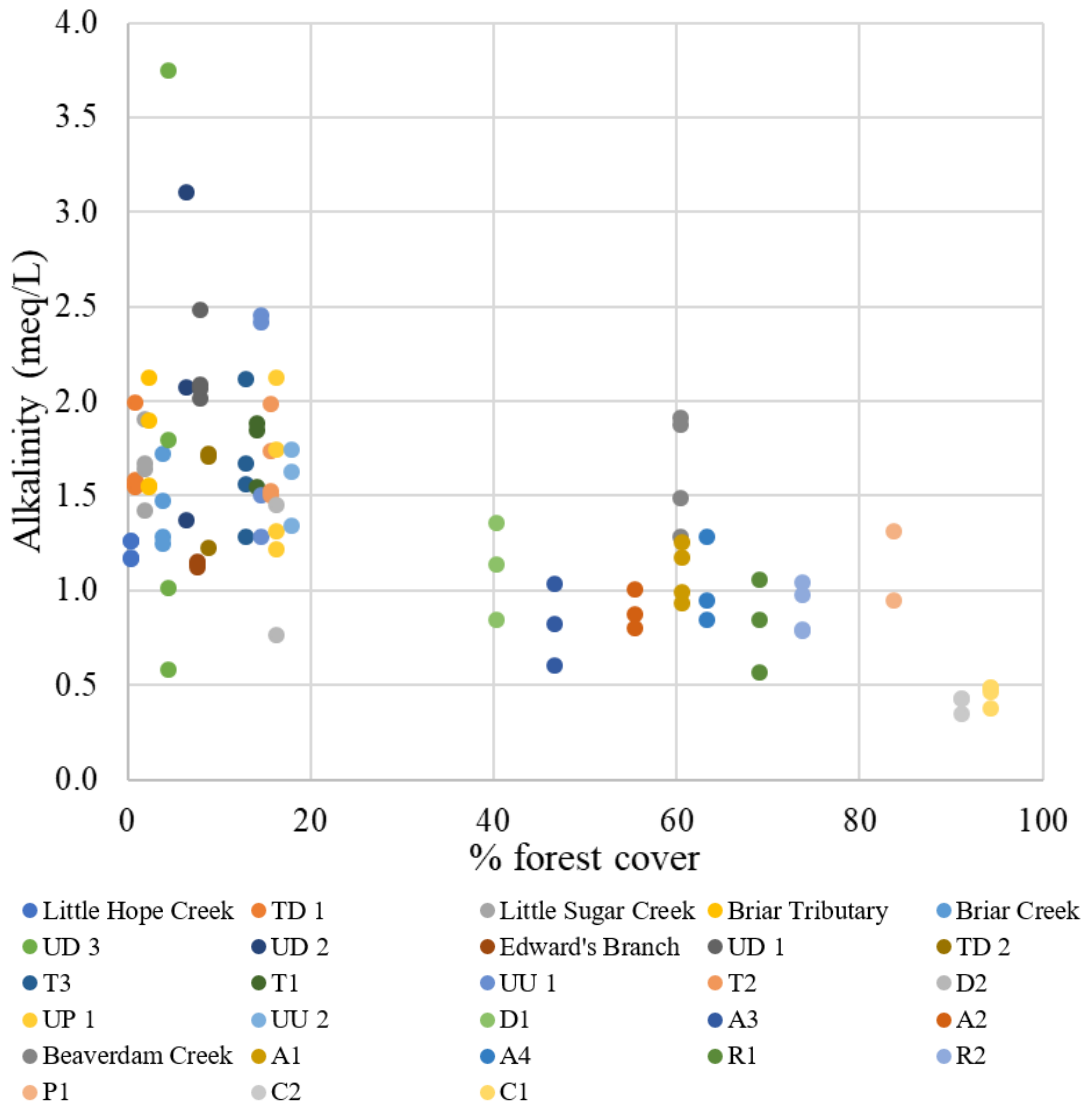
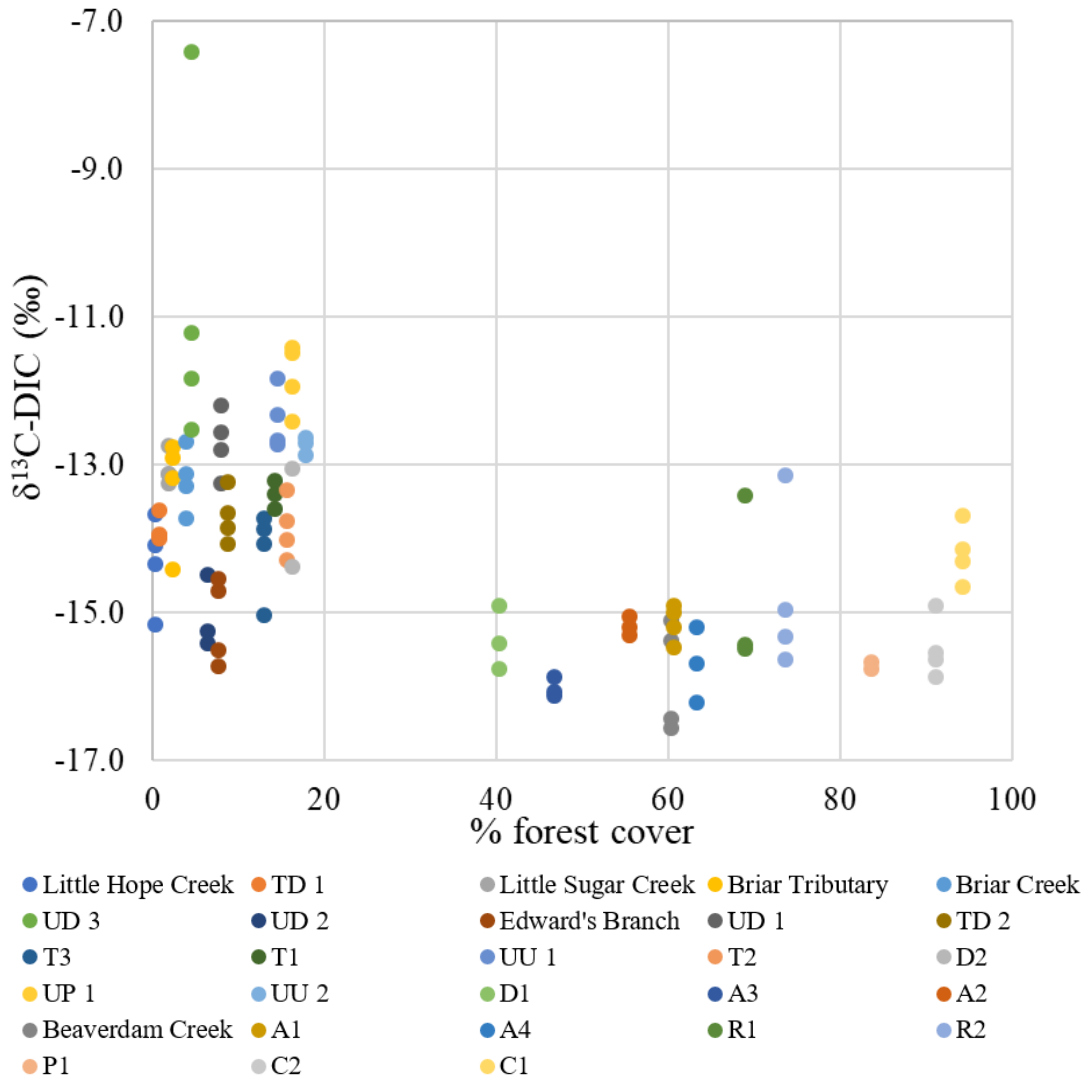


Figure 53: Percent forest cover vs. alkalinity concentration (June 2017- October 2017)



5. Discussion

5.1 Watershed-scale discharge

Watershed area, discharge, and amount of impervious cover are important components when understanding concentrations fluxes. Figure 55 and Figure 56 express how estimated annual baseflow (m^3/year) is correlated with watershed area and percent impervious cover. From Figure 55, there was a strong positive relationship between log watershed area (hectares) and log estimated annual baseflow (m^3/year) (correlation coefficient 0.74). A linear regression was done on the non-log values of watershed area and estimated annual baseflow. The linear regression equation was:

$$y=(2\text{E}+06)x - (1\text{E}+08) \quad (10)$$
$$R^2= 0.53$$

Watersheds with larger area generally had higher estimated annual baseflow. T1 (TC group) had the largest watershed area of 1186 hectares and estimated annual baseflow of $4.0 \times 10^6 \text{ m}^3/\text{year}$ (Table 5). UD 1 (TC group) has the smallest watershed area of 11 hectares and estimated annual baseflow of $3.8 \times 10^4 \text{ m}^3/\text{year}$ although not the smallest annual baseflow. D2 (RC group) has the smallest estimated annual baseflow of $2.0 \times 10^3 \text{ m}^3/\text{year}$ and a watershed area of 47 hectares.

In addition to watershed area, percent impervious cover can explain trends in discharge. Higher percent impervious cover may be associated with discharge per hectare of watershed area (correlation coefficient 0.61) (Figure 56). UP 1, UD 1, UD 2, and UD 3 had the four highest baseflow per unit watershed area. Additionally, they have some of the highest percent impervious covers. In this study, discharge measurements were taken during baseflow. Increased storm runoff in urban areas does not explain this trend between impervious cover and discharge per hectare of watershed area because storm events were not measured. “The urban watershed continuum” (Kaushal and Belt, 2012) explains possible sources of increased discharge in urban watersheds: leaking drinking water pipes often explain this increase in baseflow of urban watersheds. In this study, watersheds with higher percent impervious cover exhibited higher fluoride concentrations (Figure 44). Fluoride is added to drinking water and it can identify

possible leaks from pipes. Using the information from Figures Figure 44 and Figure 56 we can determine that leaky pipes might be increasing baseflow discharge within urban watersheds.

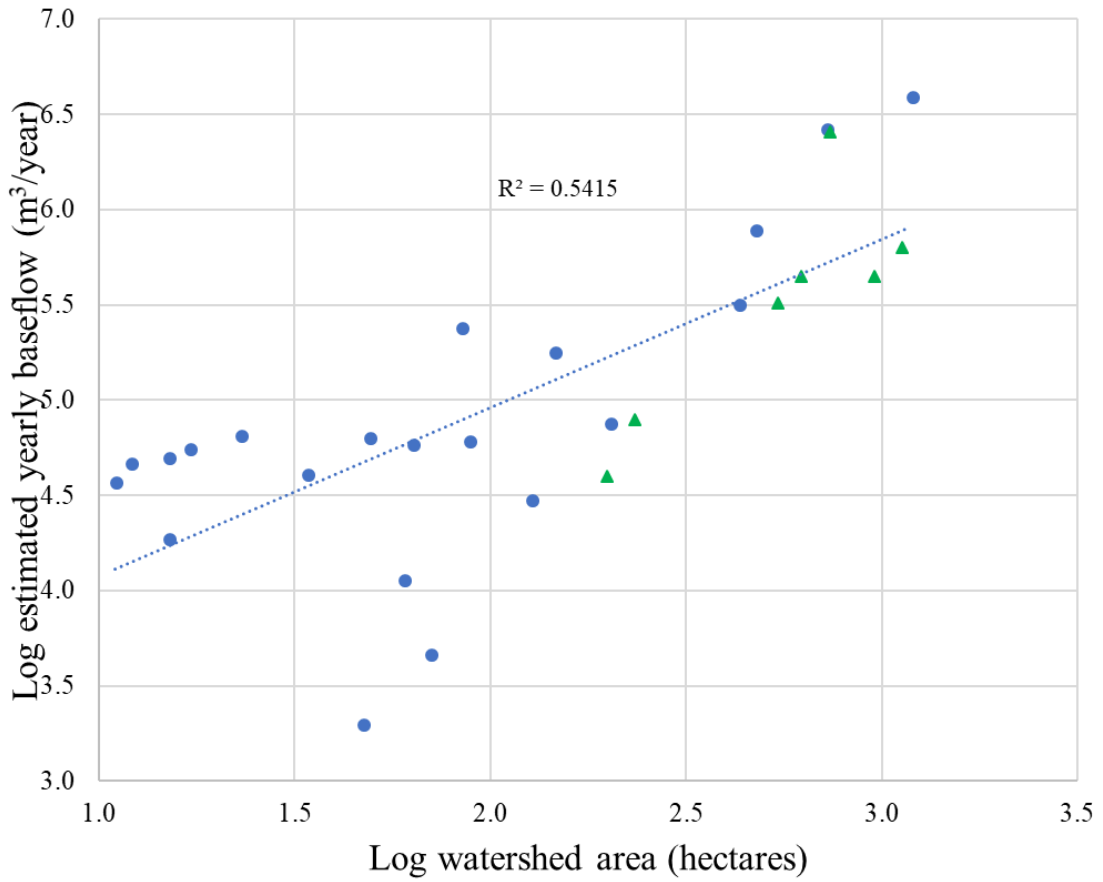


Figure 55: Watershed area vs. estimated yearly baseflow in a log scale. Blue dots represent field measurements of discharge and green triangles represent discharge measured by USGS gauges. Note: discharge measurements were during baseflow.

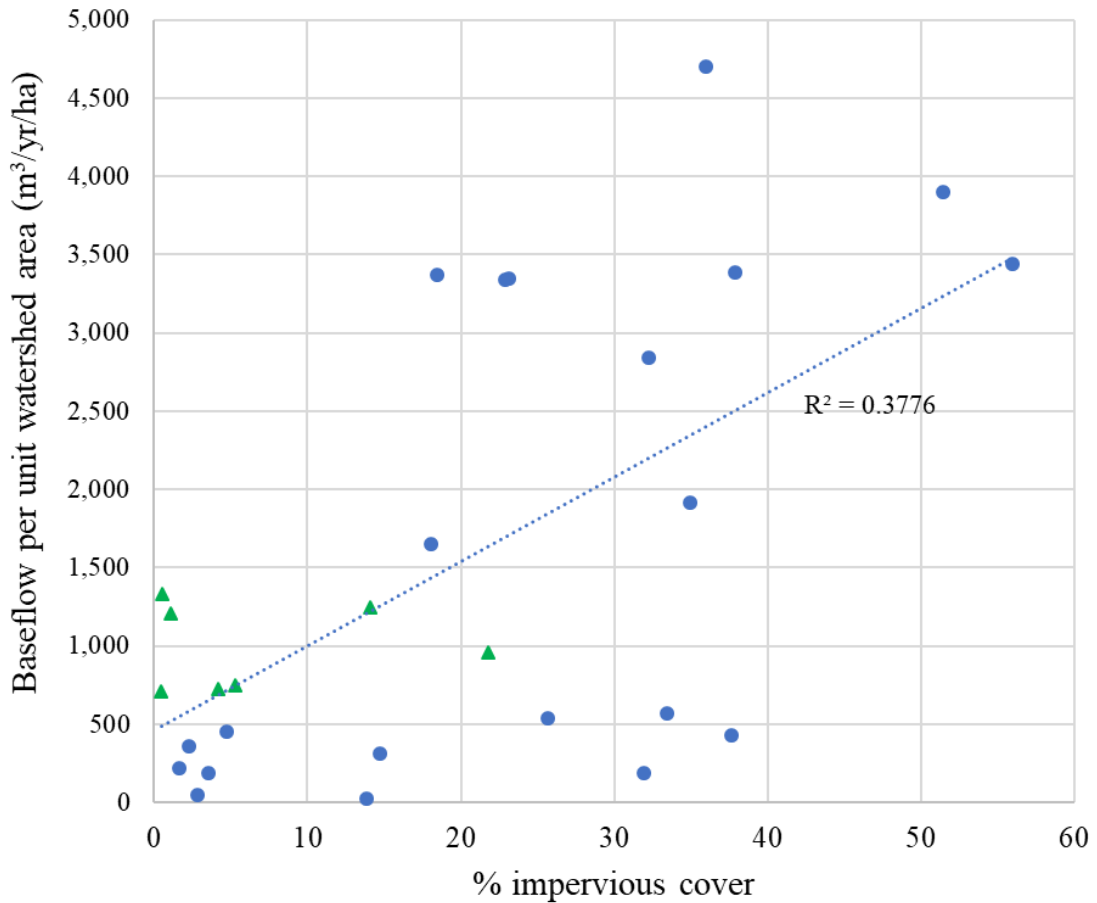


Figure 56: Percent impervious cover vs. baseflow per unit watershed area. Blue dots represent field measurements of discharge and green triangles represent discharge measured by USGS gauges. Note: discharge measurements were during baseflow.

5.2 Watershed-scale fluxes of DOC and DIC

In addition to concentrations of DOC and DIC, fluxes were calculated for all watersheds. Fluxes generally explain the discharge per unit area. In this study, fluxes are normalized for watershed area so that DOC and DIC flux can be compared across all watersheds. Table 10 lists DOC and DIC baseflow flux for all sites.

Table 10: Mean DOC and DIC baseflow fluxes (kg C/hectare/year) for all 28 watersheds

Group	Site	Watershed area (hectares)	% Impervious cover	Mean DOC baseflow flux (kg C /ha /year)	Mean DIC baseflow flux (kg C /ha /year)
RC	C1	88	0.5	2.1	5.2
RC	C2	34	1.1	3.6	8.1
RC	A1	202	2.1	0.9	5.8
RC	A2	49	0.6	3.5	18.9
RC	A3	60	3.4	1.3	2.4
RC	A4	70	2.7	0.2	1.0
RC	R1	623	4.2	1.8	9.2
RC	R2	430	5.3	1.5	9.2
RC	D1	145	14.1	3.3	17.2
RC	D2	47	13.7	0.2	0.6
RC	P1	127	1.45	1.9	3.9
MC	Beaverdam Creek	960	4.6	2.3	11.8
MC	Briar Creek	1132	25.5	1.7	10.8
MC	Briar Tributary	235	14.6	0.9	7.0
MC	Edward's Branch	199	31.8	0.4	3.2
MC	Little Hope Creek	546	33.3	1.3	10.1
MC	Little Sugar Creek	719	37.5	7.8	80.8
TC	T1	1186	23.0	14.1	81.2
TC	T2	739	18.3	9.9	79.8
TC	T3	474	17.9	4.3	35.4
TC	TD 1	84	32.1	12.4	69.0
TC	TD 2	63	21.8	2.3	21.7
TC	UD 1	11	55.8	12.7	94.1
TC	UD 2	12	51.3	15.4	104.5
TC	UD 3	15	37.7	12.8	75.8
TC	UP 1	23	35.8	10.7	51.7
TC	UU 1	17	22.7	13.4	77.0
TC	UU2	15	34.8	3.5	24.3

Mean DOC baseflow flux is strongly positively correlated to mean DIC baseflow flux (correlation coefficient 0.81). This strong correlation is mostly attributed to baseflow per unit area of watershed (Figure 56). DIC and DOC concentrations, themselves, are not strongly correlated (correlation coefficient 0.06). SUVA values for all sites were plotted against DOC baseflow flux

and DIC baseflow flux (Figure 58 and Figure 59). SUVA is weakly correlated with both DOC baseflow flux (correlation coefficient -0.09) and DIC baseflow flux (correlation coefficient -0.06). Although the overall correlation is weak, the high DOC and DIC fluxes occur at low SUVA values. The high DIC and DOC baseflow fluxes occur at higher percent impervious cover. Low SUVA values also occur at high percent impervious cover. This trend supports our hypotheses that lower SUVA values and greater fluxes will occur at more urbanized streams.

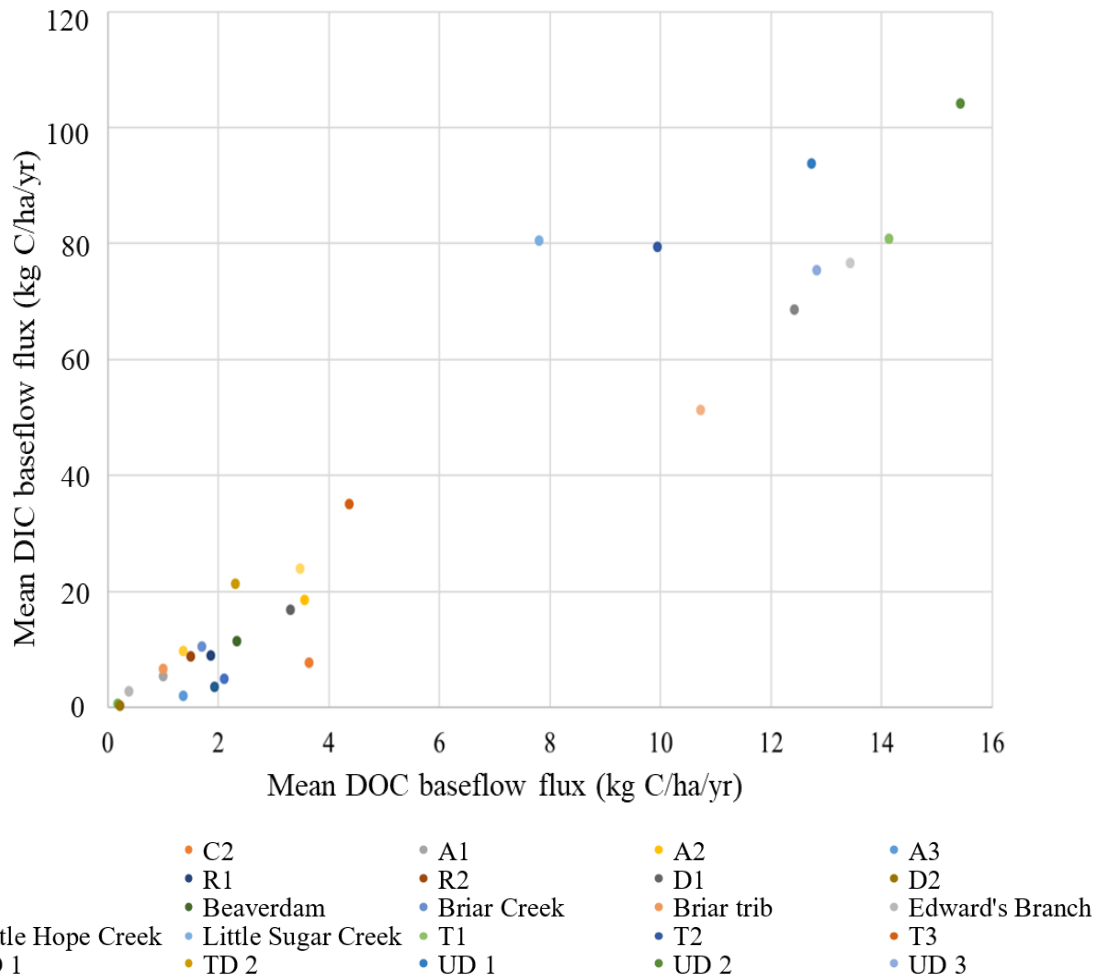


Figure 57: Mean DOC baseflow flux vs. Mean DIC baseflow flux

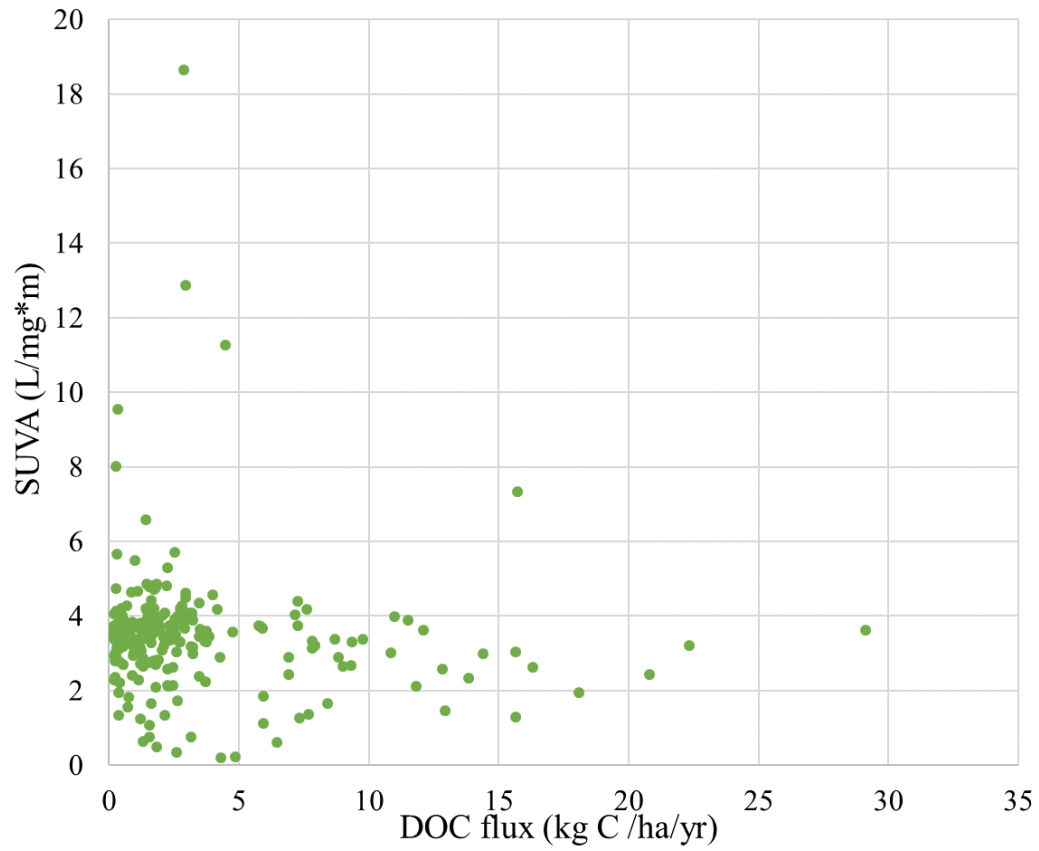


Figure 58: DOC flux vs. SUVA

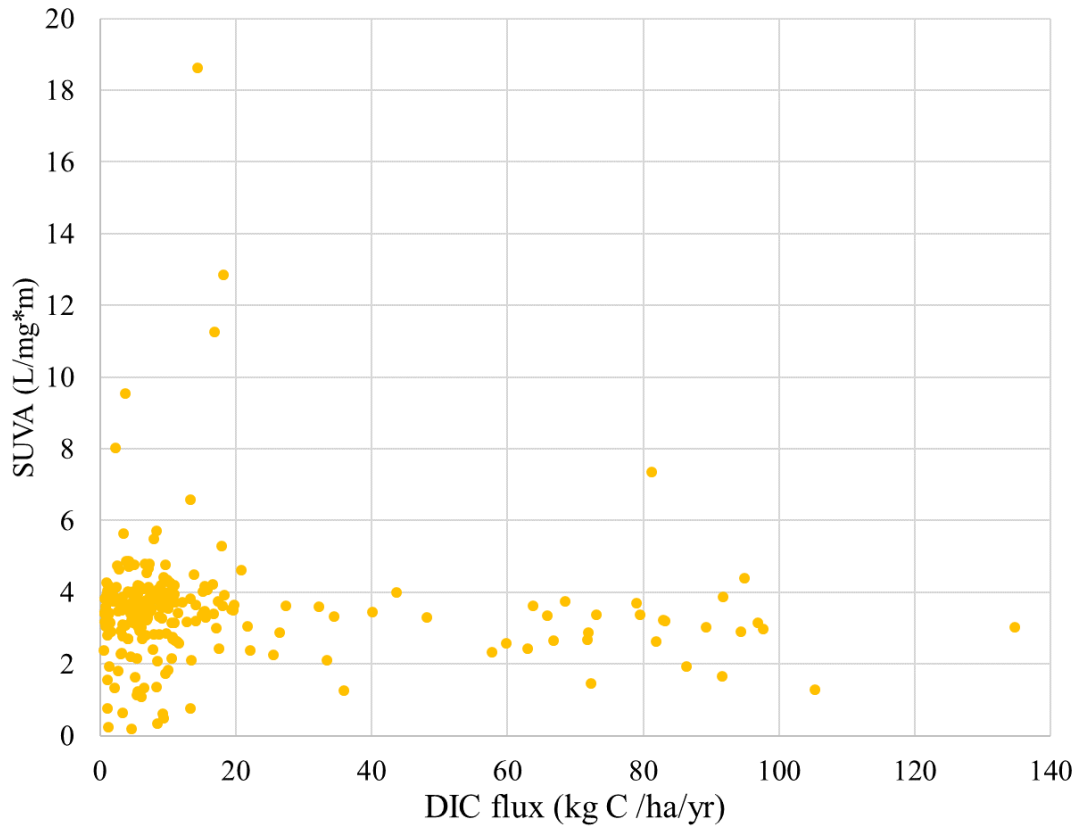


Figure 59: DIC flux vs. SUVA

5.3 DOC concentrations, DOC fluxes, and SUVA values: Response to urbanization and comparison to other studies

5.3.1 Comparison of DOC concentrations and SUVA values to other urban stream systems in the Piedmont region

DOC concentration (mg/L) had a weak negative relationship with percent impervious cover in this study (correlation coefficient -0.17). Figure 11 and Figure 12 illustrate the DOC concentration (mg/L) was primarily decreasing as percent impervious cover increases. Lu et al. (2014) observed that DOC concentration was higher in forested-dominated watersheds than cropland-dominated and urban development-dominated watersheds. This likely occurred because DOC is no longer derived from terrestrial plants in urban watersheds.

As with DOC concentrations, SUVA was weakly negatively correlated with percent impervious cover (correlation coefficient -0.15). While the negative correlation between SUVA and impervious cover is weak, Figure 14 shows that the highest SUVA values occurred in non-urban streams, consistent with previous observations from small forested watersheds. Aitkenhead-Peterson et al. (2009) stated that most DOC in forested streams is dominated by allochthonous inputs represented by high SUVA values. Imberger et al. (2014) determined that urbanized streams increase algae contributions which thus increases labile DOC represented by lower SUVA values. Parr et al. (2015) studied over 100 headwater streams along an urbanization gradient and found that more urbanized streams had more autochthonous dissolved organic matter. There was a distinct shift from allochthonous DOM to autochthonous DOM along the urbanization gradient. In this study, however, our data were weakly consistent with this shift in allochthonous to autochthonous DOM trend from prior literature. Hagen et al. (2010) stated that agricultural streams can have allochthonous inputs of DOC due to high sediment loads. This study did have some of the highest SUVA values occurring at the agricultural stream A2 in Reedy Creek. Increased sediment loads and subsequent limited algal growth may explain the high SUVA values in the agriculture streams.

5.3.1.1 Temporal variation of DOC concentrations compared to other studies

DOC concentrations of the RC group showed temporal variation. From Figure 15, high DOC concentrations occurred in the late summer to early fall of 2016 and in October 2017. The peaks that occurred in August were found at the sites draining agricultural land (A3, A4, D2). Molinero and Burke (2009) found that pasture watersheds had higher DOC concentrations than forest watersheds. Additionally, their DOC maximums also occurred in the autumn months. This is a result of leaf fall and leaf litter inputs (allochthonous) into the stream. Leaves enter the stream as POC and as they move downstream, they are decomposed and dissolved into DOC (Molinero and Burke, 2009).

5.3.2 Urbanization as a controlling variable on DOC fluxes and reactivity in streams of the study

In contrast to DOC concentration which slightly decreased as impervious cover increased, mean DOC flux increased as percent impervious cover increased (Figure 60). DOC flux has a strong positive correlation with percent impervious cover (correlation coefficient 0.65). Similarly, Sickman et al. (2007) found a positive relationship between total organic carbon (DOC + POC) flux and percent urbanization. Sickman et al. (2007) further explained that TOC yields increased in urbanized areas due to sewage inputs. From “the urban watershed continuum (Kaushal and Belt, 2012),” urban systems have large fluxes of organic carbon. This is due to storm drain networks such as gutters and pipes that store large amounts of leaf litter. Large storm events can flush out the leaves and runoff into streams. Additionally, organic carbon fluxes increase in urban watersheds due to the inputs from algal and sewage sources (Kaushal and Belt, 2012).

Mean DOC baseflow flux increased with increasing percent impervious cover, however, the largest DOC fluxes do not occur with the highest percent impervious cover (Figure 60). UD 2, T1 and UU 1 (TC group) have the highest DOC baseflow fluxes of all 28 sites (15.4, 14.1, and 13.4 kg C/ha/yr, respectively). Their impervious cover ranged from 22.7% to 51.3 %. Additionally, the lowest DOC baseflow fluxes did not occur with the lowest percent impervious

cover. Edward's (MC group), D2, and A4 had the lowest mean DOC fluxes: 0.35, 0.19, and 0.15 kg C/ha/yr. Their impervious cover ranged from 2.72% (A4) to 13.7% (D2) to 31.8% (Edward's). A main contributor to flux is discharge. Mean DOC baseflow flux was moderately positively correlated with discharge (correlation coefficient 0.36). This means that study watersheds with lower discharge likely have lower DOC fluxes. Watersheds D2 and A4 had the lowest annual baseflow (m^3/year) out of all watersheds: $2.0 \times 10^3 \text{ m}^3/\text{year}$ and $4.7 \times 10^3 \text{ m}^3/\text{year}$, respectively. Additionally, T1 had the largest annual baseflow ($4.1 \times 10^6 \text{ m}^3/\text{year}$) and one of the highest DOC fluxes. DOC baseflow flux and watershed area are not correlated (correlation coefficient -0.02). Focusing on correlation coefficients, DOC baseflow flux is associated with impervious cover. Extra sources of DOC in urban areas contributes to the larger fluxes in urban watersheds. Comparing Figure 56 and Figure 60, there are distinct similarities. Both of these figures suggest that the differences in DOC baseflow flux might be driven by differences in discharge per unit watershed area, not solely DOC concentrations. Additionally, mean DOC flux is strongly positively correlated with discharge per unit watershed area (correlation coefficient 0.95).

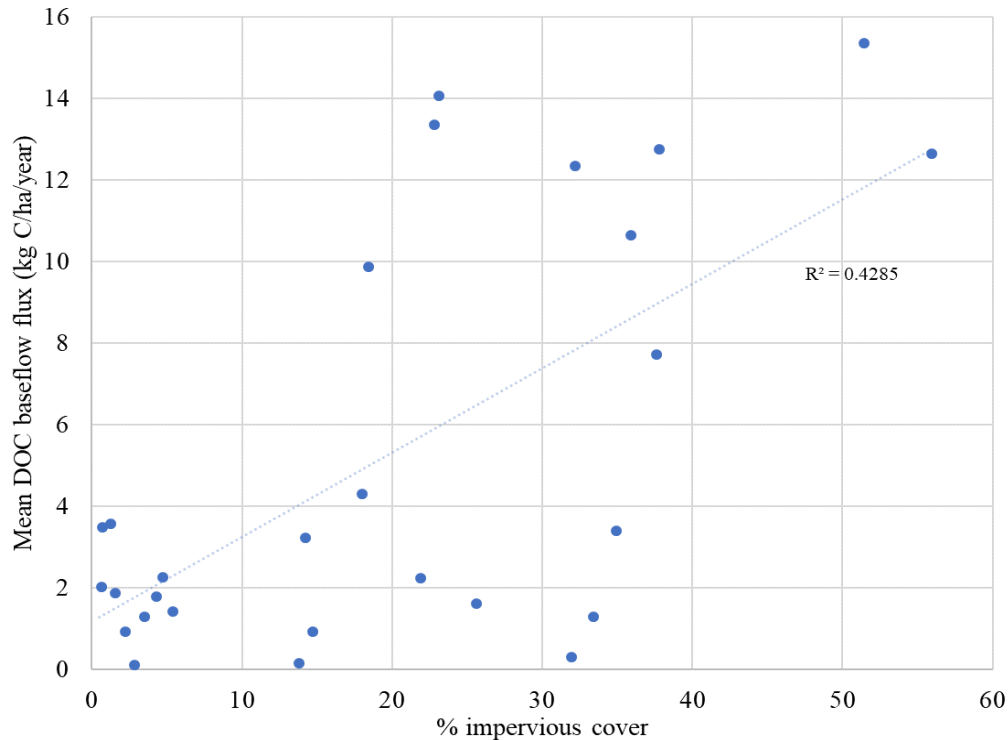


Figure 60: Percent impervious cover vs. mean baseflow DOC flux for all 28 watersheds

5.4 DIC, alkalinity, and $\delta^{13}\text{C}$ -DIC

5.4.1 Comparison of DIC, alkalinity, and $\delta^{13}\text{C}$ -DIC to other urban stream studies

Both DIC concentration and alkalinity concentration increased as percent impervious cover increased in this study (Figure 24 and Figure 26). Similarly, Lu et al. (2014) found that DIC concentrations and bicarbonate (HCO_3^-) were higher in urban-dominated watersheds compared to forested-dominated, pasture-dominated, and cropland-dominated watersheds. This increase in DIC (mM) was due to carbonate weathering. It should be noted that Lu et al. (2014) was studied on carbonate sedimentary rock geology, whereas this study is on non-carbonate crystalline silicate rocks. Forested watersheds are more likely to have developed soil layers (O horizon) which protects carbonates from weathering, thus the lower DIC concentrations. Like this study, Moore et al. (2017) studied watersheds on an urbanization gradient in the Maryland Piedmont. Moore et al. (2017) found that alkalinity and DIC increased as percent impervious surface cover increased, attributed to the weathering of silicate minerals/concrete. Likewise, in a study done by

Barnes and Raymond (2009), DIC concentrations were found to be 4.7 times higher in urban streams than forested streams. Additionally, agricultural streams had DIC concentrations 3.3 times greater than forested streams. Tippler et al. (2014) found that HCO_3^- concentrations were 18 times higher in urban streams compared to nonurban reference streams. In the Eastern U.S., Kaushal et al. (2013) studied long term trends in alkalinity of 97 streams. They found that alkalinity was 5-6 times greater in agricultural streams than forested streams due to the application of lime. They also determined that the increase in alkalinity in urban areas was due to impervious surfaces and concrete. Additionally, in Baltimore, Maryland, Kaushal et al. (2017) determined that DIC concentrations increased with percent impervious surface cover. Kaushal et al. (2017) suggested that this increase in DIC and alkalinity concentrations resulted from liming of lawns and carbonate weathering of concrete.

In most related studies, concrete (carbonate) weathering is the major source of DIC and alkalinity concentrations in urban watersheds (Kaushal et al. 2013, Peters 2014, Tipper et al. 2014, Kaushal et al. 2017, and Moore et al. 2017). In urban watersheds, these terrestrial inputs of DIC seem to overwhelm instream metabolism.

In this study, $\delta^{13}\text{C}$ -DIC values were lower (more negative) with low percent impervious cover and higher (more positive) with high percent impervious cover (Figure 36). $\delta^{13}\text{C}$ -DIC values had a strong positive correlation with percent impervious cover (correlation coefficient=0.60) (Table 9). From Lu et al. (2014), $\delta^{13}\text{C}$ -DIC values were higher (more positive) in cropland, urban, and pasture watersheds than forested. Higher $\delta^{13}\text{C}$ -DIC values were due to greater contributions of DIC (bicarbonate) from carbonate mineral weathering or C4 vegetation (Lu et al. 2014). However, Lu et al. (2014) was in a carbonate rock geology unlike this study area. Contrasting with this study's results, Barnes and Raymond (2009) found $\delta^{13}\text{C}$ -DIC values more enriched (more positive) in forested watersheds than agricultural and urban watersheds. Forested watersheds averaged -10.4‰, while agricultural and urban watersheds averaged -13.2‰ and -14.7‰, respectively. Barnes and Raymond (2009) determined that the forested streams were

most enriched, as a result of photosynthesis and atmospheric invasion. Lower DIC concentrations in undeveloped watersheds causes the atmospheric effect to be comparatively larger. The agricultural and urban streams' depleted $\delta^{13}\text{C}$ -DIC values and high DIC concentrations were due to increased chemical weathering (land use disturbance i.e. construction) and CO_2 production (septic systems increase CO_2 loading).

$\delta^{13}\text{C}$ -DIC values were enriched (more positive) in streams with high percent impervious cover (Figure 36). Urban streams, compared to forested, are more likely to have instream primary production (Imberger et al. 2014, Parr et al. 2015). In urban areas, natural vegetation is removed and this can decrease allochthonous (or terrestrial sourced) inputs. Additionally, increased light and nutrients in urban areas can increase autochthonous input (Parr et al. 2015). *In situ* primary production will uptake CO_2 , resulting in streams having a more "atmospheric" $\delta^{13}\text{C}$ -DIC signature. Atmospheric CO_2 has a $\delta^{13}\text{C}$ -DIC value of -7‰ (Clark and Fritz, 1997). This might explain why this study's urban streams have more positive $\delta^{13}\text{C}$ -DIC values than the forested streams.

$\delta^{13}\text{C}$ -DIC expressed seasonal trends at Reedy Creek. Enriched values (more positive) were found in the spring of 2017 and more negative values were found in summer 2016 and 2017 (Figure 37). The enriched $\delta^{13}\text{C}$ -DIC values corresponded with lower DIC concentrations in spring 2017 (Figure 29). Photosynthesis and atmospheric CO_2 have a greater effect on $\delta^{13}\text{C}$ -DIC since the DIC concentrations are smaller, thus producing the more positive $\delta^{13}\text{C}$ -DIC values (Barnes and Raymond, 2009). Additionally, soil temperatures are colder in spring months, compared to summer, which results in less soil respiration. Soil respiration shifts $\delta^{13}\text{C}$ -DIC values to be more negative, so this lack of soil respiration could push $\delta^{13}\text{C}$ -DIC values to be more positive in spring 2017.

5.4.2 Role of urban land cover controlling, DIC, alkalinity, and $\delta^{13}\text{C}$ -DIC fluxes

DIC baseflow flux has a strong positive relationship with percent impervious cover (correlation coefficient 0.73) (Figure 61). Barnes and Raymond (2009) found similar trends: DIC

yield ($\text{mol}\cdot\text{m}^2/\text{year}$) was 7.8 times greater in urban watersheds than forested watersheds. In their study, the percent of watershed in urban land use was positively correlated with DIC yield ($R^2 = 0.546$). This was a result of increased carbonate mineral weathering in urban areas, wastewater effluent, and the application of lime. Additionally, site differences between DIC flux are due to differences in discharge per unit area watershed (Figure 56). Mean DIC flux is strongly correlated with discharge per unit area watershed (correlation coefficient 0.98).

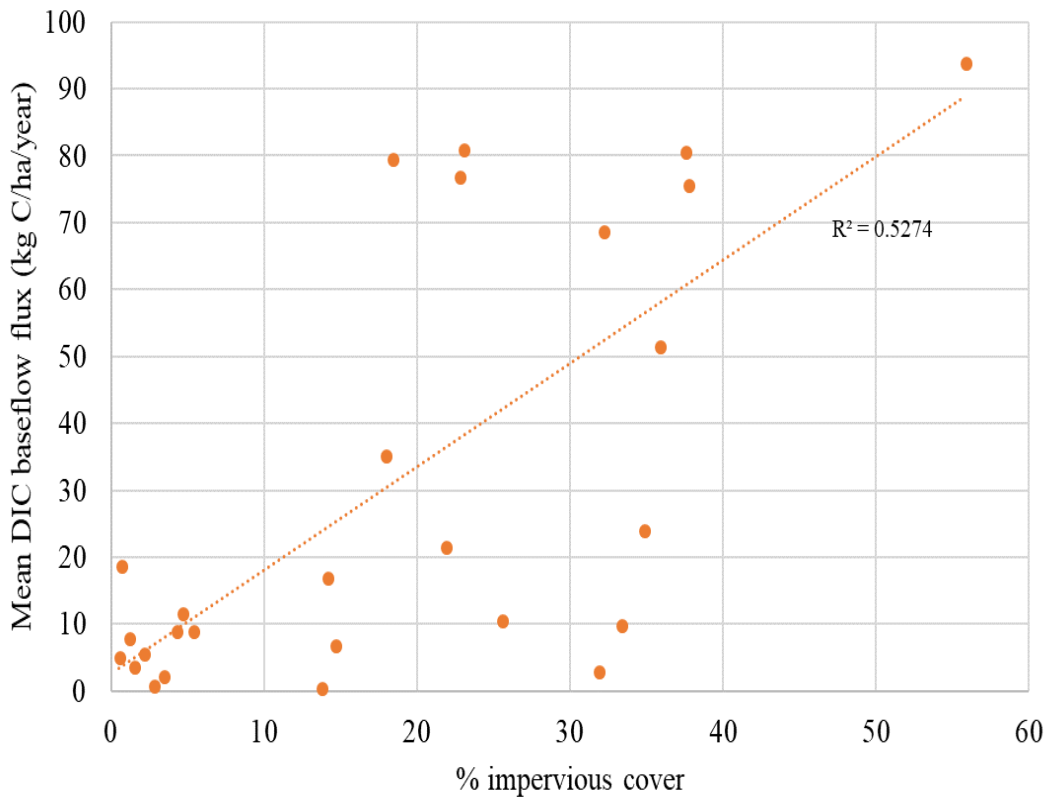


Figure 61: Percent impervious cover vs. Mean DIC baseflow flux (kg C/ha/year) for all 28 watersheds

5.5 Cations and anions

5.5.1 Comparison of cations and anions to other urban stream studies

All measured cation concentrations for this study (Na^+ , K^+ , Mg^{2+} , and Ca^{2+}) had strong positive correlations with percent impervious cover (correlation coefficient >0.5) (Figure 40, Figure 41, Figure 42, Figure 43 and Table 9: Correlation coefficient of multiple parameters versus percent impervious cover. Green shading indicates there is an association between the two parameters and red shading indicates there is no association. F^- , Cl^- , and SO_4^{2-} were strongly positively correlated with percent impervious cover. PO_4^{3-} and NO_3^- were not correlated with percent impervious cover (Table 9). Moore et al. (2017) studied sources of major ion concentrations in urban watersheds in the Maryland Piedmont. They found that Mg^{2+} , K^+ , Ca^{2+} , Na^+ , Cl^- , and SO_4^{2-} increased with increased percent impervious surface cover. Moore et al. (2017) determined that the increase in calcium was likely due to concrete weathering. High chloride concentrations were attributed to road salts and concrete weathering. High sulfate concentrations were also due to concrete weathering and building materials (i.e. drywall). Concrete and drywall are composed of gypsum ($\text{CaSO}_4 \cdot 2\text{H}_2\text{O}$), which dissolves during weathering, and thus sulfate concentrations increase (Moore et al. 2017). Kaushal et al. (2017) also found that Mg^{2+} , Ca^{2+} , and Na^+ increased with increased percent impervious cover as a result of carbonate weathering (concrete). Kaushal et al. (2017) concluded that road salts, liming of grasses, and sewage leaks were additional sources of cations. Magnesium occurs naturally in sediments and in minerals such as dolomite. Magnesium is also found in fertilizers and lime applications. The increase use of fertilizers and limes in urban areas may explain this increase of Mg^{2+} with higher percent impervious cover (Figure 42). Potassium is also found in fertilizers, which can explain the increase of K^+ with increased percent impervious cover (Figure 41). Additionally, plants and algae utilize K^+ in photosynthesis, which increases the concentration of K^+ in their tissues (Tripler et al. 2006 and Talling 2012). Higher primary production in urban streams due to decreased canopy cover could also explain the higher K^+ concentrations.

Although there were many nondetectable levels of PO_4^{3-} in this study, PO_4^{3-} slightly increased as percent impervious cover increased, if nondetectable values are treated as 0 (Figure 47). PO_4^{3-} can occur in the organic matter found in sewage waste (USGS, 2018). Waste water treatment plants exist in urban areas and their effluent contributes large amounts of PO_4^{3-} into streams. Urban fertilizer use is also a source of phosphate. Additionally, PO_4^{3-} occurs in soils, and soil erosion contributes phosphate into the stream. Urban streams are characterized by high storm runoff which deposits phosphate (from fertilizers and soils) into the streams. Fluoride (F^-) concentrations increased with increasing percent impervious cover (Figure 44). There was a strong positive correlation between the two. In U.S. public water supplies, fluoride is added as a prevention of tooth decay. Leaks from wastewater and drinking water pipes in urban areas can explain why F^- concentrations are higher in urban streams, compared to forested (Hibbs and Sharp, 2012; Kaushal and Belt, 2012). Leaky pipes from city tap water is most likely the cause of increased F^- concentrations in the urban watersheds.

Nitrate (NO_3^-) does not have a strong correlation with percent impervious cover, however, two streams from this study exhibited high nitrate concentrations (Figure 46). A2 and A3 had the highest nitrate concentrations. A2 and A3 watersheds are characterized by agriculture land uses (Figure 5). Agriculture lands use high amounts of nitrogen fertilizer (ammonia/ammonium $\text{NH}_3/\text{NH}_4^+$) to fertilize crops. Through nitrification, aerobic bacteria use oxygen and convert nitrogen gas to nitrite (NO_2^-) and then nitrate (NO_3^-). Excessive use of N fertilizers causes high amounts of nitrate in the soil. High NO_3^- in soils can be leached and further accumulate in water (Quan et al. 2016). Additionally, phosphate (PO_4^{3-}) can be sourced from agricultural fertilizers. After application, a large proportion of phosphate runs off into waterways. Figure 47 indicates that the watersheds draining agriculture land uses had higher phosphate concentrations than urban land uses.

5.6 Percent forest cover

Percent forest cover was used in comparison to percent impervious cover for DOC concentration, SUVA values, DIC concentration, alkalinity concentration and $\delta^{13}\text{C}$ -DIC (Figure 50-Figure 54). The opposite trends occur for DIC concentration, alkalinity concentration, and $\delta^{13}\text{C}$ -DIC when percent forest cover is on the x-axis compared to percent impervious cover. Sites with higher forest cover have lower DIC concentrations, alkalinity concentrations, and more negative $\delta^{13}\text{C}$ -DIC values. Percent forest cover was used mainly to determine if there are any trends in SUVA values. There was a weak negative relationship between SUVA values and percent impervious cover so it was determined that there might be a slight positive relationship between SUVA values and percent forest cover. However, there was no relationship between SUVA values and percent forest cover (correlation coefficient 0.06).

5.7 Hypotheses testing

The main hypotheses of this study were that watersheds with higher percent impervious area would have: 1) lower SUVA values, 2) higher DIC concentrations, 3) higher alkalinity values (Figure 8). To test these hypotheses, SUVA values from this study were plotted against DIC concentration (Figure 62) and alkalinity (Figure 63). From these two figures, it appears that there are distinct differences in DIC and alkalinity concentrations among land uses, but SUVA values are not as distinct. There are weak negative correlations between DIC concentration and SUVA (correlation coefficient -0.19) and between alkalinity and SUVA (correlation coefficient -0.15). To further test these relationships, critical values for Pearson's Correlation Coefficient were calculated (Siegle, D., 2009). The critical values for both alkalinity concentration versus SUVA values and DIC concentration versus SUVA values was 0.195. At a significance level of 0.05, there is not a statistically significant relationship between alkalinity concentrations and SUVA values. However, DIC concentration versus SUVA values is at the boundary of significance, meaning that there is a statistically significant difference between DIC concentrations and SUVA values. Overall, this study supported our hypotheses that watersheds

with higher percent impervious cover will have higher DIC and alkalinity concentrations. However, our hypothesis of lower SUVA values at higher percent impervious cover was not supported.

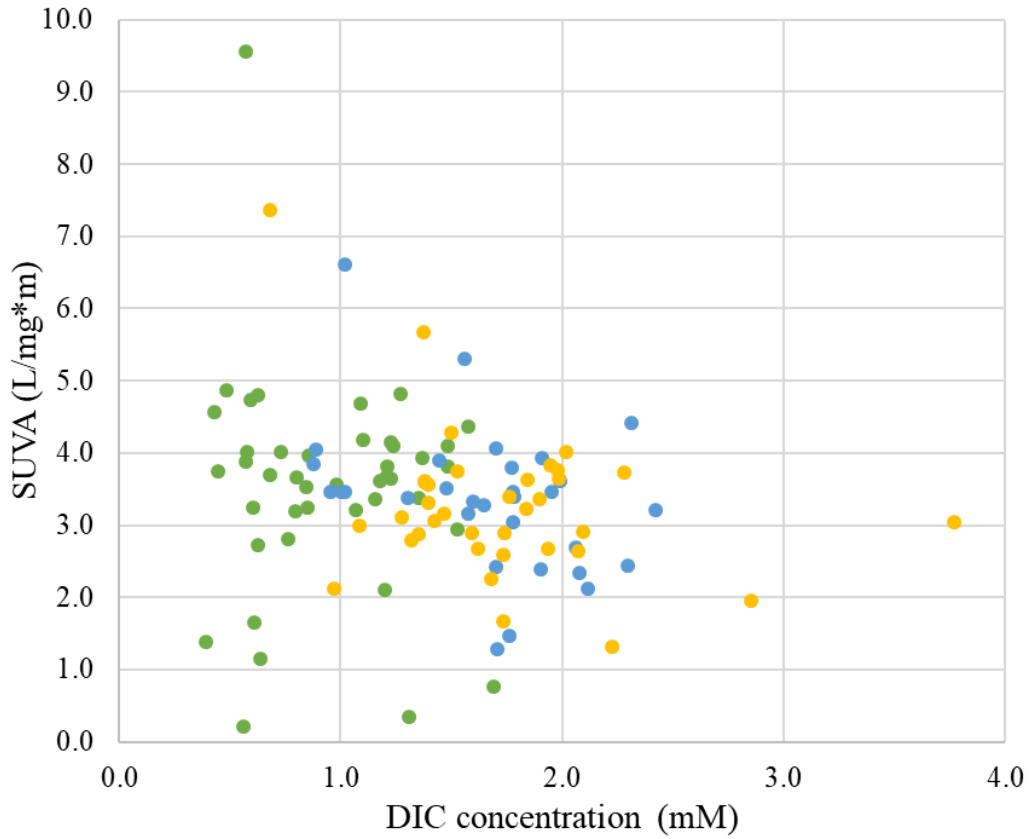


Figure 62: DIC concentration (mM) vs. SUVA (L/mg*m) for all sites June 2017-October 2017. Correlation coefficient -0.19. Green represent low percent impervious cover (0.49-5.33%). Blue represent intermediate percent impervious cover (13.7-23.0%). Orange represent high percent impervious cover (25.5-55.8%).

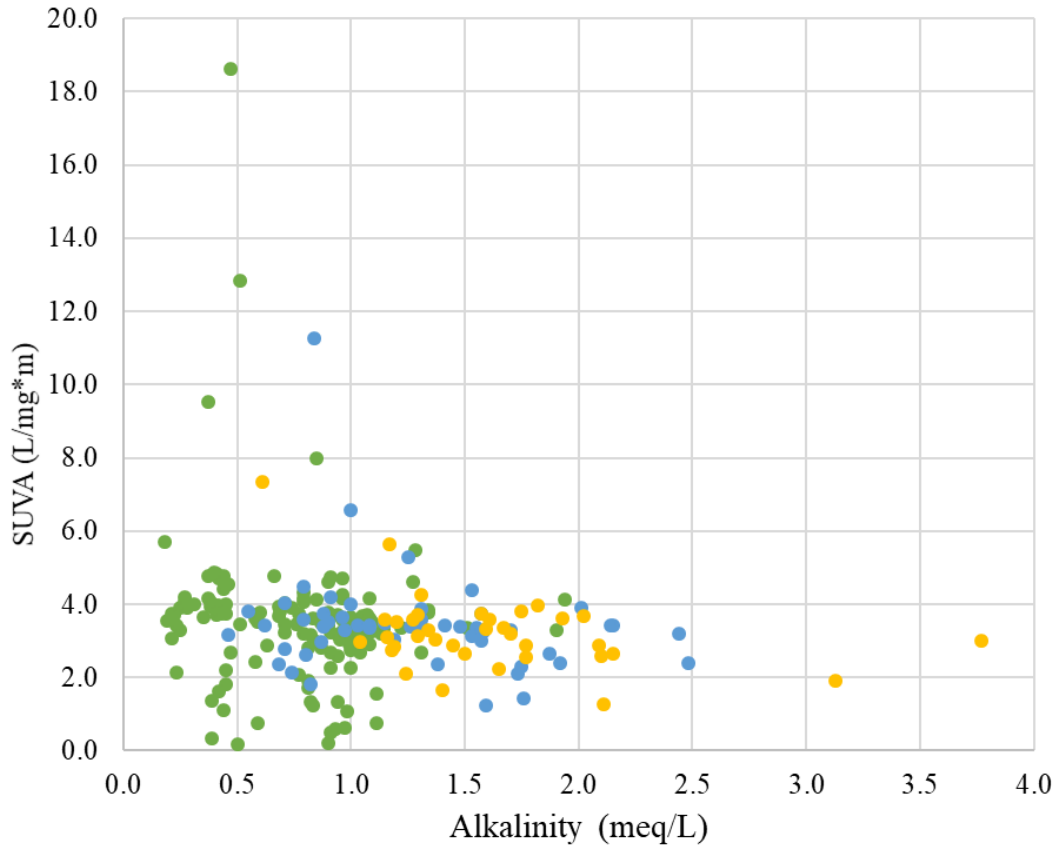


Figure 63: Alkalinity (meq/L) vs. SUVA (L/mg*m) for all sites June 2017-October 2017. Correlation coefficient -0.15. Green represent low percent impervious cover (0.49-5.33%). Blue represent intermediate percent impervious cover (13.7-23.0%). Orange represent high percent impervious cover (25.5-55.8%).

6. Conclusions

The goal of this study was to determine the potential alterations to carbon processes in streams across varying land uses. Streams with land uses ranging from pre-restoration forested to urbanized were examined; 28 streams in total. Our results suggested that there are distinct shifts of dissolved inorganic carbon, alkalinity, major cations, and major anions (F^- , Cl^- , and SO_4^{2-}) from forested watersheds to urban watersheds. There were significant relationships between DIC concentration, alkalinity, $\delta^{13}C$ -DIC, Na^+ , K^+ , Mg^{2+} , Ca^{2+} , F^- , Cl^- , and SO_4^{2-} with increased percent impervious cover. These strong positive correlations were attributed to the increased chemical weathering of concrete materials. However, there was not significant relationships between DOC concentration and SUVA values with percent impervious cover. DOC concentrations tend to overlap across land uses. Although SUVA values did not have a significant relationship with percent impervious cover, high SUVA values were found in more forested streams. Our results suggest that the increase in inorganic carbon and major cations and anions can be attributed to increased impervious surfaces in headwaters of the Southeastern Piedmont. Future studies might consider including forested watersheds that are not planned for restoration. A greater urbanization gradient would also be beneficial in measuring how SUVA values change.

Understanding how urbanization effects headwater and low-order streams is important for the global carbon cycle. Urban areas have increased chemical weathering which has increased bicarbonate/alkalinity concentrations in waters. Urban areas also increase the input from autochthonous sources compared to allochthonous sources. This study is important in understanding the changes in carbon processes in forested to urban watersheds in the Southeastern Piedmont (United States). Urban areas will continue to grow and it is important to examine all watersheds to determine impacts on the carbon cycle.

References

- Aitkenhead-Peterson, J.A., Steele, M.K., Nahar, N., and Santhy, K., 2009, Dissolved organic carbon and nitrogen in urban and rural watersheds of south central Texas: land use and land management influences, *Biogeochemistry*, v. 96, pp. 119-129, doi: 10.1007/s10533-009-9348-2
- Barnes, R.T., and Raymond, P.A., 2009, The contribution of agricultural and urban activities to inorganic carbon fluxes within temperate watersheds, *Chemical Geology*, v. 266, p. 327-336, doi: 10.1016/j.chemgeo.2009.06.018
- Campeau, A., Bishop, K., Nilsson, M.B., Klemedtsson, L., Laudon, H., Leith, F.I., Oquist, M., and Wallin, M.B., 2018, Stable carbon isotopes reveal soil-stream DIC linkages in contrasting headwater catchments, *Journal of Geophysical Research: Biogeosciences*, v. 123, pp. 149-167, doi: 10.1002/2017JG004083
- Clark, I. D., and Fritz, P., 1997, *Environmental Isotopes in Hydrogeology*, Lewis Publishers, 328 pp.
- Cole, J.J., Prairie, Y.T., Caraco, N.F., McDowell, W.H., Tranvik, L.J., Striegl, R.G., Duarte, C.M., Kortelainen, P., Downing, J.A., Middleburg, J.J., and Melack, J., 2007, Plumbing the global carbon cycle: integrating inland waters into the terrestrial carbon budget, *Ecosystems*, v. 10, pp. 171-184, doi: 10.1007/s10021-006-9013-8
- Doctor, D.H., Kendall, C., Sebestyen, S.D., Shanley, J.B., Ohte, N., and Boyer, E. W., 2008, Carbon isotope fractionation of dissolved inorganic carbon (DIC) due to outgassing of carbon dioxide from a headwater stream, *Hydrological Processes*, v. 22, pp. 2410-2423, doi: 10.1002/hyp.6833
- Finlay, J.C., 2003, Controls of streamwater dissolved inorganic carbon dynamics in a forested watershed, *Biogeochemistry*, v. 62, pp. 231-252

- Hagen, E.M., McTammany, M.E., Webster, J.R., and Benfield, E.F., 2010, Shifts in allochthonous input and autochthonous production in streams along agricultural land-use gradient, *Hydrobiologia*, v. 655, pp. 61-77
- Helie, J.F., Hillaire-Marcel, C., and Rondeau, B., 2002, Seasonal changes in the sources and fluxes of dissolved inorganic carbon through the St. Lawrence River— isotopic and chemical restraint, *Chemical Geology*, v. 186, pp. 117-138
- Hibbs, B.J., Sharp, J.M., 2012. Hydrogeological impacts of urbanization. *Environmental & Engineering Geoscience* 18, 3–24. <https://doi.org/10.2113/gseegeosci.18.1.3>
- Homer, C.G., Dewitz, J.A., Yang, L., Jin, S., Danielson, P., Xian, G., Coulston, J., Herold, N.D., Wickham, J.D., and Megown, K., 2015, Completion of the 2011 National Land Cover Database for the conterminous United States—Representing a decade of land cover change information. *Photogrammetric Engineering and Remote Sensing*, v. 81, no. 5, p. 345-354
- Hotchkiss, E., Hall, J.O., Sponseller, Butman, D., Klaminder, J., Laudon, H., Rosvall, M., and Karlsson, J., (2015), Sources of and processes controlling CO₂ emissions change with the size of streams and rivers, *Nature Geoscience*, v. 8, pp. 696–699, <https://doi.org/10.1038/ngeo2507>.
- Imberger, S.J., Cook, P.L.M., Grace, M.R., and Thompson, R.M., 2014, Tracing carbon sources in small urbanizing streams: catchment-scale stormwater drainage overwhelms the effects of reach-scale riparian vegetation, *Freshwater Biology*, v. 59, p. 168-186, doi: 10.1111/fwb.12256.
- Kaushal, S.S., and Belt, K.T., 2012, The urban watershed continuum: evolving spatial and temporal dimensions, *Urban Ecosystems*, v. 14, pp. 409-435, doi: 10.1007/s11252-012-0226-7
- Kaushal, S.S., Mayer, P.M., Vidon, P.G., Smith, R.M., and Pennino, M.J., 2014, Land use and climate variability amplify carbon, nutrient, and contaminant pulses: a review with management implications, *U.S. Environmental Protection Agency Papers*, paper 238

- Kaushal, S.S., Delaney-Newcomb, K., Findlay, S.E.G., Newcomer, T.A., Duan, S., Pennino, M.J., Svirichi, G.M., Sides-Raley, A.M., Walbridge, M.R., and Belt, K.T., 2014, Longitudinal patterns in carbon and nitrogen fluxes and stream metabolism along an urban watershed continuum, *Biogeochemistry*, v. 121, pp. 23-44, doi: 10.1007/s10533-014-9979-9
- Kaushal, S.S., Duan, S., Doody, T.R., Haq, S., Smith, R.M., Newcomer Johnson, T.A., Delaney-Newcomb, K., Gorman, J., Bowman, N., Mayer, P.M., Wood, K.L., Belt, K.T., and Stack, W.P., 2017, Human-accelerated weathering increase salinization, major ions, and alkalization in fresh water across land use, *Applied Geochemistry*, v. 83, pp. 121-135, <https://doi.org/10.1016/j.apgeochem.2017.02.006>
- Lu, Y.H., Bauer, J.E., Canuel, E.A., Chambers, R.M., Yamashita, Y., Jaffe, R., and Barrett, A., 2014, Effects of land use on sources and ages of inorganic and organic carbon in temperate headwater streams, *Biogeochemistry*, v. 119, pp. 275-292, doi: 10.1007/s10533-014-9965-2
- Marx, A., Dusek, J., Kankovec, J., Sanda, M., Vogel, T., van Geldern, R., Hartmann, J., and Barth, J.A.C., 2017, A review of CO₂ and associated carbon dynamics in headwater streams: a global perspective, *Reviews of Geophysics*, v. 55, pp. 560-585
- McMillan, S., and Clinton, S., 2013, Reedy Creek Restoration Study, proposal submitted to Charlotte Mecklenburg Stormwater Services
- Meyer, J.L., Paul, M.J., and Taulbee, W.K., 2005, Stream ecosystem function in urbanizing landscapes, *Journal of the North American Benthological Society*, v. 24, pp. 602-612
- Miller, M.P., Boyer, E.W., McKnight, D.M., Brown, M.G., Gabor, R.S., Hunsaker, C.T., Iavorivska, L., Inamdar, S., Johnson, D.W., Kaplan, L.A., Lin, H., McDowell, W.H., and Perdrial, J.N., 2016, Variation of organic matter quantity and quality in streams at Critical Zone Observatory watersheds, *Water Resources Research*, doi: 10.1002/2016WR018970

- Molinero, J., and Burke, R.A., 2009, Effects of land use on dissolved organic matter biogeochemistry in piedmont headwater streams of the Southeastern United States, *Hydrobiologia*, v. 635, pp. 289-308, doi: 10.1007/s10750-009-9921-7
- Moore, J., Bird, D.L., Dobbis, S.K., and Woodward, G., 2017, Nonpoint source contributions drive elevated major ion and dissolved inorganic carbon concentrations in urban watersheds, *Environmental Science & Technology Letters*, v. 4, pp. 198-204, doi: 10.1021/acs.estlett.7b00096
- O'Driscoll, M., Clinton, S., Jefferson, A., Manda, A., and McMillan, S., 2010, Urbanization effects on watershed hydrology and in-stream processes in the southern United States, *Water*, v. 2, pp. 605-648
- Parr, T.B., Cronan, C.S., Ohno, T., Findlay, S.E.G, Smith, S.M.C, and Simon, K.S., 2015, Urbanization changes the composition and bioavailability of dissolved organic matter in headwater streams, *Limnology and Oceanography*, v. 00, 2015, pp. 1-27
- Paul, M.J., and Meyer, J.L., 2001, Streams in the urban landscape, *Annual Review of Ecology and Systematics*, v. 32, pp. 333- 365
- Peters, N.E., 2009, Effects of urbanization on stream water quality in the city of Atlanta, Georgia, USA, *Hydrological Processes*, v. 23, pp. 2860-2878, doi:10.1002/hyp.7373
- Quan, Z., Huang, B., Lu, C., Shi, Y., Chen, X., Zhang, H., and Fang, Y., 2016, The fate of fertilizer nitrogen in a high nitrate accumulated agricultural soil, *Scientific Reports*, v. 6, doi: 10.1038/srep21539
- Raymond, R.A., and Cole, J.J, 2003, Increase in the export of alkalinity from North America's largest river, *Science*, v. 301, pp. 88-91, doi: 10.1126/science.1083788
- Regnier, P., et al., 2013, Anthropogenic perturbation of the carbon fluxes from land to ocean, *Nature Geoscience*, v. 6., pp. 597-607, doi: 10.1038/NGEO1830
- Schlesinger, W.H. and Bernhardt, E.S., 2013, *Biogeochemistry: An Analysis of Global Change*. 3rd edition, Elsevier, 688pp.

- Sickman, J.O., Zanoli, M.J., and Mann, H.L., 2007, Effects of urbanization on organic carbon loads in the Sacramento River, California, *Water Resources Research*, v. 43, W11422, doi:10.1029/2007WR005954
- Singh, N.K., Reyes, W.M., Bernhardt, E.S., Bhattacharya, R., Meyer, J.L., Knoepp, J.D., Emanuel, R.E., 2016, Hydro-climatological influences on multi-decadal trends of dissolved organic carbon in a Southern Appalachian headwater stream. *Journal of Environmental Quality*, v.45, pp.1286–1295
- Stanley, E.H., Powers, S.M., Lottig, N.R., Buffam, I., and Crawford, J.T., 2012, Contemporary changes in dissolved organic carbon (DOC) in human-dominated rivers: is there a role for DOC management? *Freshwater Biology*, v. 57, p. 26-42, doi: 10.1111/j.1365-2427.2011.02613.x
- Talling, J.F., 2010, Potassium- a non-limiting nutrient in freshwater? *Freshwater Reviews*, v. 3, pp. 97-104, doi: 10.1608/FRJ-3.2.1
- Tippler, C., Wright, I.A., Davies, P.J., and Hanlon, A., 2014, The influence of concrete on the geochemical qualities of urban streams, *Marine and Freshwater Research*, v. 65, pp. 1009-1017, <https://doi.org/10.1071/MF13164>
- Tripler, C.E., Kaushal, S.S., Likens, G.E., and Walter, M.T., 2006, Patterns in potassium dynamics in forested ecosystems, *Ecology Letters*, v. 9, pp. 451-466, doi: 10.1111/j.146-0248.2006.00891.x
- U.S. Geological Survey, Howard Perlman, 2018, Phosphorus and Water, <http://water.usgs.gov/edu/phosphorus.html>
- Weishaar, J.L., Aiken, G.R., Bergamaschi, B.A., Fram, M.S., Fujii, R., and Mopper, K., 2003, Evaluation of specific ultraviolet absorbance as an indicator of the chemical composition and reactivity of dissolved organic carbon, *Environmental Science & Technology*, v. 37, no. 20, pp. 4702-4708, doi: 10.1021/es030360x

APPENDIX A: Data table of all parameters for the MC and TC groups

Date	Site	DOC (mg/L)	SUVA (L/mg ² m)	pH	Alkalinity (meq/L)	DIC (mM)	δ ¹³ C-DIC (‰)	Sodium (ppm)	Potassium (ppm)	Magnesium (ppm)	Calcium (ppm)	Fluoride (ppm)	Chloride (ppm)	NO ₃ ⁻ as N (ppm)	PO ₄ ³⁻ (ppm)	SO ₄ ²⁻ (ppm)
6/29/2017	Beaverdam	3.73	4.39	7.75	1.30	1.47	-15.1	5.54	3.45	5.39	15.2	0.14	4.82	0.08	0.00	4.07
8/4/2017	Beaverdam	4.43	3.25	7.05	1.89	2.49	-16.4	5.65	3.38	6.99	19.1	0.15	5.46	0.03	0.00	2.03
8/30/2017	Beaverdam	4.49	2.14	7.02	1.93	2.79	-16.5	5.31	3.41	7.03	19.5	0.15	4.44	0.04	0.00	2.13
9/26/2017	Beaverdam	7.30	4.12	7.36	1.50	1.74	-15.3	5.07	3.25	5.66	15.4	0.15	4.43	0.03	0.00	2.47
6/29/2017	Briar Creek	2.69	3.87	7.71	1.26	1.37	-13.1	9.11	2.20	4.53	16.6	0.10	6.80	0.45	0.00	5.20
8/4/2017	Briar Creek	2.22	4.32	7.28	1.49	1.61	-12.6	9.48	2.40	5.00	18.5	0.11	6.85	0.11	0.00	5.65
8/30/2017	Briar Creek	2.12	3.64	7.68	1.74	1.94	-13.7	9.93	3.13	5.62	23.5	0.10	6.78	0.15	0.00	7.89
9/26/2017	Briar Creek	4.91	2.71	7.51	1.30	1.49	-13.3	8.29	2.83	4.38	16.3	0.11	6.67	0.07	0.00	4.65
6/29/2017	Briar Trib	2.41	3.31	7.65	1.91	1.90	-13.1	12.4	3.41	8.57	26.7	0.26	15.9	0.48	0.07	17.3
8/4/2017	Briar Trib	2.75	3.50	7.86	1.57	1.69	-12.7	11.4	4.67	7.47	24.7	0.28	13.5	0.90	0.43	20.5
8/30/2017	Briar Trib	2.59	3.82	7.43	1.56	1.64	-12.9	9.13	3.75	7.20	23.9	0.31	11.9	0.33	0.25	16.2
9/26/2017	Briar Trib	3.99	2.46	7.77	2.14	1.76	-14.4	15.4	3.86	7.13	23.3	0.29	20.6	0.11	0.19	13.1
6/29/2017	Edward's	1.19	5.70	7.61	1.16	1.36	-15.7	8.25	1.49	4.75	15.1	0.11	5.64	0.45	0.04	5.71
8/4/2017	Edward's	1.65	3.15	7.74	1.17	1.31	-14.7	8.26	1.33	4.40	13.4	0.08	4.92	0.29	0.13	4.20
8/30/2017	Edward's	1.57	3.64	7.58	1.15	1.27	-14.5	8.40	1.57	4.22	13.3	0.08	5.53	0.29	0.10	4.40
9/26/2017	Edward's	2.55	2.83	7.66	1.14	1.37	-15.5	8.34	1.85	4.45	13.9	0.08	5.00	0.19	0.15	3.94
6/29/2017	Little Hope	1.89	3.59	7.60	1.28	1.46	-14.3	9.34	2.46	5.68	20.8	0.13	8.57	0.66	0.07	16.0
8/4/2017	Little Hope	2.03	2.91	7.72	1.19	1.38	-14.0	9.26	2.78	5.24	19.9	0.15	9.66	0.52	0.10	16.1
8/30/2017	Little Hope	2.09	3.77	7.65	1.18	1.34	-13.6	9.79	3.21	5.46	20.4	0.16	9.58	0.54	0.18	18.3
9/26/2017	Little Hope	3.07	3.19	7.60	1.28	1.52	-15.1	9.28	3.53	5.72	21.2	0.17	9.89	0.18	0.11	18.3
6/29/2017	Little Sugar	2.08	3.27	7.84	1.69	1.83	-13.2	10.3	2.54	6.87	25.8	0.12	10.8	0.33	0.25	16.2
8/4/2017	Little Sugar	2.29	2.93	8.79	1.66	1.75	-13.1	9.99	3.32	7.12	25.5	0.19	10.5	0.45	0.06	3.63
8/30/2017	Little Sugar	1.81	3.42	8.28	1.44	1.58	-13.1	9.24	2.74	6.63	22.9	0.26	10.4	1.69	0.11	4.24
9/26/2017	Little Sugar	6.60		8.13	1.92	1.97	-12.7	10.6	2.82	8.36	27.3	0.17	10.9	0.09	0.00	3.24
7/27/2017	T1	2.74	3.25	7.84	1.86	2.05	-13.6	10.9	2.82	8.54	22.7	0.13	11.4	0.34	0.00	11.8
9/6/2017	T1	3.19	3.07	7.69	1.56	1.77	-13.2	9.95	3.05	8.01	21.3	0.14	11.9	0.27	0.00	10.8
9/27/2017	T1	3.75	2.72	7.77	1.90	2.20	-13.4	12.2	3.67	9.33	24.4	0.20	13.1	0.15	0.00	12.2
6/28/2017	T2			7.67	1.75	1.94	-13.7	9.90	2.33	8.26	20.2	0.09	9.71	0.43	0.00	7.79
7/27/2017	T2	2.84	4.44	7.54	1.54	1.75	-13.3	10.8	2.80	6.58	17.6	0.10	9.82	0.22	0.00	6.43
9/5/2017	T2	2.10	3.43	7.78	1.52	1.77	-14.0	9.05	2.60	7.54	19.3	0.09	8.68	0.29	0.00	7.93
9/27/2017	T2	4.34	1.50	7.86	2.00	2.30	-14.2	11.5	3.11	9.45	23.4					
6/28/2017	T3	1.57	3.50	7.77	1.58	1.77	-13.7	8.69	2.09	7.51	18.3	0.08	7.48	0.95	0.00	7.38
7/27/2017	T3	2.19	3.65	7.63	1.69	1.70	-13.8	8.97	2.40	7.23	17.7	0.09	7.62	0.74	0.06	8.20
9/5/2017	T3	2.26	3.37	7.62	1.30	1.59	-14.0	7.67	2.69	6.55	16.5	0.08	6.94	0.47	0.00	6.35
9/27/2017	T3	10.05	1.31	7.67	2.13	1.98	-15.0	8.94	3.36	7.93	19.4	0.08	8.46	0.05	0.00	6.47
6/28/2017	TD 1	2.68	3.80	7.88	1.60	1.83	-13.9	10.2	2.72	7.31	20.8	0.08	10.1	0.46	0.00	10.3
7/27/2017	TD 1	2.48	3.66	7.92	1.58	1.89	-14.0	10.0	2.54	8.14	20.3	0.10	9.90	0.42	0.00	9.09
9/5/2017	TD 1	2.00	3.76	7.71	1.56	1.97	-13.6	10.5	2.94	7.37	21.1	0.09	9.76	0.39	0.09	10.3
9/27/2017	TD 1	2.57	3.39	7.78	2.01	2.27	-13.9	12.2	3.09	8.36	23.2	0.09	10.6	0.12	0.00	10.4

Date	Site	DOC (mg/L)	SUVA (L/mg ² m)	pH	Alkalinity (meq/L)	DIC (mM)	$\delta^{13}\text{C-DIC}$ (‰)	Sodium (ppm)	Potassium (ppm)	Magnesium (ppm)	Calcium (ppm)	Fluoride (ppm)	Chloride (ppm)	NO ₃ ⁻ as N (ppm)	PO ₄ ³⁻ (ppm)	SO ₄ ²⁻ (ppm)
6/28/2017	TD 2			7.43	2.16	1.90	-14.0	11.1	2.99	7.26	19.4					
7/27/2017	TD 2	2.34	3.97	7.52	1.72	2.10	-13.8	11.1	3.24	7.63	22.1	0.10	10.5	0.37	0.14	10.4
9/5/2017	TD 2	2.28	5.34	7.55	1.24	1.55	-13.2	8.64	2.54	5.89	15.8	0.09	8.03	0.20	0.00	6.08
9/27/2017	TD 2	5.24	2.16	7.34	1.74	2.06	-13.6	11.9	3.05	7.58	19.7	0.10	11.3	0.10	0.00	6.47
6/30/2017	UD1	2.42	1.98	7.92	2.08	2.08	-13.2	16.9	4.06	9.30	28.4	0.65	16.2	0.63	0.00	26.8
7/27/2017	UD1	2.54	2.95	8.26	2.10	2.21	-12.5	18.2	4.97	10.5	35.2	0.80	24.9	0.57	0.09	32.9
9/5/2017	UD1	4.53	1.35	7.81	2.03	2.28	-12.2	18.0	4.87	9.90	30.7	0.69	18.8	0.32	0.00	29.8
10/2/2017	UD1	3.64	1.71	7.34	2.50	2.54	-12.8	18.2	4.47	11.7	33.1	0.57	17.5	0.50	0.04	7.24
6/30/2017	UD2	3.96	3.03	7.59	2.09	2.06	-15.4	14.4	3.92	8.90	31.5	0.27	14.8	0.13	0.00	22.9
7/27/2017	UD2	4.12	2.67	7.77	3.12	2.84	-14.5	15.3	5.42	11.1	37.8	0.38	18.1	0.10	0.07	4.44
9/5/2017	UD2	3.58	3.08	7.46	1.39	1.73	-15.2	8.44	3.79	6.59	24.7	0.25	10.8	0.07	0.00	8.71
6/30/2017	UD3	4.65	3.68	7.14	0.60	0.67	-11.8	3.99	2.77	3.11	8.33	0.16	4.24	0.23	0.00	4.32
7/27/2017	UD3	3.25	7.40	7.13	1.81	2.01	-11.2	9.34	2.90	7.91	18.3	0.20	7.75	0.29	0.00	4.27
9/5/2017	UD3	4.08	4.05	7.41	1.03	1.07	-7.4	7.59	2.71	5.33	11.9	0.17	5.98	0.16	0.00	6.96
10/2/2017	UD3	3.10		7.04	3.76	3.76	-12.5	23.5	3.58	16.8	37.9	0.16	19.6	0.31	0.00	3.74
6/30/2017	UP1	4.43	2.71	7.68	1.23	0.96	-11.9	11.5	2.30	5.63	13.6	0.08	16.2	0.12	0.00	8.04
7/27/2017	UP1	3.23	3.35	8.33	2.14	1.92	-11.4	22.9	3.54	16.1	35.4	0.20	51.9	0.78	0.00	24.7
9/5/2017	UP1	4.12	2.62	7.69	1.76	1.72	-11.4	17.0	3.20	13.8	30.9	0.14	42.1	0.71	0.08	20.8
10/2/2017	UP1	3.43	2.16	7.65	1.33	1.39	-12.4	12.7	2.72	9.87	23.0	0.40	27.4	0.02	0.00	3.61
6/30/2017	UU1	6.21	3.93	7.43	1.30	1.43	-12.6	12.0	6.48	9.29	25.8	0.25	21.4	2.49	0.13	21.3
7/27/2017	UU1	2.32	3.19	7.78	2.47	2.28	-11.8	22.2	2.52	15.7	33.1	0.11	35.7	0.20	0.00	26.4
9/5/2017	UU1	3.32	2.38	7.58	1.52	1.56	-12.7	15.5	2.12	9.72	21.1	0.10	22.1	0.10	0.00	14.9
10/2/2017	UU1	2.87	2.47	7.63	2.43	2.41	-12.3	22.0	2.67	16.4	34.4	0.11	40.2	0.02	0.00	5.04
6/28/2017	UU2	2.00	3.09	8.00	1.76	1.73	-12.6	17.3	3.10	11.0	26.6	0.11	24.7	0.34	0.00	20.4
7/27/2017	UU2	2.80	2.93	7.77	1.64	1.67	-12.8	16.9	3.49	10.1	25.4	0.12	25.8	0.20	0.00	19.5
9/5/2017	UU2	3.31	2.29	7.67	1.36	1.42	-12.7	13.1	3.21	8.32	20.9	0.10	20.1	0.25	0.00	15.4

APPENDIX B: Data table of all parameters for RC group

Date	Site	DOC (mg/L)	SUVA (L/mg ^m m)	pH	Alkalinity (meq/L)	DIC (mM)	δ ¹³ C-DIC (‰)	Sodium (ppm)	Potassium (ppm)	Magnesium (ppm)	Calcium (ppm)	Fluoride (ppm)	Chloride (ppm)	NO ₃ ⁻ as N (ppm)	PO ₄ ³⁻ (ppm)	SO ₄ ²⁻ (ppm)
5/31/2016	A1	2.51	3.75		1.04	1.05	-14.0	9.53	1.37	4.55	12.2	0.09	6.14	0.99	0.10	3.44
6/1/2016	A1	3.94			0.97	1.03	-15.9	9.32	1.27	4.52	11.9					
6/2/2016	A1				1.13	1.02	-14.7	9.36	1.26	4.23	11.4					
6/6/2016	A1					1.10	-15.0	9.04	1.43	4.43	11.8					
6/7/2016	A1				0.97	1.00	-15.8									
6/9/2016	A1				0.82	1.05	-15.4	9.56	1.25	4.49	12.1	0.08	6.09	1.02	0.10	3.23
6/14/2016	A1				0.67			9.60	1.22	4.60	12.5					
6/16/2016	A1				0.95	1.07	-15.5	9.31	1.40	4.55	12.6	0.08	7.18	0.86	0.10	3.00
6/17/2016	A1				1.07	1.26	-15.4					0.11	7.13	0.90	0.11	3.01
6/20/2016	A1				0.99	1.10	-15.0	9.64	1.24	4.47	12.2	0.08	5.74	0.99	0.09	3.00
6/21/2016	A1	16.2				1.16	-15.5	9.58	1.24	4.50	12.5					
6/27/2016	A1				1.03			10.1	1.24	4.54	12.6	0.08	6.21	0.93	0.08	2.97
6/28/2016	A1				1.07			9.60	1.31	4.38	12.2					
6/30/2016	A1				0.94			8.38	1.50	4.02	11.0	0.10	4.60	0.75	0.00	3.01
7/5/2016	A1					1.17	-15.5					0.11	5.11	0.84	0.09	2.84
7/6/2016	A1							9.71	1.31	4.43	12.5	0.12	4.75	0.82	0.12	2.75
7/21/2016	A1	16.2			2.08	1.30	-15.5					0.12	5.31	0.77	0.10	2.94
7/28/2016	A1	2.46	5.53	7.56	1.12	1.31	-15.9	10.6	1.28	4.53	5.07	0.18	5.11	0.64	0.00	2.89
8/4/2016	A1	2.95	1.29	7.44		1.16	-16.3					0.12	4.58	0.53	0.00	2.97
8/9/2016	A1	3.68										0.12	4.88	0.55	0.12	3.65
8/16/2016	A1	15.5										0.12	5.21	0.69	0.14	2.99
9/7/2016	A1	2.04		7.61	1.26	1.39	-13.6	9.62	1.57	4.51	12.8	0.11	3.76	0.30	0.16	2.57
9/13/2016	A1	2.50		7.20								0.12	4.10	0.00	0.00	2.58
9/20/2016	A1	2.34	3.08					11.1	3.15	4.71	13.6					
9/28/2016	A1							8.42	2.49	3.87	10.6	0.12	4.76	0.38	0.00	5.31
9/28/2016	A1	3.81						8.42	2.49	3.87	10.6	0.13	4.10	0.04	0.09	2.49
10/4/2016	A1	2.97	2.76					9.36	1.87	4.16	12.6					
10/12/2016	A1	3.09	3.11		0.69			9.71	2.93	4.15	11.2	0.10	6.46	0.93	0.00	6.39
10/18/2016	A1	2.35			0.98			9.66	2.16	4.51	12.2	0.11	6.11	0.61	0.14	4.42
10/25/2016	A1	2.00	3.66		1.04	1.26	-14.4	9.86	1.94	4.82	13.1	0.11	5.76	0.55	0.12	3.67
11/1/2016	A1	2.09			1.08			10.2	1.97	4.88	13.4	0.11	5.70	0.35	0.09	3.28
11/8/2016	A1	1.87			1.11			10.1	1.81	4.92	13.5	0.11	5.65	0.48	0.00	3.28
11/14/2016	A1	1.68	3.34	7.59	1.10	1.27	-12.6	9.93	1.66	4.79	13.2	0.09	5.64	0.67	0.03	3.32
11/21/2016	A1				1.12	1.37	-13.6	9.74	1.65	5.01	13.5	0.09	5.83	0.65	0.00	3.53
11/29/2016	A1	3.50		6.79				9.96	3.22	5.04	13.9	0.09	6.49	0.42	0.00	3.55
12/7/2016	A1	3.91	1.13	6.99				8.10	2.03	3.88	9.74	0.09	5.22	0.36	0.00	3.90
12/13/2016	A1			7.05		1.04	-14.9	9.43	1.63	4.30	11.3	0.09	3.75	0.02	0.05	1.56
1/4/2017	A1	4.58		6.79				6.39	2.18	3.05	7.30	0.08	5.30	0.95	0.06	6.87
1/12/2017	A1	3.46		6.84				7.90	1.71	3.50	8.93	0.08	7.30	0.93	0.00	6.82
1/19/2017	A1	2.10	3.48	7.05	0.82	0.91	-13.2	12.1	2.38	5.42	11.2	0.08	6.10	0.89	0.00	5.70
1/20/2017	A1	2.41	3.20	6.63	0.78			8.35	1.68	3.92	10.4					
1/26/2017	A1	3.38		6.85	0.49			7.07	1.86	3.31	9.16	0.07	5.37	0.82	0.08	6.45
2/2/2017	A1			7.00	0.77											
2/3/2017	A1			7.00				8.41	1.43	3.81	10.4	0.08	5.30	0.94	0.00	4.91
2/10/2017	A1	2.04		7.00	0.83			8.39	1.30	4.17	10.9	0.07	5.63	0.88	0.06	4.43
2/17/2017	A1	1.94	3.71	7.34	0.89			8.51	1.38	3.89	10.8	0.07	5.55	0.81	0.00	4.09
2/24/2017	A1			7.21	0.95			8.83	1.30	4.01	11.0	0.07	5.44	0.64	0.00	3.77
3/3/2017	A1			7.19				8.55	1.28	4.18	11.1	0.07	5.70	0.67	0.00	3.93
3/8/2017	A1	1.79		7.58				8.99	1.27	4.05	11.0	0.08	5.61	0.59	0.00	3.82
3/16/2017	A1	1.68	3.58	6.24	0.75	1.14	-12.9	8.50	1.03	4.17	11.0	0.07	5.60	0.92	0.00	4.14
3/24/2017	A1	1.60		7.49	0.98			8.81	1.21	4.24	11.5	0.07	5.46	0.74	0.00	3.88
3/30/2017	A1	1.98		7.48	1.04			8.66	1.47	4.08	11.5	0.07	4.92	0.61	0.00	3.69
4/7/2017	A1	3.15		7.40	0.58			6.82	1.26	3.29	8.49	0.08	4.72	0.53	0.00	5.16
4/13/2017	A1			7.42	0.90			8.43	1.27	4.03	11.0	0.08	4.76	0.67	0.00	4.26
4/21/2017	A1			7.23	1.02			9.06	1.48	4.39	12.0	0.08	4.80	0.83	0.06	3.66

Date	Site	DOC (mg/L)	SUVA (L/mg ² ·m)	pH	Alkalinity (meq/L)	DIC (mM)	δ ¹³ C-DIC (‰)	Sodium (ppm)	Potassium (ppm)	Magnesium (ppm)	Calcium (ppm)	Fluoride (ppm)	Chloride (ppm)	NO ₃ ⁻ as N (ppm)	PO ₄ ³⁻ (ppm)	SO ₄ ²⁻ (ppm)
4/28/2017	A1	3.20	3.44			0.93	-15.2	7.09	1.78	3.40	8.56	0.08	4.46	0.71	0.00	4.83
5/5/2017	A1	6.74		7.47				6.18	2.54	3.39	8.40	0.10	4.68	0.50	0.00	3.83
5/17/2017	A1			7.39				8.94	1.53	4.34	11.6	0.09	4.79	0.98	0.06	3.63
5/26/2017	A1	3.58		6.72	0.68	0.84	-15.1	6.60	1.65	3.55	8.95	0.08	4.34	0.67	0.00	4.19
5/31/2017	A1	3.01		6.95	0.74			8.26	1.75	4.34	11.3	0.09	4.65	0.91	0.11	3.75
6/14/2017	A1	5.90			0.36			3.58	2.17	1.84	4.68	0.08	2.95	0.37	0.08	4.03
6/20/2017	A1	2.87	3.28	6.83	0.83			8.10	1.94	3.71	10.2	0.09	4.35	0.76	0.00	3.84
6/26/2017	A1	3.40		7.40	1.21			8.48	1.75	4.36	11.2					
7/7/2017	A1	2.60		7.10	0.98	1.14	-15.3	8.47	1.85	4.44	11.6	0.10	4.49	0.80	0.06	3.34
7/25/2017	A1			7.14	1.01	1.21	-15.4	8.85	1.69	4.37	11.8	0.09	4.32	0.72	0.02	3.37
8/2/2017	A1	3.19	2.76	7.09				9.27	1.41	4.65	13.0	0.09	4.89	0.86	0.04	3.13
8/10/2017	A1	2.12	3.73	7.40		1.22	-14.9	8.68	1.49	4.36	12.1	0.09	4.34	0.70	0.00	3.09
8/15/2017	A1			7.14	0.95	0.97	-15.2	7.36	1.77	3.64	9.92	0.09	3.94	0.54	0.00	2.99
8/28/2017	A1							9.37	1.53	4.72	13.4	0.09	4.45	0.66	0.04	2.88
9/6/2017	A1					1.36	-15.2	9.11	1.57	4.61	13.0	0.09	4.48	0.56	0.00	2.93
9/20/2017	A1	2.00	3.69		1.19	1.34	-15.0	9.36	1.73	4.59	13.1	0.08	5.24	0.45	0.06	3.63
9/25/2017	A1	2.28	2.98		1.27			9.71	1.88	4.86	13.9	0.09	5.25	0.27	0.00	3.61
10/6/2017	A1	2.17	3.27	7.90				9.76	1.70	5.04	14.1	0.09	4.81	0.14	0.00	2.84
10/13/2017	A1			6.65		1.68	-16.1					0.09	4.88	0.00	0.00	2.36
10/19/2017	A1	2.51	3.39	7.46		1.47	-14.5	9.19	2.08	4.89	13.3	0.08	5.00	0.25	0.00	3.10
10/25/2017	A1			7.70				8.16	1.96	4.43	11.8	0.08	5.20	0.33	0.00	3.58
10/30/2017	A1			7.67				9.15	1.84	4.74	12.8	0.08	5.27	0.49	0.00	3.33
5/31/2016	A2	2.11	18.7			0.89	-15.6	10.1	1.41	5.42	13.9	0.09	7.56	2.52	0.00	4.53
6/6/2016	A2					0.33	-17.7									
6/17/2016	A2				0.89			9.91	1.35	4.93	13.3					
6/21/2016	A2				0.81	0.94	-15.3	9.75	1.20	5.09	13.7					
6/30/2016	A2				0.90			9.50	1.35	4.96	13.3	0.09	7.22	2.47	0.00	3.83
7/6/2016	A2				0.93			9.95	1.19	4.93	13.4	0.11	7.12	2.86	0.27	3.74
7/28/2016	A2	2.17	4.66	7.49	0.94	1.13	-16.2	10.4	1.28	4.85	13.4	0.11	7.32	2.16	0.21	3.80
8/4/2016	A2	2.17	12.9	7.40	0.83	0.96	-15.7					0.11	6.97	2.19	0.20	3.47
10/25/2016	A2					1.12	-14.5	9.63	1.99	5.29	13.5	0.09	7.98	2.44	0.18	4.29
11/14/2016	A2	1.53	3.53	7.31	0.96	1.09	-13.6	9.69	1.68	5.41	14.3	0.08	7.96	2.90	0.12	4.07
12/7/2016	A2	5.18	2.49	6.88				6.51	1.19	3.78	11.0	0.08	6.82	0.93	0.18	3.77
1/19/2017	A2			7.15	0.83	0.93	-12.8	8.80	1.89	5.28	13.4	0.07	10.1	2.60	0.08	8.32
2/17/2017	A2			7.46	0.89											
3/16/2017	A2	1.41	3.68	6.96	0.85	1.12	-12.3	9.13	1.04	5.36	13.6	0.07	8.23	2.88	0.07	5.11
4/28/2017	A2	3.08	4.22			0.95	-14.9					0.08	5.67	1.83	0.13	5.56
5/26/2017	A2	4.93		6.79	0.68	0.79	-14.5	6.67	2.04	4.21	9.67	0.08	5.20	1.57	0.11	5.34
6/20/2017	A2			6.98	0.78			7.93	2.58	4.55	10.8	0.09	5.73	2.20	0.13	4.70
7/25/2017	A2			7.43	0.89	1.09	-15.0	8.71	1.73	4.72	11.7	0.08	6.22	2.09	0.15	3.93
8/15/2017	A2			7.16	0.82	1.26	-15.3	8.23	1.75	4.61	12.0	0.08	6.46	1.80	0.14	3.65
9/20/2017	A2	2.32	3.23		1.02	1.23	-15.2	9.21	1.78	4.96	12.8	0.07	7.51	1.69	0.11	4.24
10/19/2017	A2	2.60	3.70	7.38		1.30	-14.6	8.48	1.91	5.24	12.5	0.08	7.19	0.84	0.18	3.27
5/31/2016	A3	3.28	1.61					10.4	1.48	4.12	10.6	0.10	6.45	0.93	0.00	3.42
6/6/2016	A3					0.91	-15.9	9.64	1.56	4.13	10.5	0.08	7.58	0.76	0.07	3.12
6/17/2016	A3							10.8	1.63	4.20	11.3	0.10	6.61	0.70	0.11	3.00
6/21/2016	A3							10.4	1.36	5.15	11.0	0.11	6.49	0.65	0.00	3.00
6/30/2016	A3					0.77	-16.3	7.45	1.58	3.39	8.68	0.08	7.58	0.76	0.07	3.12
7/6/2016	A3				1.08			10.3	1.44	4.20	11.0	0.12	6.16	0.42	0.00	2.59
7/28/2016	A3	1.61	1.99	7.18	1.10	1.90	-18.9	11.5	1.01	4.13	12.8					
8/4/2016	A3	24.8	0.28	6.92	0.89	1.06	-17.3					0.12	4.63	0.22	0.07	3.31
9/20/2016	A3	1.51	1.39			1.93	-17.9					0.09	3.50	0.21	0.20	3.25
9/28/2016	A3											0.10	4.60	0.36	0.25	4.13
10/25/2016	A3	2.39	3.22		0.95	1.19	-14.9	9.65	1.86	3.97	10.1	0.10	6.21	0.12	0.06	3.34
11/1/2016	A3							8.87	1.26	3.73	9.32					
11/14/2016	A3	1.84	3.21	7.35	1.00	1.28	-15.8	10.4	1.72	4.22	11.3	0.09	5.88	0.22	0.00	3.27
12/7/2016	A3	4.53		6.55				4.81	1.49	2.52	7.14	0.09	5.20	5.93	0.00	4.81

Date	Site	DOC (mg/L)	SUVA (L/mg ² ·m)	pH	Alkalinity (meq/L)	DIC (mM)	δ ¹³ C-DIC (‰)	Sodium (ppm)	Potassium (ppm)	Magnesium (ppm)	Calcium (ppm)	Fluoride (ppm)	Chloride (ppm)	NO ₃ ⁻ as N (ppm)	PO ₄ ³⁻ (ppm)	SO ₄ ²⁻ (ppm)
1/19/2017	A3	2.43	3.86	6.84	0.75	0.92	-13.5	8.88	1.39	3.73	9.44	0.08	6.31	0.62	0.00	5.18
2/17/2017	A3	2.07		7.22	0.80	0.90	-12.8					0.07	6.44	0.79	0.00	4.09
3/16/2017	A3	2.00	4.24	7.06	0.75	1.05	-12.7					0.07	6.36	0.92	0.00	3.87
4/28/2017	A3	3.15	4.32		0.57	0.77	-14.6	7.52	1.46	3.08	7.62	0.08	5.35	0.54	0.13	4.94
5/26/2017	A3	4.91		6.76	0.62	0.72	-15.6	6.76	1.46	2.93	7.23	0.08	4.97	0.55	0.00	4.36
6/20/2017	A3	2.45	3.96	6.80	0.70			8.59	1.58	3.36	8.02	0.09	5.09	0.69	0.00	4.00
7/25/2017	A3			7.07	0.84	1.08	-16.0	8.82	1.63	3.80	9.57	0.09	4.80	0.42	0.07	4.30
8/15/2017	A3			7.26	0.62	0.84	-16.1	6.23	1.74	3.01	7.56	0.08	3.81	0.37	0.03	3.20
9/20/2017	A3	2.52	3.42		1.05	1.16	-15.8	9.02	1.97	3.98	10.4	0.08	5.91	0.09	0.00	3.24
10/18/2017	A3	15.9	0.81													
5/31/2016	A4	2.73	8.06		0.99	1.04	-15.6	7.89	1.88	3.49	9.86	0.11	4.12	0.21	0.00	2.38
6/6/2016	A4				0.55	-15.5	7.85	1.47	3.51	9.99						
6/17/2016	A4				0.94	-15.0	8.60	1.38	4.02	11.1						
6/21/2016	A4				0.84	1.04	-15.0	9.05	1.29	5.05	11.8	0.11	6.16	0.23	0.00	2.07
6/30/2016	A4				0.95	0.99	-15.2	8.02	1.56	3.68	10.1	0.08	4.19	0.22	0.02	1.77
7/6/2016	A4				1.11			8.97	1.36	4.14	11.7	0.11	3.73	0.19	0.00	1.99
7/28/2016	A4	1.75	3.54	7.76	1.28	1.49	-16.1	10.3	1.19	4.84	14.4	0.11	3.82	0.26	0.00	2.11
8/4/2016	A4	2.74	4.78	7.23	1.12	1.14	-16.7					0.12	3.75	0.23	0.10	2.42
9/20/2016	A4	18.5	0.68		1.44	1.56	-15.6									
10/25/2016	A4	1.57	2.99		1.19	1.42	-16.2	9.60	1.39	4.74	13.9	0.10	5.65	0.15	0.00	2.92
11/14/2016	A4	1.75	2.34	8.30	1.24	1.47	-14.9	9.34	1.18	4.72	13.9	0.09	3.70	0.14	0.02	2.74
12/7/2016	A4	2.89	3.80	6.87				7.19	1.93	2.85	7.49	0.10	4.62	0.14	0.00	3.68
1/19/2017	A4	1.93	3.79	6.85	0.73	0.80	-13.3	7.11	1.30	2.97	8.29	0.08	4.12	0.14	0.00	3.70
2/17/2017	A4	2.74	2.96	6.98	0.72			7.34	1.22	3.04	8.37					
3/16/2017	A4	1.66	4.10	7.08	0.68	0.94	-12.8	7.40	1.05	3.12	8.43	0.07	3.98	0.13	0.00	3.05
4/28/2017	A4	3.54	3.53		0.98	0.68	-14.5	5.94	1.69	2.58	6.79	0.08	3.46	0.17	0.00	3.49
5/26/2017	A4	4.57		6.68	0.68	0.85	-15.4	6.05	1.55	2.86	7.38	0.08	3.61	0.19	0.00	2.95
6/20/2017	A4	3.01	4.18	7.20	0.70			7.13	1.64	3.01	7.65	0.09	3.45	0.22	0.00	2.65
7/25/2017	A4			7.15	0.96	1.19	-15.6	8.05	1.57	3.64	10.1	0.09	3.56	0.21	0.00	2.21
8/15/2017	A4			7.70	0.86	1.06	-15.2	7.05	1.76	3.35	9.24	0.09	3.29	0.19	0.00	2.09
9/20/2017	A4		3.68		1.30	1.47	-16.2	9.22	1.46	4.59	13.2	0.08	4.06	0.20	0.06	3.01
10/19/2017	A4	1.98	3.59	7.21	1.20	-15.9	8.07	2.06	3.91	9.97	0.08	5.05	0.00	0.00	3.49	
5/31/2016	C1	2.81	3.13		0.57											
6/1/2016	C1	3.39			0.41	0.42	-14.3	6.02	1.33	1.61	4.31	0.21		0.21	0.07	1.67
6/2/2016	C1							6.37	1.31	1.59	4.23					
6/6/2016	C1				0.44	0.45	-15.7	5.85	1.34	1.55	4.12					
6/7/2016	C1				0.40							0.07	4.83	0.19	0.04	1.06
6/9/2016	C1				0.22											
6/14/2016	C1				0.21	0.46	-15.3					0.08	5.69	0.21	0.06	1.04
6/16/2016	C1				0.43			4.02	0.99	1.09	2.83	0.07	4.88	0.17	0.05	0.90
6/17/2016	C1				0.40			6.25	1.49	1.67	4.69					
6/20/2016	C1				0.42	0.51	-14.7	6.21	1.38	1.64	4.43					
6/21/2016	C1	9.23			0.30	0.50	-15.5	5.74	1.16	1.44	3.98	0.11	6.51	0.23	0.06	1.32
6/27/2016	C1							6.18	1.29	1.56	4.22	0.05	3.50	0.18	0.04	0.98
6/28/2016	C1				0.20			6.16	1.35	1.66	4.44	0.08	5.23	0.13	0.00	1.25
6/30/2016	C1				0.37			5.89	1.43	1.56	4.17	0.05	3.39	0.17	0.04	0.98
7/5/2016	C1				0.52	-16.2						0.10	3.58	0.01	0.00	1.22
7/6/2016	C1				0.45	0.53	-14.8	6.30	1.34	1.59	4.42	0.10	4.13	0.13	0.00	1.28
7/21/2016	C1	9.23			0.49	0.62	-15.6					0.09	3.39	0.13	0.00	1.24
7/28/2016	C1	2.62	0.10	7.54		0.65	-16.1	6.93	1.52	2.57	5.68	0.08	5.28	0.16	0.00	1.38
7/28/2016	C1	2.62	3.82													
8/4/2016	C1			7.15								0.10	3.13	0.10	0.07	1.27
8/9/2016	C1	3.16			0.51	0.61	-14.5					0.10	3.26	0.09	0.00	1.36
8/16/2016	C1	2.76										0.10	2.88	0.09	0.10	1.12
9/7/2016	C1	2.87		6.85		0.58	-13.8	6.39	1.42	1.64	5.24	0.11	2.98	0.07	0.11	1.20
9/13/2016	C1															
9/21/2016	C1	2.64	3.79			0.87	-14.7					0.10	3.29	0.06	0.00	1.27

Date	Site	DOC (mg/L)	SUVA (L/mg ² ·m)	pH	Alkalinity (meq/L)	DIC (mM)	δ ¹³ C-DIC (‰)	Sodium (ppm)	Potassium (ppm)	Magnesium (ppm)	Calcium (ppm)	Fluoride (ppm)	Chloride (ppm)	NO ₃ ⁻ as N (ppm)	PO ₄ ³⁻ (ppm)	SO ₄ ²⁻ (ppm)
9/28/2016	C1	4.17						6.77	2.04	1.82	4.78	0.10	3.38	0.04	0.00	1.73
10/4/2016	C1	3.10	2.20					2.47	0.78	0.84	2.46	0.09	3.46	0.06	0.00	1.43
10/12/2016	C1	2.88	3.47		0.30			6.41	1.65	1.51	4.20	0.09	3.53	0.08	0.00	1.89
10/18/2016	C1	2.79						6.39	1.62	1.78	5.01	0.09	3.58	0.00	0.00	1.49
10/26/2016	C1	2.07	3.96		0.77	0.63	-15.2	6.32	1.58	1.80	4.84					
11/1/2016	C1	2.35			0.40			6.49	1.81	1.86	4.89	0.09	3.50	0.01	0.00	1.35
11/9/2016	C1				0.44			6.37	1.85	1.80	4.67	0.09	3.34	0.02	0.00	1.37
11/16/2016	C1	1.93	4.26	7.09	0.57	0.55	-14.2	6.40	1.54	1.80	4.52	0.08	3.34	0.00	0.00	1.47
11/21/2016	C1				0.43	0.62	-16.2	6.36	1.76	1.87	4.83	0.07	3.45	0.00	0.00	1.40
11/29/2016	C1	5.51		6.35				6.24	3.40	1.93	4.88	0.11	3.96	0.00	0.00	1.62
12/7/2016	C1	3.66	4.07	7.18				6.51	2.11	1.59	4.20	0.08	3.41	0.22	0.29	1.84
12/13/2016	C1			6.73				6.52	1.60	1.58	4.28	0.10	5.18	0.38	0.23	4.21
1/4/2017	C1	5.00		6.59	0.23			5.31	1.42	1.24	3.23	0.07	3.67	0.02	0.00	3.81
1/12/2017	C1	3.11		6.56	0.32			5.98	1.17	1.44	3.66	0.07	4.00	0.02	0.04	3.26
1/19/2017	C1	2.56	3.99	6.82	0.37	0.47	-13.2	5.91	1.23	1.53	4.28	0.06	3.62	0.02	0.00	2.46
1/26/2017	C1	4.33		6.68	0.20			4.93	1.38	1.28	2.85	0.06	3.82	0.02	0.00	3.53
2/2/2017	C1	3.27		7.03				5.54	1.38	1.56	3.66	0.06	3.38	0.05	0.00	2.91
2/10/2017	C1	2.75		6.98	0.35			5.62	1.21	1.53	4.13	0.06	3.38	0.06	0.00	2.40
2/17/2017	C1	2.50	4.92	7.08	0.39			5.53	1.17	1.38	3.58	0.06	3.37	0.06	0.00	2.12
2/24/2017	C1	2.54		6.95	0.44			5.85	1.23	1.46	3.89	0.06	3.37	0.00	0.08	1.81
3/3/2017	C1			6.95				5.49	1.14	1.32	3.58	0.06	3.43	0.03	0.00	1.82
3/8/2017	C1	2.78		6.96				5.58	1.20	1.32	3.67	0.06	3.37	0.00	0.00	1.78
3/16/2017	C1	2.33	4.03	6.99	0.35	0.50	-10.0	5.58	1.03	1.36	3.25	0.06	3.53	0.01	0.00	2.01
3/24/2017	C1	2.48		7.54	0.38			5.86	1.16	1.32	3.62	0.06	3.90	0.00	0.00	1.98
3/30/2017	C1	3.40		7.29	0.41			5.86	1.30	1.52	4.38	0.06	3.62	0.02	0.10	1.77
4/7/2017	C1	4.29		7.16	0.26			5.06	1.30	1.26	3.25	0.07	4.00	0.05	0.00	2.95
4/13/2017	C1			6.89	0.41			5.63	1.34	1.51	4.13	0.07	3.34	0.02	0.00	2.28
4/21/2017	C1			6.76	0.46			5.80	1.49	1.71	4.52	0.07	3.33	0.08	0.00	1.78
4/28/2017	C1	4.50	3.93	6.59	0.22	0.37	-14.8					0.07	3.05	0.11	0.00	2.80
5/5/2017	C1	7.68		6.69				5.14	1.69	1.43	3.68	0.09	4.45	0.06	0.00	2.37
5/17/2017	C1			7.23				8.76	1.70	4.79	12.4	0.10	4.64	0.73	0.12	4.64
5/26/2017	C1	4.93		6.42	0.40	0.42	-15.6	4.84	1.39	1.40	3.22	0.07	3.34	0.12	0.00	2.21
5/31/2017	C1	3.21		6.44	0.39			5.34	1.35	1.56	4.04	0.07	3.17	0.15	0.05	1.61
6/14/2017	C1	6.68			0.24			3.66	1.42	1.32	2.79	0.07	2.91	0.08	0.00	2.77
6/21/2017	C1	5.56	4.61	6.87	0.57			4.83	1.44	1.41	3.37	0.07	3.48	0.10	0.00	1.55
6/26/2017	C1	3.73		7.42	0.40			5.47	1.36	1.49	4.03	0.07	3.24	0.13	0.00	1.87
7/7/2017	C1	3.78		6.73	0.39	0.47	-14.9	5.25	1.40	1.52	3.81	0.08	3.16	0.12	0.00	1.71
7/25/2017	C1			7.16	0.48	0.58	-14.3	5.89	1.49	1.69	4.37	0.08	3.23	0.12	0.00	1.43
8/2/2017	C1	1.96	4.91	6.90	0.60	0.60	-13.4	6.03	1.30	1.59	4.51	0.07	3.19	0.10	0.00	1.48
8/10/2017	C1	2.33	4.76	6.90		0.56	-13.6	5.89	1.36	1.54	4.47					
9/6/2017	C1					0.62	-14.1	5.97	1.54	1.84	4.93	0.07	3.11	0.06	0.00	1.34
9/20/2017	C1	2.19	1.69		0.50	0.62	-14.6	6.09	1.66	1.54	4.61	0.06	3.73	0.03	0.00	2.10
9/25/2017	C1	2.55	3.92		0.50			6.21	1.69	1.70	4.99	0.06	3.70	0.05	0.00	2.07
10/6/2017	C1	2.11	4.83	7.33				6.38	1.85	1.92	5.34	0.07	3.72	0.00	0.00	1.57
10/13/2017	C1			7.12		0.78	-16.2					0.07	3.73	0.00	0.00	1.41
10/20/2017	C1	8.33	1.18	7.02				6.00	1.68	1.65	4.35	0.06	3.79	0.00	0.00	1.45
10/25/2017	C1			7.43				5.92	1.92	1.60	4.27	0.06	3.78	0.00	0.00	1.48
10/30/2017	C1			7.76				6.14	1.79	1.70	4.52	0.06	3.88	0.00	0.00	1.43
6/21/2016	C2				0.34	0.50	-15.5	6.07	1.23	1.37	3.73	0.06	4.37	0.20	0.03	0.95
6/30/2016	C2				0.36			5.94	1.38	1.42	3.75	0.05	3.50	0.17	0.03	0.91
7/28/2016	C2	2.22	3.83	7.51	0.49	0.64	-17.4	6.49	1.44	1.63	4.42	0.09	3.29	0.13	0.00	1.26
8/4/2016	C2			7.06								0.09	3.36	0.12	0.00	1.25
9/21/2016	C2	1.43	4.82			0.81	-16.7	6.89	1.40	2.04	5.64	0.09	2.76	0.05	0.07	1.27
10/26/2016	C2	1.88	3.77		0.42	0.56	-15.2	6.41	1.54	1.62	4.40					
11/4/2016	C2				0.81			6.40	1.77	1.62	4.17	0.08	3.29	0.02	0.06	1.28
11/16/2016	C2	2.01	5.76	6.77	0.49	0.61	-16.4	6.32	1.69	1.60	4.00	0.07	3.96	0.03	0.00	1.49
11/21/2016	C2				0.46			6.40	1.75	1.71	4.72	0.07	3.27	0.00	0.00	1.36

Date	Site	DOC (mg/L)	SUVA (L/mg·m)	pH	Alkalinity (meq/L)	DIC (mM)	$\delta^{13}\text{C-DIC}$ (‰)	Sodium (ppm)	Potassium (ppm)	Magnesium (ppm)	Calcium (ppm)	Fluoride (ppm)	Chloride (ppm)	NO ₃ ⁻ as N (ppm)	PO ₄ ³⁻ (ppm)	SO ₄ ²⁻ (ppm)
11/29/2016	C2	4.87		6.31				6.30	3.33	1.73	4.26					
12/7/2016	C2	3.85	3.61	6.61				3.21	1.03	0.99	2.60	0.08	3.42	0.02	0.00	1.50
12/13/2016	C2			6.71				6.10	1.41	1.48	3.95	0.08	3.29	0.02	0.00	1.49
1/4/2017	C2	5.46		6.46	0.23			5.34	1.41	1.13	2.92	0.07	3.76	0.00	0.00	3.99
1/12/2017	C2	3.24		6.48	0.64			6.00	1.28	1.33	3.33	0.07	4.36	0.04	0.00	3.34
1/19/2017	C2	2.97	3.37	7.00	0.38	0.47	-13.5	6.11	1.27	1.51	5.83	0.07	3.37	0.03	0.00	2.34
1/26/2017	C2	4.61		6.75	0.18			4.96	1.47	1.08	2.46	0.06	4.00	0.07	0.08	3.53
2/2/2017	C2	4.00		7.24	0.26			5.41	1.26	1.32	3.08	0.06	3.39	0.07	0.00	2.49
2/10/2017	C2	2.78		7.32	0.34			5.44	1.18	1.26	3.26	0.07	3.28	0.12	0.07	2.17
2/17/2017	C2	2.46	4.14	6.81	0.31	0.42	-14.0	5.62	1.25	1.28	3.32					
2/24/2017	C2	2.61		6.77				5.66	1.34	1.21	3.37	0.06	3.27	0.04	0.00	1.77
3/3/2017	C2			6.78				5.49	1.15	1.21	3.22	0.06	3.38	0.00	0.00	1.87
3/8/2017	C2	2.63		7.07				5.58	1.61	1.08	3.22	0.06	3.33	0.03	0.00	1.68
3/16/2017	C2	2.42	3.96	6.42	0.29	0.49	-12.4	5.61	1.10	1.24	3.15	0.06	3.58	0.05	0.00	1.98
3/24/2017	C2	2.44		7.34	0.35			5.86	1.22	1.25	3.51	0.06	3.88	0.07	0.00	1.91
3/30/2017	C2	3.14		7.33	0.43			5.77	1.33	1.35	3.66	0.06	3.80	0.06	0.08	1.68
4/7/2017	C2	4.90		7.16	0.24			4.96	1.32	1.17	2.86	0.07	3.97	0.08	0.00	2.83
4/13/2017	C2			7.08	0.38			5.35	1.32	1.31	3.58	0.07	3.45	0.07	0.00	1.86
4/21/2017	C2			6.74	0.41			5.77	1.51	1.65	4.26	0.07	3.29	0.10	0.00	1.40
4/28/2017	C2	4.82	3.71	6.80	0.26	0.29	-14.0	4.32	1.44	1.17	2.63	0.08	3.11	0.11	0.00	2.66
5/5/2017	C2	7.57		6.82				5.14	1.66	1.34	3.16	0.07	4.56	0.06	0.00	1.97
5/17/2017	C2			6.93				5.62	1.34	1.41	3.72	0.07	3.24	0.17	0.00	1.44
5/26/2017	C2	5.28		6.35	0.30	0.38	-16.1	4.78	1.36	1.39	3.04	0.07	3.25	0.12	0.00	2.07
5/31/2017	C2	3.70		6.41	0.40			5.34	1.36	1.41	3.51	0.07	3.39	0.19	0.00	1.95
6/14/2017	C2	6.63			0.17			3.66	1.47	1.09	2.43	0.07	3.02	0.08	0.00	2.60
6/21/2017	C2	6.21	4.22	6.80	0.27			4.79	1.42	1.29	3.06	0.07	3.70	0.10	0.00	1.48
6/26/2017	C2	4.40		7.63	0.37			5.47	1.61	1.55	3.61	0.07	3.39	0.14	0.00	1.48
7/7/2017	C2	3.95		6.69	0.36	0.43	-15.4	5.18	1.39	1.39	3.36	0.08	3.20	0.13	0.00	1.52
7/25/2017	C2			6.65	0.44	0.56	-15.8	6.02	1.64	1.56	4.19	0.07	3.25	0.12	0.00	1.27
8/2/2017	C2	1.77	4.85	6.62		0.56	-14.8	6.08	1.35	1.46	4.15					
8/10/2017	C2	2.57	4.12	6.91		0.55	-14.9	5.84	1.37	1.54	4.14	0.07	3.18	0.13	0.02	1.28
8/16/2017	C2			6.68												
8/21/2017	C2											0.07	3.22	0.11	0.00	1.27
8/28/2017	C2							6.10	1.42	1.63	4.28	0.07	3.23	0.11	0.00	1.30
9/6/2017	C2					0.59	-15.5	5.93	1.44	1.43	4.18	0.07	3.17	0.10	0.02	1.23
9/20/2017	C2	2.07	0.39		0.44	0.61	-15.6	6.00	1.58	1.44	4.19	0.06	3.74	0.08	0.00	2.07
9/25/2017	C2	6.28	1.42													
10/6/2017	C2	1.85	3.78	7.38				6.26	1.72	1.61	4.92	0.07	3.73	0.06	0.08	1.35
10/13/2017	C2			7.03								0.07	3.79	0.00	0.00	1.24
10/19/2017	C2							5.95	1.69	1.45	4.05	0.06	3.81	0.00	0.00	1.36
10/20/2017	C2	2.10	4.05	7.12				8.14	1.05	7.84	16.2	0.09	4.38	0.05	0.16	2.07
10/25/2017	C2			7.80				5.85	1.76	1.46	3.78	0.07	3.79	0.04	0.00	1.41
10/30/2017	C2			8.18				5.91	1.64	1.50	3.95	0.06	3.78	0.04	0.00	1.41
5/31/2016	D1	1.91	2.20		0.70	0.69	-15.1	8.65	1.68	4.97	12.8	0.08	7.96	0.70	0.10	4.40
6/1/2016	D1	2.65						8.62	1.72	4.78	13.0					
6/2/2016	D1					0.81	-14.5									
6/6/2016	D1				0.78	0.83	-16.1	6.34	1.85	3.59	9.32	0.08	8.07	0.56		3.80
6/7/2016	D1				0.81			5.27	2.87	3.17	8.87	0.10	5.44	0.62	0.00	3.88
6/9/2016	D1				1.14	1.01	-15.2									
6/14/2016	D1					1.01	-15.2	7.55	1.36	4.18	10.7					
6/16/2016	D1				0.95			4.89	1.38	2.66	6.48					
6/17/2016	D1				0.89			8.48	2.13	4.78	12.4					
6/20/2016	D1					0.75	-13.1	9.17	1.82	4.77	13.0					
6/21/2016	D1	1.43			0.96	1.17	-15.7	9.52	1.66	5.23	13.5					
6/27/2016	D1				1.02			9.23	1.49	4.65	12.4	0.08	4.99	0.69	0.17	4.15
6/28/2016	D1							4.74	1.28	2.56	6.69	0.10	5.66	0.83	0.00	4.56
6/30/2016	D1				0.45			5.16	2.12	2.93	7.86	0.10	4.58	0.67	0.11	4.74

Date	Site	DOC (mg/L)	SUVA (L/mg ² ·m)	pH	Alkalinity (meq/L)	DIC (mM)	δ ¹³ C-DIC (‰)	Sodium (ppm)	Potassium (ppm)	Magnesium (ppm)	Calcium (ppm)	Fluoride (ppm)	Chloride (ppm)	NO ₃ ⁻ as N (ppm)	PO ₄ ³⁻ (ppm)	SO ₄ ²⁻ (ppm)
7/5/2016	D1					1.11	-15.9	8.81	1.70	4.48	11.9	0.11	4.74	0.69	0.13	4.01
7/6/2016	D1				0.87			7.88	1.83	4.07	10.9	0.11	4.41	0.63	0.15	4.33
7/15/2016	D1				1.07											
7/21/2016	D1	1.43				1.19	-15.4					0.12	4.72	0.56	0.14	3.65
7/28/2016	D1	2.31	4.54	7.05	0.79	0.91	-16.5	6.88	2.04	3.37	9.20	0.11	3.61	0.37	0.00	3.93
8/4/2016	D1			7.24		0.74	-16.4					0.10	3.70	0.36	0.16	3.36
8/9/2016	D1	5.88				0.65	-12.0					0.13	4.47	0.27	0.08	3.42
8/16/2016	D1	2.49			0.76							0.12	4.51	0.47	0.11	3.68
9/7/2016	D1	1.74		7.17		1.11	-14.1	7.69	2.17	3.83	10.4	0.11	4.09	0.33	0.23	3.51
9/13/2016	D1	2.10		7.19								0.14	6.62	0.21	0.20	3.44
9/21/2016	D1	1.91	2.67			1.13	-14.2	8.58	2.59	3.99	11.2	0.11	4.15	0.09	0.00	3.22
9/28/2016	D1	5.76						5.85	3.44	2.96	7.72	0.13	4.63	0.19	0.00	4.96
10/4/2016	D1	4.71	1.89		1.54			6.60	2.74	3.62	9.91	0.11	4.04	0.28	0.00	4.80
10/12/2016	D1	3.53	11.3		0.68			7.18	3.19	4.07	10.7	0.11	5.20	0.50	0.00	7.01
10/18/2016	D1	2.65						8.67	2.68	4.82	12.8	0.11	5.21	0.25	0.00	4.67
10/25/2016	D1	2.53	3.04		1.33	1.10	-13.8	7.57	2.65	4.58	12.1	0.11	6.07	0.27	0.13	5.92
11/1/2016	D1	2.32			1.52			8.53	2.63	4.97	13.1	0.11	4.93	0.06	0.15	4.37
11/9/2016	D1	1.93			1.07			8.92	2.38	5.72	18.1	0.11	4.78	0.06	0.13	3.79
11/16/2016	D1	1.80	3.44	6.51	1.13	1.14	-14.4	8.90	1.91	5.44	13.6	0.10	4.84	0.10	0.00	3.85
11/21/2016	D1				1.07	1.28	-15.3	8.74	2.95	4.90	12.3	0.09	5.46	0.00	0.01	3.72
11/29/2016	D1	4.12		6.70								0.09	5.70	0.12	0.15	3.53
12/7/2016	D1	4.58	3.80	7.06				4.96	2.51	3.10	8.45	0.11	4.80	0.27	0.12	7.02
12/13/2016	D1			7.29				8.29	1.94	4.60	11.9	0.10	6.85	0.89	0.00	4.33
1/4/2017	D1	4.82		6.68	0.66			5.39	3.64	3.17	8.27	0.10	4.52	0.49	0.07	12.4
1/12/2017	D1	3.39		6.82	0.64							0.09	30.0	0.43	0.00	6.92
1/19/2017	D1	1.82	3.58	7.31	0.98	1.09	-12.8	10.9	1.66	4.33	11.0	0.09	6.99	0.27	0.04	5.27
1/26/2017	D1	2.96		6.78	0.73			7.79	2.09	3.83	9.69	0.08	5.59	0.43	0.00	6.85
2/2/2017	D1	1.59		7.16	0.83			8.39	1.66	4.42	11.2	0.08	5.17	0.44	0.12	5.73
2/3/2017	D1			6.02	0.96											
2/10/2017	D1	2.86		7.06	0.80			7.79	1.80	4.23	10.7	0.08	6.17	0.43	0.00	6.23
2/17/2017	D1	2.14	4.26	7.70	0.82	0.92	-12.1	8.09	1.89	4.16	10.7					
2/24/2017	D1	1.81		8.18	0.99			8.50	1.74	4.46	11.9	0.08	5.23	0.03	0.00	4.94
3/3/2017	D1			7.27				6.97	1.93	4.05	10.2	0.14	5.95	0.29	0.00	7.49
3/8/2017	D1	2.39		8.22				7.95	1.61	3.84	9.88					
3/16/2017	D1	2.29	3.71	8.67	0.80	1.03	-12.2					0.08	5.38	0.26	0.00	5.67
3/24/2017	D1	2.03		9.06	0.93			7.97	1.42	4.38	11.2	0.09	5.21	0.03	0.00	5.29
3/30/2017	D1	2.62		7.52	1.02			8.27	1.74	4.63	12.3	0.08	4.86	0.15	0.00	4.96
4/7/2017	D1	3.37		7.14	0.79			6.50	2.02	3.85	10.1	0.09	4.44	0.32	0.00	6.44
4/13/2017	D1			7.31	0.99			8.00	1.59	4.62	11.9	0.09	4.56	0.22	0.00	5.41
4/21/2017	D1			7.03	0.99			8.30	2.06	4.73	12.3	0.10	4.79	0.50	0.00	5.13
4/28/2017	D1	2.95	3.36	7.14	0.83	1.00	-15.4	7.06	2.26	4.26	11.0	0.09	4.31	0.48	0.03	6.86
5/5/2017	D1	7.45		7.32				4.76	2.80	2.84	7.59	0.10	4.13	0.33	0.00	5.05
5/17/2017	D1			7.17				8.67	1.66	4.75	12.1	0.09	4.89	0.73	0.08	4.62
5/26/2017	D1	4.49		6.92	0.75	0.88	-14.5	5.69	2.76	3.49	9.16	0.09	4.00	0.31	0.03	6.22
5/31/2017	D1	2.88		6.67	0.87			7.14	2.31	4.03	10.6	0.09	4.24	0.55	0.12	5.35
6/14/2017	D1	6.02			0.54			3.91	3.62	2.87	7.45	0.10	3.26	0.20	0.00	6.38
6/21/2017	D1	5.68	4.08	6.55	0.61			4.68	2.87	3.11	8.17	0.09	3.49	0.33	0.10	4.38
6/26/2017	D1	2.55		7.25	0.90			7.42	2.41	4.12	10.6	0.09	4.48	0.59	0.00	4.89
7/7/2017	D1	2.36		7.24	0.86	1.01	-15.1	6.88	2.82	4.04	10.4	0.12	4.62	0.58	0.08	5.55
7/25/2017	D1			7.21	1.15	1.01	-15.7	6.66	2.79	3.79	9.50	0.08	4.45	0.55	0.07	5.24
8/2/2017	D1	1.07	6.64	7.19												
8/10/2017	D1	2.71	3.50	7.22		0.99	-14.9	6.64	2.15	4.00	10.2	0.08	4.05	0.50	0.03	4.36
8/16/2017	D1			6.90												
8/28/2017	D1							8.17	2.27	4.33	11.2	0.08	4.53	0.47	0.13	3.89
9/6/2017	D1							7.84	2.12	4.22	11.1	0.08	4.27	0.31	0.09	3.60
9/20/2017	D1	1.78	3.49			1.29	-15.4	8.21	2.51	4.36	11.8	0.08	4.98	0.28	0.14	4.21
9/25/2017	D1	1.85	3.41		1.37			8.38	2.52	4.48	12.0	0.08	4.76	0.15	0.14	4.18

Date	Site	DOC (mg/L)	SUVA (L/mg ² ·m)	pH	Alkalinity (meq/L)	DIC (mM)	δ ¹³ C-DIC (‰)	Sodium (ppm)	Potassium (ppm)	Magnesium (ppm)	Calcium (ppm)	Fluoride (ppm)	Chloride (ppm)	NO ₃ ⁻ as N (ppm)	PO ₄ ³⁻ (ppm)	SO ₄ ²⁻ (ppm)
10/6/2017	D1	2.00	3.55	7.32				8.47	2.34	4.65	12.4	0.08	4.60	0.08	0.23	3.78
10/13/2017	D1			7.08		1.46	-17.4					0.09	4.80	0.04	0.27	3.26
10/20/2017	D1	2.72	2.43	7.20				7.05	2.30	4.05	10.5	0.08	4.85	0.35	0.19	3.94
10/25/2017	D1			7.37				5.74	3.45	3.54	8.93	0.08	4.97	0.31	0.07	4.14
10/30/2017	D1			7.77				7.55	2.32	4.54	11.3	0.08	5.11	0.35	0.13	3.89
5/31/2016	D2	3.85	2.42			0.49	-15.1	9.33	2.45	6.51	16.0					
6/2/2016	D2				1.18	1.23	-13.5									
6/6/2016	D2					1.03	-13.8	7.46	2.36	5.29	13.1	0.10	8.56	0.98	0.04	3.66
6/17/2016	D2											0.11	8.73	1.94	0.07	4.43
6/21/2016	D2				1.40	1.54	-13.5	13.8	2.27	8.52	20.3					
6/30/2016	D2				0.70							0.11	6.38	0.80	0.00	6.10
7/6/2016	D2				1.25			10.9	2.51	6.95	16.6	0.13	9.02	1.53	0.00	5.01
7/28/2016	D2	3.54	2.85	7.18	1.56			13.5	2.63	7.70	19.5	0.13	11.6	1.49	0.00	6.10
8/4/2016	D2	17.6		7.38	0.80							0.10	3.83	0.43	0.14	3.01
9/21/2016	D2	3.64	3.66			1.22	-15.1	9.10	2.85	4.32	11.4	0.13	4.48	0.02	0.10	2.12
9/28/2016	D2											0.12	4.71	0.14	0.00	
10/26/2016	D2	4.78	3.09		0.94	1.07	-12.4	6.76	4.37	5.61	13.8					
11/16/2016	D2	2.95	3.46	6.40	1.60	1.78	-13.3	11.7	2.95	9.14	22.4	0.10	11.8	1.86	0.00	5.77
12/7/2016	D2			6.91				6.29	4.19	4.38	9.75	0.12	5.58	0.30	0.00	11.8
1/19/2017	D2	3.14	3.44	7.42	1.30	1.40	-11.4	9.13	2.68	7.26	17.1	0.09	8.13	1.51	0.00	8.20
2/17/2017	D2	3.77	3.48	7.46		0.96	-10.6	7.34	3.12	5.07	12.4					
3/16/2017	D2	4.07	3.44	8.38	0.76	0.93	-9.4	7.34	2.75	4.85	11.6	0.09	6.52	0.85	0.00	9.20
4/28/2017	D2	5.44	3.22	7.16	0.72	0.90	-12.0	5.77	3.38	4.01	10.4	0.11	5.11	0.58	0.00	10.0
5/26/2017	D2	6.24		7.16	0.66	0.87	-12.0	4.88	3.60	3.44	9.18	0.11	4.29	0.23	0.00	7.38
6/21/2017	D2	6.25	3.87	7.99	0.67			4.14	4.23	3.41	8.74	0.11	3.78	0.35	0.00	5.48
7/25/2017	D2			7.13	0.78	0.94	-13.0	6.16	3.76	4.38	9.98	0.10	5.35	0.77	0.00	6.17
8/16/2017	D2			8.05												
9/20/2017	D2	3.49	3.50		1.47	1.69	-14.3	9.78	3.85	7.40	17.5	0.09	9.74	1.30	0.00	5.46
10/20/2017	D2	3.78	4.10	6.99				12.2	3.50	9.36	19.6	0.09	12.7	1.19	0.07	6.58
5/31/2016	P1	2.89	1.87		0.87	0.83	-15.7	6.04	1.16	3.81	11.4	0.08	3.42	0.10	0.02	2.63
6/6/2016	P1							5.21	1.26	3.28	10.4	0.09	10.8	0.09	0.00	2.14
6/14/2016	P1											0.09	4.26	0.17	0.05	2.39
6/17/2016	P1				0.90			6.87	1.26	4.28	13.3					
6/21/2016	P1					1.45	-16.3	8.67	1.34	5.00	16.2					
6/30/2016	P1					1.18	-16.1	6.92	1.32	4.20	13.6	0.06	3.54	0.22	0.03	2.61
7/6/2016	P1				1.26			7.93	1.25	4.62	14.7	0.10	6.39	0.14	0.00	3.06
7/28/2016	P1	1.82	4.06	7.44	1.24	1.35	-16.6	8.65	1.35	4.78	15.6	0.10	3.21	0.16	0.00	3.04
8/4/2016	P1	2.56		7.20	1.44	1.36	-16.7					0.11	3.09	0.16	0.00	3.08
9/21/2016	P1	1.92	2.76			1.50	-15.0	8.42	1.51	4.75	15.7	0.10	3.07	0.05	0.00	3.09
10/26/2016	P1	1.37	2.26		1.33			8.94	1.29	5.30	16.4					
11/16/2016	P1	1.13	3.73	6.40		1.60	-11.9	9.14	1.22	5.27	16.5	0.09	3.15	0.00	0.00	3.71
12/7/2016	P1	4.39	2.32	7.04				2.04	0.88	1.70	7.35	0.10	1.81	0.02	0.00	1.17
1/19/2017	P1			7.50	0.85	1.00	-12.8	5.67	1.54	3.34	10.8	0.07	2.81	0.04	0.00	3.11
2/3/2017	P1			6.95	0.81			5.48	1.50	3.13	9.95					
2/17/2017	P1	3.33	4.68	7.85	0.65			4.89	1.95	2.68	8.97	0.07	3.13	0.01	0.00	2.71
3/16/2017	P1	3.41	3.90	7.57	0.67	0.89	-11.2	5.16	1.40	2.92	9.01	0.07	3.27	0.02	0.00	2.65
4/28/2017	P1	4.41	3.83	7.14	0.49	0.70	-14.8					0.08	2.78	0.07	0.00	2.86
5/26/2017	P1	4.19		6.82	0.60	0.67	-14.6	3.44	1.34	2.26	6.77	0.08	2.46	0.07	0.00	2.36
6/21/2017	P1	5.09		7.02	0.44			2.82	1.51	1.99	6.75	0.08	2.17	0.05	0.00	1.68
7/25/2017	P1			6.99	0.96	1.19	-15.6	5.95	1.37	3.53	11.5	0.08	2.70	0.06	0.00	2.72
8/16/2017	P1			7.37												
9/20/2017	P1	1.10	9.59		1.33	1.52	-15.7	8.45	1.33	4.68	15.3	0.07	3.58	0.07	0.00	4.10
10/20/2017	P1	17.8	0.25	7.17				8.38	1.31	4.87	14.6	0.08	3.63	0.00	0.00	3.61
5/31/2016	R1	2.17	4.85		0.90	0.82	-16.0					0.09	6.05	0.49	0.00	3.45
6/1/2016	R1	2.81				0.27	-15.9	7.86	1.41	4.22	11.4					
6/2/2016	R1					0.96	-15.9	8.30	1.30	4.19	11.2					
6/6/2016	R1					1.14	-15.2	7.09	1.47	3.87	10.5	0.09	8.23	0.42	0.00	2.97

Date	Site	DOC (mg/L)	SUVA (L/mg ² ·m)	pH	Alkalinity (meq/L)	DIC (mM)	δ ¹³ C-DIC (‰)	Sodium (ppm)	Potassium (ppm)	Magnesium (ppm)	Calcium (ppm)	Fluoride (ppm)	Chloride (ppm)	NO ₃ ⁻ as N (ppm)	PO ₄ ³⁻ (ppm)	SO ₄ ²⁻ (ppm)
6/7/2016	R1				1.10	0.90	-15.4	7.60	1.56	3.95	10.9	0.11	6.60	0.46	0.00	3.25
6/9/2016	R1															
6/14/2016	R1							8.73	1.38	4.41	15.6					
6/16/2016	R1				0.89			8.03	1.49	4.18	11.3					
6/17/2016	R1					1.10	-15.7	8.34	1.55	4.07	11.0	0.09	2.66	0.08	0.00	1.38
6/20/2016	R1				0.93	0.99	-15.5	8.32	1.27	4.24	11.5	0.07	4.99	0.53	0.08	3.18
6/21/2016	R1	1.61			0.93	1.11	-15.2	8.42	1.36	4.26	11.7					
6/23/2016	R1											0.09	5.40	0.52	0.00	3.23
6/27/2016	R1				1.02			8.55	1.23	4.25	11.7	0.07	4.50	0.47	0.07	3.14
6/28/2016	R1							7.95	1.36	4.01	10.9	0.09	2.45	0.20	0.00	1.70
6/30/2016	R1				0.68			6.37	1.64	3.37	9.00	0.07	4.00	0.53	0.07	3.21
7/5/2016	R1					1.07	-16.2					0.11	4.44	0.17	0.00	3.06
7/6/2016	R1				0.95			8.04	1.38	4.17	11.4	0.11	4.44	0.26	0.00	3.11
7/21/2016	R1	1.61				1.24	-16.5					0.49	4.01	0.01	0.00	2.97
7/28/2016	R1	2.23	3.81	7.45	0.95	1.18	-15.6	7.98	1.52	4.08	11.4	0.12	3.53	0.25	0.00	3.11
8/4/2016	R1	2.54	2.88	7.11		0.90	-16.4					0.11	3.07	0.19	0.06	2.78
8/9/2016	R1	13.8			0.73							0.13	3.68	0.19	0.00	2.74
8/16/2016	R1	2.49										0.11	2.17	0.13	0.09	1.76
9/7/2016	R1	1.87				1.24	-14.6					0.11	3.30	0.13	0.15	3.00
9/20/2016	R1	2.09	0.81			1.52	-14.7	1.94	0.50	1.52	6.59	0.12	3.81	0.03	0.07	3.15
10/25/2016	R1	2.17	4.24		1.07	1.25	-14.8	7.33	2.36	4.38	11.9	0.11	4.36	0.10	0.08	4.44
11/14/2016	R1	2.40	2.75	7.11	1.10	1.22	-12.9	8.33	1.66	4.55	12.4	0.09	4.13	0.08	0.00	3.23
12/7/2016	R1	3.75	3.36	6.91				5.80	2.15	3.40	9.38	0.06	2.45	0.04	0.07	2.09
1/19/2017	R1	1.93	4.20	7.07				8.31	1.47	3.94	12.1	0.08	5.01	0.31	0.00	5.08
2/17/2017	R1	1.69	3.43	7.10	0.89			7.40	1.29	3.89	10.6					
3/16/2017	R1	2.15	4.47	7.40	0.80	0.99	-12.3	6.82	1.35	3.53	9.61	0.07	4.16	0.25	0.11	4.17
4/28/2017	R1	3.30	3.58			0.80	-14.5	5.71	1.63	3.02	7.77	0.08	3.46	0.32	0.00	5.07
5/26/2017	R1	4.53		6.55	0.65	0.75	-14.6	5.33	1.91	2.98	7.96	0.08	3.43	0.27	0.00	4.21
6/20/2017	R1	2.47	3.84	6.93	0.76			6.69	1.78	3.50	9.23	0.09	3.57	0.38	0.00	4.05
7/25/2017	R1			6.92	0.86	1.06	-15.5	6.98	1.89	3.78	9.95	0.08	3.64	0.37	0.00	3.68
8/15/2017	R1			7.01	0.58	0.79	-13.4	4.53	2.20	2.68	7.84	0.08	3.00	0.19	0.02	2.52
9/20/2017	R1	1.97	4.00		1.07	1.22	-15.4	7.91	1.91	4.19	11.8	0.08	4.39	0.14	0.00	3.66
10/19/2017	R1			7.25		1.24	-14.6	7.08	2.18	4.21	11.0	0.08	4.24	0.13	0.00	3.31
5/31/2016	R2	3.44	1.77		0.98	1.04	-15.8					0.08	3.63	0.33	0.00	3.45
6/6/2016	R2							6.39	1.63	3.34	9.26					
6/17/2016	R2				0.78	0.95	-15.7	7.37	1.47	3.98	10.9					
6/21/2016	R2				0.93	1.02	-16.0	7.77	1.28	4.13	11.3	0.10	4.10	0.32	0.08	3.27
6/30/2016	R2				0.59	0.70	-15.4	5.54	1.65	3.04	8.21	0.07	3.40	0.43	0.06	3.46
7/6/2016	R2				0.92											
7/28/2016	R2	2.36	2.88	7.39	0.81	1.01	-16.5	7.11	1.57	3.80	10.6	0.11	3.19	0.21	0.00	3.31
8/4/2016	R2	2.75	1.38	7.38	1.02	1.00	-16.4					0.11	3.48	0.26	0.09	2.74
9/13/2016	R2	2.04		7.24		1.27	-14.6					0.10	3.42	0.08	0.00	2.99
9/20/2016	R2	2.37	0.55									0.12	3.46	0.03	0.10	3.13
9/28/2016	R2	4.83				0.81	-12.4	5.64	2.67	2.96	8.46					
10/4/2016	R2	8.56	0.65		0.97			6.90	2.33	3.79	10.6	0.11	3.98	0.17	0.00	4.08
10/12/2016	R2	2.92	2.64	2.57	0.60			6.66	2.33	3.64	10.2	0.10	4.04	0.22	0.00	4.83
10/18/2016	R2	2.34			0.82			7.66	2.23	4.14	11.6	0.11	4.30	0.11	0.11	3.78
10/25/2016	R2	2.24	3.62		1.08	1.17	-13.9	7.33	2.36	4.38	11.9	0.10	4.69	0.05	0.07	4.89
11/1/2016	R2	1.94			1.27			7.90	2.13	4.44	12.1	0.11	4.09	0.01	0.10	3.51
11/8/2016	R2	1.73			1.01	1.19	-13.6	7.93	1.86	4.49	12.3	0.10	3.98	0.02	0.09	3.39
11/14/2016	R2	1.92	2.81	7.37	1.07	1.21	-13.9	7.92	1.76	4.43	12.2	0.09	3.81	0.00	0.00	3.34
11/21/2016	R2				1.04			8.23	1.72	4.77	13.0	0.08	3.91	0.00	0.00	3.39
11/29/2016	R2	3.53		6.48				8.01	2.49	4.29	11.3	0.09	4.52	0.00	0.06	3.31
12/7/2016	R2	4.22	3.20	6.82				5.18	2.14	3.12	8.79	0.10	3.44	0.07	0.00	3.60
12/13/2016	R2			6.88	0.78			7.41	1.64	3.86	10.5	0.09	3.85	0.11	0.04	3.55
1/4/2017	R2	4.46		6.70				4.82	2.35	2.56	7.13	0.06	3.43	0.16	0.00	6.18
1/12/2017	R2	3.05		6.72	0.60			12.5	2.18	3.22	9.04	0.09	13.5	0.14	0.00	4.95

Date	Site	DOC (mg/L)	SUVA (L/mg ² ·m)	pH	Alkalinity (meq/L)	DIC (mM)	δ ¹³ C-DIC (‰)	Sodium (ppm)	Potassium (ppm)	Magnesium (ppm)	Calcium (ppm)	Fluoride (ppm)	Chloride (ppm)	NO ₃ ⁻ as N (ppm)	PO ₄ ³⁻ (ppm)	SO ₄ ²⁻ (ppm)
1/19/2017	R2	1.91	3.78	7.15	0.89	0.99	-14.3	7.86	1.32	3.75	10.9	0.08	4.30	0.07	0.00	4.71
1/20/2017	R2	2.07	3.33	6.55				7.87	1.41	3.69	9.99					
1/26/2017	R2	3.33		6.90	0.67			5.58	1.63	2.89	7.52	0.07	3.79	0.18	0.00	6.26
2/2/2017	R2	4.42		7.10	0.73			1.86	0.47	1.29	5.00	0.08	3.60	0.15	0.00	5.42
2/10/2017	R2	2.80		6.80	0.73			6.23	1.37	3.51	9.45	0.07	3.98	0.19	0.00	4.89
2/17/2017	R2	2.24	4.25	7.23	0.77							0.07	3.88	0.11	0.00	4.82
2/24/2017	R2	2.08		7.12	0.85			6.91	1.38	3.66	10.0	0.07	3.74	0.00	0.00	4.22
3/3/2017	R2			6.99				6.61	1.66	3.65	9.73	0.09	4.19	0.06	0.00	4.54
3/8/2017	R2	2.56		7.98				6.90	1.31	3.58	9.73	0.08	3.85	0.01	0.00	4.18
3/16/2017	R2	2.34	3.98	7.40	0.79	0.98	-13.5	6.31	1.18	3.53	9.41	0.07	3.81	0.07	0.00	4.15
3/24/2017	R2	3.85		7.59	0.82			6.72	1.21	3.68	10.1					
3/30/2017	R2			7.45	0.85	0.93	-14.4	6.69	2.24	3.15	9.59	0.07	3.75	0.03	0.00	3.83
4/7/2017	R2	3.60		7.48	0.58			5.19	1.38	2.91	7.99	0.08	3.55	0.14	0.00	4.96
4/13/2017	R2			7.39	0.80			6.58	1.29	3.76	10.2	0.09	3.82	0.04	0.00	4.82
4/21/2017	R2			7.05	0.90			7.14	1.56	3.90	10.6	0.09	3.78	0.19	0.04	4.39
4/28/2017	R2	3.26	3.77		0.70	0.73	-14.7	7.91	3.04	4.44	11.5	0.08	3.22	0.22	0.00	5.33
5/5/2017	R2	6.34		7.55				5.16	2.31	2.94	7.60	0.09	3.84	0.33	0.00	3.79
5/17/2017	R2			7.44				6.99	1.42	3.79	10.1	0.09	3.43	0.32	0.09	3.91
5/26/2017	R2	4.18		6.69	0.59	0.77	-15.3	4.75	1.88	2.77	7.41	0.08	3.18	0.15	0.00	4.35
5/31/2017	R2	2.85		6.98	0.76			6.01	1.70	3.31	9.05	0.08	3.30	0.27	0.00	4.04
6/14/2017	R2	5.82			0.43			3.45	2.49	2.24	5.77	0.09	2.83	0.16	0.00	4.83
6/20/2017	R2	2.64	4.05	6.70	0.74			6.11	1.68	3.28	8.81	0.09	3.27	0.26	0.00	4.23
6/26/2017	R2	2.69		7.60	0.78			4.88	1.40	2.72	8.26	0.08	3.46	0.26	0.00	3.77
7/7/2017	R2	2.87		7.13	0.81	0.81	-15.2	6.66	1.89	3.62	9.52	0.11	3.70	0.38	0.00	3.73
7/25/2017	R2			7.11	0.80	0.97	-15.3	6.40	1.99	3.48	9.40	0.08	3.41	0.27	0.09	3.81
8/2/2017	R2			7.20				7.66	1.52	4.27	11.4	0.08	3.46	0.25	0.05	3.63
8/10/2017	R2	2.14	3.55	7.23		1.05	-14.9	6.90	1.62	4.02	10.9	0.08	3.51	0.30	0.03	3.14
8/15/2017	R2			7.26	0.99	0.73	-13.1	3.90	2.29	2.66	7.50	0.08	2.79	0.12	0.00	2.43
8/28/2017	R2							7.48	1.70	4.08	11.2	0.08	3.43	0.18	0.04	3.29
9/6/2017	R2							7.17	1.77	3.90	10.7	0.08	3.46	0.10	0.05	3.12
9/20/2017	R2	1.73	3.64		1.06	1.25	-15.6	7.38	1.94	3.98	11.2	0.07	4.16	0.10	0.06	3.74
9/25/2017	R2	1.72	3.85		1.06			7.61	1.93	4.20	11.8	0.08	3.98	0.06	0.04	3.75
10/6/2017	R2	2.15	2.84	7.70				7.73	2.06	4.61	12.6	0.09	3.94	0.00	0.00	3.34
10/13/2017	R2			6.94								0.09	4.02	0.00	0.16	2.85
10/19/2017	R2			6.90		1.10	-14.4	6.50	2.27	3.95	10.6	0.07	4.20	0.12	0.00	3.41
10/25/2017	R2			7.49				5.37	2.39	3.32	9.07	0.08	4.27	0.10	0.00	3.58
10/30/2017	R2			7.80				6.94	1.87	4.10	10.9	0.07	4.19	0.12	0.06	3.29